NATIONAL ADVISORY COMMITTEE FOR AERONAUTICS

TECHNICAL NOTE 2905 APP

A RAPID METHOD FOR USE IN DESIGN OF TURBINES WITHIN SPECIFIED AERODYNAMIC LIMITS

By Richard H. Cavicchi and Robert E. English

Lewis Flight Propulsion Laboratory Cleveland, Ohio

CASE FILE

NACA

Washington April 1953

TECHNICAL NOTE 2905

A RAPID METHOD FOR USE IN DESIGN OF TURBINES WITHIN SPECIFIED AERODYNAMIC LIMITS

By Richard H. Cavicchi and Robert E. English

SUMMARY

A method is presented for the rapid determination of design velocity diagrams of turbine stages within specified aerodynamic limits. This method facilitates the selection of the number of turbine stages, the determination of the necessary proximity of staging operation to design limits, and the selection of optimum work division between or among the stages for any given application. For convenience, the method is presented in both chart and tabular form. Aerodynamic limits on design were built into the method to render it suitable for analyzing turbine stages of the following types: (1) Last stage limited by zero change in magnitude of relative velocity across rotor at hub radius and with zero exit whirl, or by specified entrance relative Mach number at hub radius and with zero exit whirl; and (2) stage other than the last limited by specified Mach numbers at hub radius relative to rotor entrance and relative to following stator and by amount of turning in rotor.

Several examples are included to illustrate in detail the use of the method. It is intended that this method be used primarily for sketching out a turbine design with a minimum expenditure of time and effort. The details of the derivations of the charts and tables are also included.

INTRODUCTION

Some of the most important preliminary considerations in the design of the turbine component of an aircraft turbojet engine are the selection of the number of stages, the proximity of stage operation to the design limits, and the selection of optimum work division between or among the stages. The choice of the number of stages should be such that the turbine can drive the compressor and operate within certain aerodynamic limits imposed upon the turbine design. For designs within such aerodynamic limits, there exists the problem of determining the maximum work

capacities associated with turbines of one, two, or three stages, or, alternatively, of determining for a specified turbine work output the minimum leaving loss which can be employed for a given number of stages.

A rapid and moderately accurate method for obtaining answers to these design questions is needed. At present there are several methods for estimating the work outputs of a turbine stage for various design conditions, one example of which is shown in reference 1. This reference, the analysis of which is based upon one-dimensional flow theory, presents a graphic trial-and-error method for estimating the work output of a turbine stage. Once the value of the work output of a stage has been established, this reference provides a method for making a specific design chart for the stage to aid in the study of the relations among the turbine aerodynamic parameters. The method of this reference, however, is best suited for a different problem from those posed in connection with the present study.

In order to furnish information readily on the design characteristics of turbines within specified aerodynamic limits, a method was evolved at the NACA Lewis laboratory which embodies certain preselected design parameters. With this method, a turbine design which can satisfy its requirements while operating within specified aerodynamic design limits can be roughed out rapidly. This report presents this method in both charts and tables along with their derivations and describes in detail their use in preliminary design of turbines.

Several combinations of the following design limits were selected in the production of the charts and tables:

- (1) Specified axial component of exit critical velocity ratio
- (2) Zero change in magnitude of relative velocity of gas across a rotor-blade row
- (3) Low magnitude of exit tangential velocity from last rotor-blade row
- (4) Specified maximum relative Mach number at entrance to any blade row
- (5) Specified maximum turning of gas by rotor-blade row

These design limits were postulated in order that the method be suitable for analyzing turbine stages of the following types:

Chart I and table I:

- (1) Last stage limited by zero change in magnitude of relative velocity of gas at hub radius and zero exit whirl
- (2) Last stage limited by rotor-entrance relative Mach number at hub radius and zero exit whirl

Chart II and table II:

Stage other than the last limited by hub radius Mach numbers relative to rotor entrance and relative to following stator and by amount of turning of gas through rotor

ANALYSIS AND PREPARATION OF CHARTS AND TABLES

Assumptions

The symbols used in this report are listed in appendix A. The following assumptions were made to simplify the analysis:

- (1) Simplified radial equilibrium
- (2) Angular momentum per unit mass which is constant along a radial line (free vortex)
- (3) At mean radius, $\rho V_X A$ is constant across rotor
- (4) No radial variation in stagnation state relative to stator
- (5) Hub and mean radii constant in value from entrance to exit
- (6) Constant value of 4/3 for the ratio of specific heats

Assumption (5) is exact for a straight annulus. For a diverging annulus with constant tip diameter, it is conservative (with respect to Mach number, reaction, and turning) at the hub radius, which is the most critical section. The value of 4/3 for the ratio of specific heats was selected as an average for the range of gas temperatures used in current gas turbines. As will be discussed later, the value chosen for the ratio of specific heats has a negligible effect on the results obtained.

Factors Affecting Maximum Stage Work

One of the design limitations built into chart I and table I is that of zero change in the magnitude of the relative velocity of gas across the rotor at the hub radius, that is, $(W_1/W_2)_h = 1$. A typical

velocity diagram, the numbering system of which is applicable to any stage, is presented in figure 1. This design selection, $(W_1/W_2)_h=1$, is similar to the commonly used impulse design, which connotes zero change in static pressure across the blade row. In fact, these two types of design are identical for isentropic expansion. In general, a rise in static pressure across a blade row is avoided because of possible separation of flow and concomitant poor performance. It can be shown that for nonisentropic flow the limitation of zero velocity change yields a drop in static pressure across the blade row, the magnitude of which depends on the efficiency. Thus, in practice, this design limitation is somewhat more conservative than the impulse limitation.

The relative Mach number of the gas entering a blade row is likewise one of the main limitations used in the charts and tables. With progressively higher relative Mach numbers at the entrance to a blade row the theoretical work capacity of the row is increased; however, the tendency for local separation of flow also increases, as does the drag. An optimum entrance relative Mach number has not yet been determined. The entrance relative Mach number is highest and thus most critical at the hub radius.

For a last-stage rotor it is advisable to design for as low a value of the magnitude of the tangential component of the exit absolute velocity as possible, if no means is to be provided for utilizing the kinetic energy associated with this component of velocity. In stages other than the last stage of a multistage turbine, relatively high values of this parameter can be tolerated because of utilization of the energy associated with this parameter in subsequent staging. As a consequence, a greater proportion of the total work of a turbine can be extracted from stages other than the last.

An additional parameter to be considered is the axial component of exit critical velocity ratio $(V_x/a_{\rm cr}^{\dagger})_2$ at the exit of a last stage or single stage. When the value of this parameter reaches unity for the condition of zero exit whirl, the annulus is passing its maximum weight flow. At a value of 0.7 for the exit axial velocity ratio, a margin of about 10 percent in the weight-flow capacity exists; that is, the weight flow can be increased by 10 percent before the annulus chokes.

The turning angle of the gas flow through a blade row, as in the case of Mach number, is believed to have an upper limit for good turbine performance. A value of 120° for this parameter was arbitrarily selected for use in this report. For a rotor, the turning angle is most critical at the hub radius.

Analytical Basis for Charts, Tables, and Figures

Throughout this report the work output is presented in the nondimensional form $-gJ\Delta h^{\dagger}/U_{t}^{2}$, where the negative sign is indicative of a drop in enthalpy. This ratio, referred to as the stage-work parameter, is merely half the reciprocal of the square of the blade-tip to jet speed ratio.

Another parameter presented in the charts and tables herein is the isentropic annular area ratio $(A_2/A_1)_s$. This parameter is the ratio of the annular area behind the rotor to that ahead of the rotor with the assumption of isentropic flow and is defined by the following equation:

$$\left(\frac{A_{Z}}{A_{1}}\right)_{S} \equiv \frac{A_{Z}}{A_{1}} \left(\frac{p_{Z}''}{p_{1}''}\right)_{m}$$
(C12)

In appendix B are tabulated the general thermodynamic relations which are used throughout the analysis.

Chart I, table I, and figure 2 - last stage or single stage with zero exit whirl. - In chart I and table I are shown values of stage-work parameter $-gJ\Delta h^{\,\prime}/U_{\rm t}^2$ for various values of exit axial velocity ratio $(V_{\rm x}/a_{\rm cr}^{\,\prime})_2$, isentropic annular area ratio $(A_2/A_1)_{\rm s}$, hub-tip radius ratio r_h/r_t , and blade-speed parameter $U_t/a_{\rm cr}^{\,\prime}.2$.

Chart I, table I, and figure 2 have been prepared for use in making last-stage or single-stage designs; hence, it was found convenient to express some of the nondimensional parameters in terms of the stage-exit stagnation state relative to the stator.

Parallel designations have been used for the charts and tables. For chart I and table I, designations (a), (b), and (c) refer to values of 0.5, 0.6, and 0.7, respectively, for the exit axial velocity ratio. Subdesignation 1 identifies the set limited by zero change in the magnitude of relative velocity at the hub radius, $(W_1/W_2)_h = 1$; subdesignations 2, 3, and 4 identify the set limited by specified values of entrance relative Mach number at the hub radius of 0.6, 0.8, and 1.0, respectively.

Chart I,l and table I,l - last stage or single stage limited by zero change in magnitude of relative velocity at hub radius with zero exit whirl. - In appendix C are developed the equations used in the preparation of chart I,l, table I,l, and figure 2. The stage-work parameter was calculated from the following equation:

$$\left(\frac{-gJ\Delta h'}{U_{t}^{2}}\right)_{V_{u,2}=0} = \left(\frac{V_{u}}{U}\right)_{1,h} \left(\frac{r_{h}}{r_{t}}\right)^{2}$$
(C19)

The calculations then proceed in the following manner. Solved as a dependent variable is the isentropic annular area ratio $(A_2/A_1)_s$, which was calculated from

$$\begin{pmatrix} \frac{A_2}{A_1} \end{pmatrix}_{s} = \frac{V_{x,1}}{V_{x,2}} \left\{ \frac{\frac{k+1}{k-1} + \left(\frac{U}{a_{cr}^{\dagger}}\right)_{2,h}^{2} \left(\frac{V_{u}}{U}\right)_{1,h} \left[2 - \left(\frac{V_{u}}{U}\right)_{1,h} \frac{-2}{r^2}\right] - \left(\frac{V_{x,1}}{V_{x,2}}\right)^{2} \left(\frac{V_{x}}{a_{cr}^{\dagger}}\right)_{2}^{2}}{\frac{k+1}{k-1} - \left(\frac{V_{x}}{a_{cr}^{\dagger}}\right)_{2}^{2}} \right\}^{\frac{1}{k-1}}$$
(C18)

upon insertion of the ratio of axial velocities

$$\frac{\mathbf{v}_{x,1}}{\mathbf{v}_{x,2}} = \sqrt{1 + \left(\frac{\mathbf{u}}{\mathbf{a}_{cr}^{t}}\right)^{2}_{2,h} \left(\frac{\mathbf{a}_{cr}^{t}}{\mathbf{v}_{x}}\right)^{2}_{2} \left\{1 - \left[\left(\frac{\mathbf{v}_{u}}{\mathbf{u}}\right)_{1,h} - 1\right]^{2}\right\}}$$
 (C8)

For convenience in the construction of chart I,l and table I,l, nominal values of the parameters $(U/a_{\rm cr}^i)_{2,h}$ and $(V_u/U)_{1,h}$ were assigned for three selected values of $(V_x/a_{\rm cr}^i)_2$ and five typical values of (r_h/r_t) . Combinations of these variables were chosen so as to yield results in the practical range for turbines.

In order to obtain the charts and the data for the tables, the stage-work parameter $-\mathrm{gJ}\Delta h^{\,\prime}/U_t^2$ was plotted against isentropic annular area ratio $(A_2/A_1)_s$ for lines of constant exit blade-hub speed ratio $U_h/a_{cr,2}^{\,\prime}$, each such preliminary plot having been made for one particular value of exit axial velocity ratio $(V_x/a_{cr}^{\,\prime})_2$ and one value of hub-tip radius ratio r_h/r_t . The curves of chart I,l are merely cross plots of these preliminary plots. In the final form of chart I,l, stage-work parameter is plotted against exit blade-speed parameter with lines of constant hub-tip radius ratio, all for one particular value of exit axial velocity ratio and one value of isentropic annular area ratio. The abscissa of the charts was calculated from the exit blade-hub speed ratio $(U/a_{cr}^{\,\prime})_{2,h}$ by the simple relation

$$\frac{U_{t}}{a_{cr,2}^{\prime}} = \frac{(U/a_{cr}^{\prime})_{2,h}}{r_{h}/r_{t}}$$
 (1)

Table I,1 was produced by simply reading chart I,1 at 0.02 intervals of the blade-speed parameter over the same range presented in the chart.

The turbine weight flow has been expressed in the form of a non-dimensional parameter identified in figure 2 as exit weight-flow parameter. This parameter is calculated from the equation

$$\hat{\mathbf{w}}_{2} = \left[1 - \frac{\mathbf{k} - 1}{\mathbf{k} + 1} \left(\frac{\mathbf{v}_{x}}{\mathbf{a}_{cr}^{\dagger}}\right)^{2}\right]^{\frac{1}{\mathbf{k} - 1}} \left(\frac{\mathbf{v}_{x}}{\mathbf{a}_{cr}^{\dagger}}\right)^{2} \left[1 - \left(\frac{\mathbf{r}_{h}}{\mathbf{r}_{t}}\right)^{2}\right]$$
(C24)

which is plotted directly in figure 2.

Chart I,2,3,4 and table I,2,3,4 - last stage or single stage limited by rotor entrance relative Mach number at hub radius with zero exit whirl. - The stage-work parameter was again calculated from equation (C19). The isentropic annular area ratio was calculated from equation (C18); but for the Mach number limitation the ratio of axial velocities $V_{x,1}/V_{x,2}$ was calculated by the following equation, which is developed in appendix D:

$$\frac{V_{x,1}}{V_{x,2}} = \frac{\left(\frac{U}{a_{cr}^{\dagger}}\right)_{2,h}}{\left(\frac{V_{x}}{a_{cr}^{\dagger}}\right)_{2}} \sqrt{\frac{k+1}{2} M_{1,h}^{2}} \left[\frac{1 + \frac{k-1}{k+1} \left(\frac{U}{a_{cr}^{\dagger}}\right)_{2,h}^{2}}{\left(\frac{U}{a_{cr}^{\dagger}}\right)_{2,h}^{2} \left(1 + \frac{k-1}{2} M_{1,h}^{2}\right)} - \left[\left(\frac{V_{u}}{U}\right)_{1,h} - 1\right]^{2} \tag{D5}$$

The exit weight-flow parameter was also calculated from equation (C24), so that figure 2 also applies to this set.

In order to obtain the calculated data for preparation of chart I,2, 3,4 and table I,2,3,4 nominal values of the parameters $(U/a_{cr}^i)_{2,h}$ and $(V_u/U)_{1,h}$ were assigned for three arbitrary values of $M_{1,h}$, three values of $(V_x/a_{cr}^i)_2$, and five typical values of r_h/r_t .

The curves of chart I,2,3,4 were also obtained by cross-plotting preliminary plots at constant selected values of isentropic annular area ratio. These preliminary plots once again consisted of stage-work parameter plotted against isentropic annular area ratio with lines of constant

2754

exit blade-hub speed ratio, each preliminary plot being drawn for one particular value of entrance relative Mach number, one value of exit axial velocity ratio, and one value of hub-tip radius ratio. The final forms of chart I,2,3,4 and table I,2,3,4 are similar in manner of presentation to those of chart I,1 and table I,1.

On some of the plots of chart I,2,3,4 are shown dotted curves, which are the loci of points of zero change in the magnitude of relative velocity at the hub radius across the rotor. Equation (D8) of appendix D has been developed for the purpose of establishing these curves:

$$\left(\frac{W_{1}}{W_{2}}\right)_{h}^{2} = \frac{k+1}{2} \left[\frac{M_{1,h}^{2}}{\left(\frac{U}{a_{cr}^{\dagger}}\right)_{2,h}^{2} + \left(\frac{V_{x}}{a_{cr}^{\dagger}}\right)_{2}^{2}} \right] \left[\frac{1 + \frac{k-1}{k+1} \left(\frac{U}{a_{cr}^{\dagger}}\right)_{2,h}^{2}}{1 + \frac{k-1}{2} M_{1,h}^{2}} \right]$$
(D8)

Preliminary plots of $(W_1/W_2)_h^2$ against U_t/a_{cr}^i , 2 with lines of constant hub-tip radius ratio were made, each plot drawn for a particular value of $(V_x/a_{cr}^i)_2$ and of $M_{1,h}$. The dotted curves, depicting $(W_1/W_2)_h = 1$, on the final charts were obtained by cross-plotting these preliminary plots at a value of unity for the ratio $(W_1/W_2)_h^2$. No such dotted curves can be drawn on chart I(b)2 [combination of $(V_x/a_{cr}^i)_2 = 0.6$ and $M_{1,h} = 0.6$] or on chart I(c)2 [combination of $(V_x/a_{cr}^i)_2 = 0.7$ and $M_{1,h} = 0.6$], for, as can be easily noted from consideration of the velocity diagram, the exit axial component of velocity is approximately equal to or greater than the exit relative velocity at the hub radius. The reasons for the absence of the dotted curve in some of the plots of chart I,4 is that this locus occurs only at values of blade-speed parameter greater than that presented in the chart (0.8). In chart I,2,3,4 regions to the left of the dotted curves are indicative of a decrease in the magnitude of relative velocity across the rotor at the hub radius; whereas, regions to the right of the dotted curves are indicative of an increase.

Table I,2,3,4 was fashioned from chart I,2,3,4 in the same manner that table I,1 was read from chart I,1.

Chart II, table II, and figure 3 - stage other than last limited by hub-radius Mach numbers relative to rotor entrance and relative to following stator and by amount of turning in rotor. - Derivations of the equations used in making chart II, table II, and figure 3 are presented in appendix E. The calculations and plotting procedures for this set were somewhat more involved than those for chart I and table I.

Because chart II, table II, and figure 3 have been prepared for stages other than the last, for convenience some of the nondimensional parameters have been expressed in terms of the stage-entrance stagnation state relative to the stator.

In chart II and table II, designations (a) and (b) identify relative hub-radius Mach numbers of 0.6 and 0.8, respectively; whereas, subdesignations 1 and 2 identify the stage-work parameter $-gJ\Delta h^{\,\prime}/U_{\rm t}^2$ and the ratio of hub-radius tangential velocities $-(V_{\rm u},1/V_{\rm u},2)_{\rm h}$, respectively.

The stage-work parameter is found from the equation

$$\frac{-gJ\triangle h^{\dagger}}{U_{t}^{2}} = \left[\left(\frac{V_{u}}{U} \right)_{1,h} - \left(\frac{V_{u}}{U} \right)_{2,h} \right] \left(\frac{r_{h}}{r_{t}} \right)^{2}$$
 (E16)

where the term $-(V_u/U)_{2,h}$ provides additional work for stages other than the last without penalty, because the energy associated with this term remains available for use in subsequent stages.

The isentropic annular area ratio was calculated from the relation

$$\frac{\binom{A_{2}}{A_{1}}}{\binom{A_{2}}{A_{1}}} = \frac{V_{x,1}}{V_{x,2}} \left\{ \frac{\frac{k+1}{k-1} - \left(\frac{V_{x}}{a_{cr}^{t}}\right)_{1}^{2} - \left(\frac{V_{u}}{u}\right)_{1,h}^{2} + \left(\frac{U}{a_{cr}^{t}}\right)_{1,h}^{2} - \left(\frac{V_{u}}{u}\right)_{2,h}^{2} - 2\left(\frac{V_{u}}{u}\right)_{2,h}^{2} - 2\left(\frac{V_{u}}{u}\right$$

in which the ratio $V_{x,2}/V_{x,1}$ was found by solving the expression

$$\left(\frac{\mathbf{v}_{\mathbf{x},2}}{\mathbf{v}_{\mathbf{x},1}}\right)^{2} = \frac{1}{\left(\frac{\mathbf{v}_{\mathbf{x}}}{\mathbf{a}_{\mathrm{cr}}^{\mathsf{T}}}\right)_{1}^{2}} \left(\frac{\frac{\mathbf{k}+1}{2} \, \mathbf{M}_{h}^{2}}{1 + \frac{\mathbf{k}-1}{2} \, \mathbf{M}_{h}^{2}} \left\{1 - 2 \, \frac{\mathbf{k}-1}{\mathbf{k}+1} \left(\frac{\mathbf{U}}{\mathbf{a}_{\mathrm{cr}}^{\mathsf{T}}}\right)_{1,h}^{2} \left[\left(\frac{\mathbf{v}_{\mathbf{u}}}{\mathbf{U}}\right)_{1,h} - \left(\frac{\mathbf{v}_{\mathbf{u}}}{\mathbf{U}}\right)_{2,h}\right]\right\} - \left(\frac{\mathbf{U}}{\mathbf{a}_{\mathrm{cr}}^{\mathsf{T}}}\right)_{1,h}^{2} \left(\frac{\mathbf{v}_{\mathbf{u}}}{\mathbf{U}}\right)_{2,h}^{2} \tag{E10}$$

and the factor $(V_x/a_{cr}^i)_1^2$ from solution of

$$\left(\frac{v_{x}}{a_{cr}^{i}}\right)_{1}^{2} = \frac{\frac{k+1}{2} M_{h}^{2} \left\{1 - \frac{k-1}{k+1} \left(\frac{U}{a_{cr}^{i}}\right)_{1,h}^{2} \left[2\left(\frac{v_{u}}{U}\right)_{1,h} - 1\right]\right\}}{1 + \frac{k-1}{2} M_{h}^{2}} - \left[\left(\frac{v_{u}}{U}\right)_{1,h} - 1\right]^{2} \left(\frac{U}{a_{cr}^{i}}\right)_{1,h}^{2}$$

Turning angle at the hub radius was determined by the equation

$$\Delta \beta_{h} = -\cot^{-1} \left\{ \frac{\left[\left(\frac{V_{u}}{U} \right)_{l,h} - 1 \right] \left(\frac{U}{a_{cr}^{!}} \right)_{l,h}}{\left(\frac{V_{x}}{a_{cr}^{!}} \right)_{l}} \right\} - \cot^{-1} \left\{ \frac{\left[\left(\frac{V_{u}}{U} \right)_{2,h} - 1 \right] \left(\frac{U}{a_{cr}^{!}} \right)_{l,h}}{\frac{V_{x,2}}{V_{x,1}} \left(\frac{V_{x}}{a_{cr}^{!}} \right)_{l}} \right\}$$
(E15)

Entrance weight-flow parameter was calculated by the formula

$$\mathbf{v}_{1} = \left\{ 1 - \frac{\mathbf{k} - 1}{\mathbf{k} + 1} \left[\left(\frac{\mathbf{v}_{x}}{\mathbf{a}_{cr}^{t}} \right)_{1}^{2} + \left(\frac{\mathbf{v}_{u}}{\mathbf{U}} \right)_{1,h}^{2} \left(\frac{\mathbf{u}}{\mathbf{a}_{cr}^{t}} \right)_{1,h}^{2} - \frac{\mathbf{z}}{\mathbf{r}^{2}} \right] \right\}^{\frac{1}{\mathbf{k} - 1}} \left(\frac{\mathbf{v}_{x}}{\mathbf{a}_{cr}^{t}} \right)_{1} \left[1 - \left(\frac{\mathbf{r}_{h}}{\mathbf{r}_{t}} \right)^{2} \right]$$
(E21)

In the calculations for this set, nominal values of the parameter $(U/a_{cr}^{\dagger})_{1,h}$ were assigned along with two values of M_h and four values of (r_h/r_t) . It was by a trial-and-error process that the proper combinations of the parameters $(V_u/U)_{1,h}$ and $(V_u/U)_{2,h}$ were determined for use with the selected parameters. It was necessary that these combinations of $(V_u/U)_{1,h}$ and $(V_u/U)_{2,h}$ yield calculated values of isentropic annular area ratio of $0.8 \le (A_2/A_1)_s \le 1.2$ while simultaneously yielding values of turning angle at the hub radius near 120° .

Preliminary plots of hub turning angle $\Delta\beta_h$ against isentropic annular area ratio were drawn with lines of constant entrance blade-hub speed ratio, each such plot pertaining to one particular value of M_h , one value of (r_h/r_t) , and one value of $-(V_u/U)_{2,h}$. Similar plots were likewise made with stage-work parameter plotted as ordinate instead of hub turning angle. A value of $(U/a_{cr}^i)_{1,h}$ determined on the former plot by the intersection of a desired abscissa with the 120° ordinate established a value of $-gJ\Delta h^i/U_t^2$ on the corresponding latter plot. The corresponding value of entrance blade-speed parameter was calculated from the equation

$$\frac{U_{t}}{a_{cr,l}^{\prime}} = \frac{\left(U/a_{cr}^{\prime}\right)_{l,h}}{r_{h}/r_{t}} \tag{2}$$

in which $(U/a_{\rm cr}^i)_{1,h}$ has that value obtained from the plot of $\Delta\beta_h$ against $(A_2/A_1)_s$. Thus, these two preliminary plots yielded one point on chart II,1, in which stage-work parameter is plotted against entrance blade-speed parameter with lines of constant hub-tip radius ratio, all for one particular value of Mach number at the hub radius and one value of isentropic annular area ratio.

Preliminary plots of $-(V_u,1/V_u,2)$ against $\Delta\beta_h$ were drawn with lines of constant entrance blade-hub speed ratio, each for one particular value of M_h and one value of $-(V_u/U)_{2,h}$. This plot is independent of hub-tip radius ratio, because the parameter r_h/r_t is absent from equation (E15). This plot and the $\Delta\beta_h$ against $(A_2/A_1)_s$ preliminary plot described previously, drawn for the corresponding values of M_h and $-(V_u/U)_{2,h}$, established one point on chart II,2. In chart II,2 the ratio of tangential velocities at the hub radius is presented as the ordinate, and the parameters $U_t/a_{cr,1}$, r_h/r_t , M_h , and $(A_2/A_1)_s$ retain the same form of presentation as in chart II,1.

Table II was produced from chart II by the same procedure in which table I was prepared from chart I.

For the preparation of figure 3, preliminary plots of entrance weight-flow parameter \hat{w}_1 against hub turning angle $\Delta\beta_h$ were made, again with lines of constant entrance blade-hub speed ratio $(U/a_{cr}^i)_{1,h}$ for one particular value of each of the parameters M_h , r_h/r_t , and $-(V_u/U)_{2,h}$. The value of $(U/a_{cr}^i)_{1,h}$ established on the corresponding preliminary plot of $\Delta\beta_h$ against $(A_2/A_1)_s$ located a corresponding point on the previously mentioned \hat{w}_1 against $\Delta\beta_h$ plot, all of which yielded one point on a plot of \hat{w}_1 against $U_t/a_{cr,1}^i$ with lines of constant r_h/r_t for $(A_2/A_1)_s = 0$. This was cross-plotted in order to present figure 3 in a form similar to that of figure 2. Figure 3 is a plot of hub-tip radius radio against entrance weight-flow parameter with lines of constant entrance blade-speed parameter, drawn for an isentropic annular area ratio of 1.0 and for each of two selected rotor-entrance relative Mach numbers. For simplicity, only an isentropic annular area ratio of 1.0 is furnished in figure 3.

Determination of loss factors for use with charts and tables. Although the charts and tables were constructed on the basis of isentropic
flow, provision for including stage efficiency has been made. In
appendix F are presented the details of the development of a loss factor
which is used according to the following equation:

$$\frac{A_2}{A_1} = \left(\frac{A_2}{A_1}\right)_s e^{\frac{J\Delta s}{R}}$$
 (F6)

0

The velocity diagram and stage-work parameter as obtained from the charts or tables are unaffected upon assumption of stage efficiency; the design of the charts and tables is such that only the annular area ratio becomes affected. The charts and tables have been constructed for various isentropic annular area ratios in order that interpolation between the actual annular area ratios as calculated from equation (F6) can be used for ascertaining the stage-work parameter (and $-(V_{\rm u},1/V_{\rm u},2)_{\rm h}$ in the case of chart II and table II) associated with the desired actual annular area ratio.

Figure 4 is a plot of loss factor $e^{J\Delta s/R}$ against stage-enthalpy parameter $-gJ\Delta h^{i}/T^{i}$ with lines of constant adiabatic efficiency η . The abscissa of figure 4(a) is in terms of the exit stagnation temperature relative to the stator, because this plot is intended for use with chart I and table I. By the same token, figure 4(b) was constructed for use with chart II and table II by presenting the abscissa in terms of the entrance stagnation temperature relative to the stator.

Summary of Design Conditions Used in Charts and Tables

The following table summarizes the design conditions built into the charts and tables:

Chart and table	$\left(\frac{v_x}{a_{cr}^t}\right)_2$	$\left(\frac{W_1}{W_2}\right)_h$	Ml,h	M2,h	Vu,2	$\frac{r_{ m h}}{r_{ m t}}$	$\left(\frac{A_2}{A_1}\right)_s$	Appendix
I,1	0.5, 0.6, 0.7	1			0	0.5, 0.6, 0.7, 0.8, 0.9	0.8, 0.9, 1.0, 1.1	C
I,2,3,4	0.5, 0.6, 0.7	-	0.6, 0.8, 1.0		0	0.5, 0.6, 0.7, 0.8, 0.9	0.8, 0.9, 1.0, 1.1	D
II		-	0.6, 0.8	0.6, 0.8		0.6, 0.7, 0.8, 0.9	0.8, 1.0, 1.2	E

Chart II and table II are presented with but three annular area ratios, because this parameter has less effect here than it does in chart I and table I.

USE OF CHARTS AND TABLES

The design information of this report is presented in both chart and tabular form. The charts may be somewhat more convenient in instances in which one or two turbine designs are sought. In situations in which a survey of many turbine designs is desired, the tables may prove especially suitable. Either the charts or tables, of course, can be used for either of these purposes.

Turbine Design Requirements

The charts and tables in this report have been set up for the purpose of furnishing a turbine design to meet a given set of turbine design requirements. These requirements consist, in one form or another, of

- (1) Equivalent work per pound of gas needed to drive compressor $-\Delta h'/\theta_c'$
- (2) Equivalent weight flow per unit turbine-tip frontal area w $\sqrt{\theta_{\rm C}'}/{\rm A_F}\delta_{\rm C}'$
- (3) Equivalent blade tip speed of turbine $U_{\rm t}/\sqrt{\theta_{\rm c}^{\, \rm i}}$
- (4) Equivalent turbine-inlet stagnation temperature relative to stator T_1^i/θ_c^i
- (5) Equivalent turbine-inlet stagnation pressure relative to stator $p_1^{\prime}/\delta_c^{\prime}$

Calculation of Parameters

Before entry can be made into the charts or tables, certain parameters must be calculated in order to express the turbine design requirements in the nondimensional forms of the chart and table presentation. The following equations are therefore used:

$$T_2^i = T_1^i - \left(\frac{-\Delta h^i}{c_p}\right) \tag{3}$$

$$p_{2}' = p_{1}' \left[1 - \left(\frac{T_{1}' - T_{2}'}{\eta T_{1}'} \right) \right]^{\frac{k}{k-1}}$$
 (4)

$$\rho' = \frac{p'}{RT'}$$
 (B1)

$$a_{cr}' = \sqrt{\frac{2k}{k+1}} gRT'$$
 (B4)

$$\frac{U_{t}}{a_{cr}^{!}} = \frac{U_{t}}{\sqrt{\theta_{c}^{!}}} \sqrt{\frac{T_{c}^{!}}{518.4}} \left(\frac{1}{a_{cr}^{!}}\right)$$
 (5)

$$\hat{\mathbf{w}} = \frac{\mathbf{w} \sqrt{\theta_{c}^{'}}}{\mathbf{A_{F}} \delta_{c}^{'}} \frac{2116}{\mathbf{p_{c}^{'}}} \sqrt{\frac{518.4}{\mathbf{T_{c}^{'}}}} \left(\frac{1}{\rho' a_{cr}^{'}}\right) \tag{6}$$

Required stage-work parameter:
$$\left(\frac{-gJ\Delta h^{\dagger}}{U_{t}^{2}}\right)_{req}$$
 (7)

Enthalpy parameter:
$$\frac{-gJ\Delta h'}{T'}$$
 (8)

Use of Chart I and Table I

With a given set of turbine design requirements, the initial step in using chart I or table I is to assign limits for entrance relative Mach number at the hub radius Ml.h and exit axial velocity ratio $(V_{\rm x}/a_{\rm cr})_2$, along with annular area ratio A_2/A_1 and turbine adiabatic efficiency n. From the turbine design requirements, the parameters of the previous section can be calculated from equations (3), (4), (B1), (B4), (5), (6), (7), and (8). The exit weight-flow parameter $\hat{\mathbf{w}}_2$, calculated from equation (6), together with the assigned value of $(V_{\rm x}/a_{\rm cr}')_2$ establish the hub-tip radius ratio $r_{\rm h}/r_{\rm t}$, which is read on figure 2. Once the hub-tip radius ratio has been established, recourse to the charts or tables immediately yields the stage-work parameter at the appropriate blade-speed parameter for the even values of isentropic annular area ratios presented, at the initially selected value of exit axial velocity ratio. In all instances readings should be made from chart I, 1 and chart I, 2, from chart I, 1 and chart I, 3, or from chart I,l and chart I,4 in order that a comparison of the results from the two sets can be used to determine which is the limiting set. If the tables are being used, the word "table" is to be substituted for the word "chart" in the previous sentence.

In the calculation of the exit-enthalpy parameter $-gJ\Delta h^{\prime}/T_2^{\prime}$, there arises an ambiguity as to what value should be used for the factor $-\Delta h^{\prime}$. The following rule-of-thumb approximations are suggested for use in calculating the value of $-gJ\Delta h^{\prime}/T_2^{\prime}$ with which to enter figure 4(a). When the stage-work parameters read from chart I or table I at the even values of $(A_2/A_1)_s$ presented are of about the same magnitude as the

required value, so that a single-stage design is indicated, the value of compressor work per pound of air is suggested for the factor $-\Delta h'$. For the last stage of a multistage turbine, the value of $-\Delta h'$ is suggested which is determined by subtracting from the required enthalpy drop the sum of the design values of enthalpy drops of all stages other than the last. As will be explained later, the enthalpy drops of stages other than the last can be obtained from chart II or table II.

From the exit-enthalpy parameter $-gJ\Delta h'/T_2'$ and the turbine adiabatic efficiency η , a loss factor $e^{J\Delta s/R}$ can be read directly on figure 4(a). The abscissa in figure 4(a) is presented in terms of downstream stagnation temperature T_2' because figure 4(a) is intended for use with chart I and table I. The actual annular area ratio is calculated from the loss factor by

$$\frac{A_{2}}{A_{1}} = \left(\frac{A_{2}}{A_{1}}\right)_{S} e^{\frac{J\Delta s}{R}}$$
(F6)

The procedure is to select two isentropic annular area ratios such that the resulting values of A_2/A_1 (from eq. (F6)) encompass the desired

value of annular area ratio. If chart I is being used, a linear interpolation is then made to yield the value of stage-work parameter corresponding to the desired annular area ratio. Use of the tables involves an additional interpolation, that is, for blade-speed parameter. The following graphical method is suggested for interpolating the tables. For hub-tip radius ratio, a linear interpolation in the tables is quite satisfactory. Stage-work parameter can be read at two values of blade-speed parameter for two values of isentropic annular area ratio, the two values of each parameter being selected so as to encompass the desired value of each. The four values of stage-work parameter so obtained can be plotted with blade-speed parameter for each of the two selected isentropic annular area ratios. The two points of each area ratio can be joined by a straight line and an interpolation made between them at the desired abscissa (blade-speed parameter).

The Euler work equation (Cl) can be written as follows:

$$\frac{-gJ\triangle h!}{U_{t}^{2}} = \left(\frac{V_{u,1}}{U} - \frac{V_{u,2}}{U}\right) \left(\frac{r_{h}}{r_{t}}\right)^{2} \tag{9}$$

where the term $V_{u,2}/U$ is set equal to zero in the derivations of chart I and table I. In many instances it will be found that the stagework parameter as read from chart I or table I is not quite sufficient

to meet the work required of the stage. Selection of higher values of the aerodynamic limits $(V_x/a_{\rm cr}^i)_2$ or $M_{1,h}$ may suffice. If, however, the deficiency is small, the turbine stage can be designed to produce sufficient work by designing for a small amount of exit whirl. The equation to be used for this purpose in connection with the set of chart I and table I pertaining to zero change in the magnitude of relative velocity is

$$\left(\frac{-gJ\Delta h^{\dagger}}{U_{t}^{2}}\right)_{I,V_{u,2}\neq 0} \approx \left(\frac{-gJ\Delta h^{\dagger}}{U_{t}^{2}}\right)_{I,V_{u,2}=0} - 2\left(\frac{V_{u}}{U}\right)_{2,h} \left(\frac{r_{h}}{r_{t}}\right)^{2}$$
(10)

in which the numerical coefficient 2 has been found to be a good average value. The paralleling equation for use with the set of chart I and table I limited by Mach number is

$$\left(\frac{-gJ\Delta h^{\dagger}}{U_{t}^{2}}\right)_{M,V_{u},2\neq0} = \left(\frac{-gJ\Delta h^{\dagger}}{U_{t}^{2}}\right)_{M,V_{u},2=0} - \left(\frac{V_{u}}{U}\right)_{2,h} \left(\frac{r_{h}}{r_{t}}\right)^{2} \tag{11}$$

In both equations (10) and (11), the value used for the stage-work parameter on the left is that required of the stage; the value of $-\Delta h$ ' in this parameter coincides identically with that suggested in calculating $-gJ\Delta h$ '/ T_2 '. The stage-work parameter on the right is taken directly from chart I or table I.

Values of $(V_u/U)_{2,h}$ having been calculated from equations (10) and (11), inspection of their absolute magnitudes immediately indicates whether the particular design is limited by change in magnitude of relative velocity or by Mach number. For the values of $(V_u/U)_{2,h}$ so calculated, each set will lie within its particular limit; what is sought, however, is that set which lies within the limits of both sets. The set corresponding to the larger absolute magnitude of the two values of $(V_u/U)_{2,h}$, calculated from equations (10) and (11), is the limiting set. The reason for this statement can be seen from a consideration of the work equation

$$\frac{-gJ\Delta h^{*}}{U^{2}} = \left(\frac{V_{u}}{U}\right)_{1} - \left(\frac{V_{u}}{U}\right)_{2}$$
 (E1)

For the required value of $-gJ\Delta h^{1}/U^{2}$, the larger the absolute magnitude of $(V_{U}/U)_{2}$, the smaller can be the absolute magnitude of $(V_{U}/U)_{1}$. Smaller absolute magnitudes of $(V_{U}/U)_{1}$ are indicative of lower values of entrance relative velocity W_{1} , which in turn correspond to lower values of both W_{1}/W_{2} and $(W/a)_{1}$. The conclusion is thus that the set corresponding to the larger magnitude of $(V_{U}/U)_{2}$, h lies within both limits.

Other occasions will arise in which the value of the stage-work parameter read from chart I or table I is in excess of that required of the stage. This situation can be handled in several ways. Perhaps the simplest is to decrease the value of $(V_u/U)_{1,h}$ (see eq. (C6)) for design for less work. Other possibilities consist in selecting lower values of the aerodynamic parameters $(V_x/a_{cr}^!)_2$ or $M_{1,h}$.

Although chart I and table I are presented for but three values of $(V_{\rm X}/a_{\rm cr}^{\rm r})_2$ and three values of $M_{\rm l,h}$, linear interpolations can be made in order to yield results for any desired limits of these two parameters, provided they lie within the range of values presented herein.

Use of Chart II and Table II

Recourse is made to chart II and table II only after it has been found from chart I or table I that a single stage cannot satisfactorily meet the turbine design requirements. That is, when the value of the stage-work parameter determined from chart I or table I remains too small even after exit whirl has been employed or higher selections of $(V_x/a_{cr}^i)_2$ or $M_{l,h}$ have been made or all three of these departures have been used, additional staging is necessary.

Once it has been found necessary to resort to a multistage turbine, the procedure is to select a Mach number limit and annular area ratio for the first stage. From the turbine design requirements, the parameters necessary for entry into chart II or table II are calculated from equations (Bl), (B4), (5), (6), (7), and (8). The entrance weight-flow parameter $\hat{\mathbf{w}}_1$ calculated from equation (6), along with the assigned value of Mach number \mathbf{M}_h , and the entrance blade-speed parameter calculated from equation (5), establish the hub-tip radius ratio which is read on figure 3. At this value of hub-tip radius ratio and for the assigned Mach number, the stage-work parameter can be read at the appropriate blade-speed parameter on chart II or table II for the even values of isentropic annular area ratio presented.

Chart II and table II are furnished with an additional parameter, the ratio of tangential velocities $-(V_{\rm u},1/V_{\rm u},2)_{\rm h}$, the manner of presentation of which is identical to that used for the stage-work parameter. The purpose of including this additional parameter is to provide a means of determining the magnitudes of $V_{\rm u},1,h$ and $V_{\rm u},2,h$, which are related to the stage-work parameter by equation (E1). The value of the ratio $-(V_{\rm u},1/V_{\rm u},2)_{\rm h}$ is read from chart II or table II at the location corresponding to that used in determining stage-work parameter.

In calculating the entrance-enthalpy parameter $-gJ\Delta h^{\,\prime}/T_1^{\,\prime}$ for stages other than the last, it is suggested that the value for the factor $-\Delta h^{\,\prime}$ be determined from the stage-work parameter read from chart II or table II at an isentropic annular area ratio of 1.0 if a diverging annulus is desired. If a straight annulus is desired, the value of stage-work parameter read at an isentropic annular area ratio of 0.8 is suggested.

From the entrance-enthalpy parameter and the turbine adiabatic efficiency, a loss factor $e^{J\Delta s/R}$ can be read directly from figure 4(b). Annular area ratio is again calculated from isentropic annular area ratio by equation (F6). Isentropic annular area ratios are selected so that the resulting values of A_2/A_1 (from eq. (F6)) encompass the desired annular area ratio. If chart II is to be used, a linear interpolation then yields the values of both stage-work parameter and ratio of tangential velocities corresponding to the desired annular area ratio.

If table II is to be used, the method of interpolation of the tables suggested in the previous section can be applied to both stage-work parameter and ratio of tangential velocities.

Once the first-stage design has been accomplished in this manner, examination should be made of

to ascertain whether or not one more stage will suffice. If this difference is too greatly in excess of the stage-work parameters obtainable from chart I or table I, design of an intermediate stage can be effected in the manner described in this section. Otherwise, chart I or table I furnishes the design of the last stage to complete the turbine design.

As in the case of chart I and table I, linear interpolation can be made to yield results for any Mach numbers between 0.6 and 0.8.

Discussion of Approximations Involved

In order to estimate the sensitivity of the method to the value of the ratio of specific heats k, equations (C18) and (C24) were solved with a value of 1.40 for k. The resulting values of isentropic annular area ratio and of exit weight-flow parameter differed from the corresponding values of k of 4/3 by less than 1/2 percent.

When a design is made to produce additional work by employing exit whirl (eqs. (10) and (11)), figure 2 is no longer exact because of the absence of a $(v_u/a_{\rm cr}^i)_{2,m}^2$ term in equation (C24). For a given value of exit weight-flow parameter, a solution of equation (C24) for hub-tip radius ratio in which a value of -400 feet per second for the exit whirl was used resulted in about 1/2-percent difference from the corresponding value of v_h/r_t as read from figure 2.

An additional approximation has been made because figure 3 is presented for an isentropic annular area ratio of 1.0 only. This approximation, which avoids much complication, is reasonable because a stage other than the last is generally designed with a diverging annulus.

At this point a word of caution is introduced: when the charts or tables indicate the necessity for a multistage turbine, a rise in static pressure across stators other than the first may result. This situation is most likely to occur at high values of entrance relative Mach number and low blade speeds. Elimination of such a static-pressure rise reduces either the work output or the weight-flow capacity of the turbine.

ILLUSTRATIVE EXAMPLES

Four examples illustrating in detail the use of this method are presented in this section. In three of the examples the charts have been used; whereas the tables have been used in the remaining example. Using either charts or tables yields the same results.

Example 1

Lightly loaded single-stage turbine. - In the first illustrative example the charts are used to determine some of the design characteristics of a lightly loaded single-stage turbine capable of satisfying the turbine design requirements of a typical contemporary jet engine.

Turbine design requirements

$$-\Delta h^{\dagger}/\theta_{c}^{\dagger} = 81.9 \text{ Btu/lb}$$

$$W \sqrt{\theta_{c}^{\dagger}}/A_{F}\delta_{c}^{\dagger} = 16.0 \text{ lb/(sec)(sq ft)}$$

$$U_{t}/\sqrt{\theta_{c}^{\dagger}} = 1200 \text{ ft/sec}$$

$$T_{l}^{\dagger} = 2060^{\circ} \text{ R}$$

$$p_{l}^{\dagger} = 11,000 \text{ lb/sq ft}$$

At sea level: $\theta_c^i = 1$, $\delta_c^i = 1$

Assigned variables

$$A_2/A_1 = 1.0$$

$$(V_{x}/a_{cr}^{t})_{2} = 0.5$$

$$M_{l,h} \leq 0.8$$

$$\eta = 0.9$$

$$k = 4/3$$

Calculation of parameters:

$$c_p = \frac{k}{k-1} \frac{R}{J} = 4 \frac{R}{J} = 0.2745 \text{ Btu/(lb)(}^{\circ}R)$$

$$T_2^* = 2060 - \frac{81.9}{0.2745} = 1761.6^{\circ} R$$

$$p_2^* = 11,000 \left[1 - \left(\frac{2060 - 1761.6}{0.9(2060)} \right) \right]^4 = 5456 \text{ lb/sq ft}$$

$$\rho_2^{t} = \frac{5456}{53.4(1761.6)} = 0.0580 \text{ lb/cu ft}$$

$$a_{cr,2}^{t} = \sqrt{2(\frac{4}{7}) 32.2(53.4)(1761.6)} = 44.3 \sqrt{1761.6}$$

= 1859 ft/sec

$$\frac{U_{\rm t}}{a_{\rm cr,2}^{\rm i}} = \frac{1200}{1859} = 0.646$$

$$\hat{w}_2 = \frac{16.0}{0.0580(1859)} = 0.148$$

$$\left(\frac{-gJ\Delta h^{\dagger}}{U_{t}^{2}}\right)_{req} = \frac{25,000(81.9)}{(1200)^{2}} = 1.422$$

If the charts indicate that a single stage is sufficient, the value of $-\Delta h^{\dagger}$ of 81.9 Btu per pound can be used in equation (8):

$$\frac{-gJ\Delta h!}{T_2!} = \frac{25,000(81.9)}{1761.6} = 1162 \text{ sq ft/(sec}^2)(^{\circ}R)$$

by equation (8)

From figure 2 at \hat{w}_2 = 0.148 and $(V_x/a_{cr}^i)_2$ = 0.5, the hub-tip radius ratio r_h/r_t = 0.818.

From figure 4(a) at -gJ\Deltah'/T_2' = 1162 sq ft/(sec^2)(OR) and η = 0.9, the loss factor $e^{J\Delta s/R}$ = 1.077.

Entry into chart. - Because the desired annular area ratio is 1.0, it is necessary to interpolate the stage-work parameters read from the charts of 0.9 and of 1.0 isentropic annular area ratio. Use is made of equation (F6) in calculating the corresponding area ratios:

Chart I(a)1
$$\begin{cases} \left(\frac{-gJ\Delta h^{\dagger}}{U_{t}^{2}}\right)_{I,V_{u,2}=0} = 1.435 & \text{at } \frac{A_{2}}{A_{1}} = 0.969 \\ \left(\frac{-gJ\Delta h^{\dagger}}{U_{t}^{2}}\right)_{I,V_{u,2}=0} = 1.390 & \text{at } \frac{A_{2}}{A_{1}} = 1.077 \end{cases}$$

Interpolation
$$\left(\frac{-gJ\Delta h^{t}}{U_{t}^{2}}\right)_{I,V_{u,2}=0} = 1.422$$
 at $\frac{A_{2}}{A_{1}} = 1.0$

Chart I(a)3
$$\begin{cases} \left(\frac{-gJ\Delta h^{i}}{U_{t}^{2}}\right)_{M,V_{u,2}=0} = 1.580 & \text{at } \frac{A_{2}}{A_{1}} = 0.969 \\ \left(\frac{-gJ\Delta h^{i}}{U_{t}^{2}}\right)_{M,V_{u,2}=0} = 1.538 & \text{at } \frac{A_{2}}{A_{1}} = 1.077 \end{cases}$$

Interpolation
$$\left(\frac{-gJ\Delta h^{\dagger}}{U_{t}^{2}}\right)_{M,V_{u,2}=0} = 1.568$$
 at $\frac{A_{2}}{A_{1}} = 1.0$

The two values of stage-work parameter interpolated for an annular area ratio of 1.0 show that $(-gJ\Delta h'/U_t^2)_{I,V_{u,Z}=0} = (-gJ\Delta h'/U_t^2)_{req}$

and $(-gJ\Delta h^{i}/U_{t}^{2})_{M,V_{u},2=0} > (-gJ\Delta h^{i}/U_{t}^{2})_{req}$. Hence, a single-stage turbine with zero change in the magnitude of relative velocity at the hub radius, zero exit whirl, and an entrance relative Mach number at the hub radius less than 0.8 can satisfy the turbine design requirements.

Example 2

Heavily loaded single-stage turbine. - The object of this example is to determine by means of the charts the effect upon some of the design characteristics of example 1 of increasing the work output required of the turbine while all other turbine design requirements are unaltered.

Turbine design requirements $-\Delta h^{t}/\theta_{c}^{t} = 100.0 \text{ Btu/lb}$ $A_{2}/A_{1} = 1.0$ $\forall \sqrt{\theta_{c}^{t}}/A_{F}\delta_{c}^{t} = 16.0 \text{ lb/(sec)(sq ft)}$ $U_{t}/\sqrt{\theta_{c}^{t}} = 1200 \text{ ft/sec}$ $T_{1}^{t} = 2060^{\circ} \text{ R}$ $p_{1}^{t} = 11,000 \text{ lb/sq ft}$ Assigned variables $A_{2}/A_{1} = 1.0$ $(\nabla_{x}/a_{cr}^{t})_{2} = 0.5$ $M_{1,h} \leq 0.8$ $\eta = 0.90$ k = 4/3At sea level: $\theta_{c}^{t} = 1, \delta_{c}^{t} = 1$ $c_{p} = 0.2745 \text{ Btu/(lb)(}^{\circ}\text{R)}$

Calculation of parameters:

$$T_2^* = 2060 - \frac{100.0}{0.2745} = 1696^{\circ} R$$
 by equation (3)

$$p_2^* = 11,000 \left[1 - \left(\frac{2060 - 1696}{0.9(2060)} \right) \right]^4 = 4590 \text{ lb/sq ft}$$
 by equation (4)

$$\rho_2^{t} = \frac{4590}{53.4(1696)} = 0.0507 \text{ lb/cu ft}$$
 by equation (B1)

$$a_{cr,2}^{\dagger} = 44.3 \sqrt{1696} = 1824 \text{ ft/sec}$$
 by equation (B4)

$$\frac{U_{t}}{a_{cr,2}^{*}} = \frac{1200}{1824} = 0.658$$
 by equation (5)

$$\hat{W}_2 = \frac{16.0}{0.0507(1824)} = 0.173$$
 by equation (6)

$$\frac{\left(\frac{-gJ\Delta h^{\dagger}}{U_{t}^{2}}\right)_{req}}{\left(\frac{25,000(100.0)}{(1200)^{2}}\right)} = 1.736$$
by equation (7)

From figure 2 at \hat{w}_2 = 0.173 and $(v_x/a_{cr}^*)_2$ = 0.5, the hub-tip radius ratio r_h/r_t = 0.783.

Entry into charts. -

$$\begin{cases} \left(\frac{-gJ\Delta h^{\dagger}}{U_{t}^{2}}\right)_{I,V_{u,2}=0} = 1.326 & \text{at } \left(\frac{A_{2}}{A_{1}}\right)_{s} = 0.9 \\ \left(\frac{-gJ\Delta h^{\dagger}}{U_{t}^{2}}\right)_{I,V_{u,2}=0} = 1.284 & \text{at } \left(\frac{A_{2}}{A_{1}}\right)_{s} = 1.0 \end{cases}$$

$$\begin{cases} \left(\frac{-gJ\Delta h^{\dagger}}{U_{t}^{2}}\right)_{I,V_{u,2}=0} = 1.475 & \text{at } \left(\frac{A_{2}}{A_{1}}\right)_{s} = 0.9 \\ \left(\frac{-gJ\Delta h^{\dagger}}{U_{t}^{2}}\right)_{M,V_{u,2}=0} = 1.436 & \text{at } \left(\frac{A_{2}}{A_{1}}\right)_{s} = 1.0 \end{cases}$$
Chart I(a)3

Although the preceding stage-work parameters are all less than the value of $(-gJ\Delta h^*/U_t^2)_{req}$, the deficiency can be made up either by designing for exit whirl or by selecting a higher value of the parameter $(V_x/a_{cr}^*)_2$. In this example, exit whirl will be added in order to illustrate the procedure; and if the resulting value of $V_{u,2}$ is not excessive, a single stage will suffice. Since it is sought to determine whether a single stage can supply the necessary work, the value of $-\Delta h^*$ to be used in equation (8) is 100.0 Btu per pound:

$$\frac{-gJ\Delta h^{t}}{T_{2}^{t}}$$
 = 25,000(100.0)/1696 = 1474 sq ft/(sec²)(OR)

by equation (8)

From figure 4(a) at $-gJ\Delta h^{\dagger}/T_2^{\dagger}=1474$ sq ft/(sec²)(°R) and $\eta=0.9$, $e^{J\Delta s/R}=1.10$. Hence, $(A_2/A_1)_s=0.9$ corresponds to $(A_2/A_1)=0.99$, and $(A_2/A_1)_s=1.0$ corresponds to $(A_2/A_1)=1.10$, by equation (F6). It is necessary to determine the magnitude of the tangential component of exit velocity for each case before it can be decided whether the turbine is limited by zero change in the magnitude of relative velocity or by Mach number. Interpolation of the stage-work parameter from the chart I(a)1 values at an annular area ratio of 1.0 yields $(-gJ\Delta h^{\dagger}/U_t^2)_{I,V_{U,2}=0}=1.322$. A similar interpolation of the corresponding parameters from chart I(a)3 yields $(-gJ\Delta h^{\dagger}/U_t^2)_{M,V_{U,2}=0}=1.471$.

The use of equation (10) gives for the design limited by zero change in the magnitude of relative velocity at the hub radius

$$\left(\frac{V_u}{U}\right)_{2,h} = -\frac{1}{2} \left(\frac{1}{0.783}\right)^2 (1.736-1.322) = -0.338$$

Application of equation (11) to the design limited by 0.8 entrance relative Mach number at the hub radius yields

$$\left(\frac{v_u}{U}\right)_{2,h} = -\left(\frac{1}{0.783}\right)^2 (1.736-1.471) = -0.432$$

Because a greater amount of exit whirl is needed for the latter design, the turbine design is limited by the 0.8 entrance relative Mach number. The tangential component of exit absolute velocity at the hub radius is

$$V_{u,2,h} = -0.432(0.783)(1200) = -406 \text{ ft/sec}$$

This amount of exit whirl is high; in fact the energy associated with this whirl is

$$\frac{V_{u,2,h}^2/2gJ}{-\Delta h^{t}}$$
 (100) = 3.3 percent

This amount of energy, which is usually a loss, could be reduced by selecting a higher value of $(v_x/a_{cr})_2$, because the higher value of stage-work parameter so obtained would necessitate less exit whirl.

Example 3

High-speed, high-weight-flow single-stage turbine. - The tables are next to be applied for determining some of the design characteristics of a high-speed high-weight-flow turbine such as might be used to drive a supersonic compressor.

Turbine design requirements	Assigned variables
$-\Delta h'/\theta_c' = 73.0 \text{ Btu/lb}$	$A_2/A_1 = 1.0$
$w \sqrt{\theta_c^t} / A_F \delta_c^t = 30.0 \text{ lb/(sec)(sq ft)}$	$(v_x/a_{cr}^t)_2 = ?$
$U_t / \sqrt{\theta_c^*} = 1400 \text{ ft/sec}$	$M_{l,h} \leq 0.8$
$T_1 = 1960^{\circ} R$	η = 0.85
p; = 8500 lb/sq ft	k = 4/3
At sea level: $\theta_{c}^{i} = 1$, $\delta_{c}^{i} = 1$	$c_p = 0.2745 \text{ Btu/(lb)(}^{\circ}\text{R)}$

Calculation of parameters:

$$T_2' = 1960 - \frac{73.0}{0.2745} = 1694^{\circ} R$$
 by equation (3)

$$p_2^t = 8500 \left[1 - \left(\frac{1960 - 1694}{0.85(1960)} \right) \right]^4 = 4242 \text{ lb/sq ft}$$
 by equation (4)

$$\rho_2^{\bullet} = \frac{4242}{53.4(1694)} = 0.0469 \text{ lb/cu ft}$$
 by equation (B1)

$$a_{cr,2}^{r} = 44.3 \sqrt{1694} = 1823 \text{ ft/sec}$$
 by equation (B4)

$$\frac{U_t}{a_{cr,2}} = \frac{1400}{1823} = 0.768$$
 by equation (5)

$$\hat{w}_2 = \frac{30.0}{0.0469(1823)} = 0.351$$
 by equation (6)

$$\frac{\left(\frac{-gJ\Delta h^{t}}{U_{t}^{2}}\right)_{req} = \frac{25,000(73.0)}{(1400)^{2}} = 0.931$$
 by equation (7)

For this case it is found necessary to choose a value of either 0.6 or 0.7 for $(V_x/a_{cr}^i)_2$, because the exit weight-flow parameter is so high that a value of 0.5 would yield a hub-tip radius ratio less than 0.5, which is the lowest value used in preparing the charts and tables. In this example, a value of 0.7 will be used for $(V_x/a_{cr}^i)_2$. From figure 2 at $\hat{v}_2 = 0.351$ and $(V_x/a_{cr}^i)_2 = 0.7$, the hub-tip radius ratio $v_1/v_2 = 0.614$.

Entry into tables. - Because $(V_x/a_{\rm cr}^i)_2 = 0.7$ is to be used, table I(c) will be employed. A cursory observation of table I(c) at $U_t/a_{\rm cr}^i, 2 = 0.76$ and 0.78 indicates that the stage-work parameters are sufficiently close to the value of $(-gJ\Delta h^i/U_t^2)_{\rm req}$ that a single-stage turbine will suffice; consequently, the value of $-\Delta h^i$ to be used in the exit-enthalpy parameter is 73.0 Btu per pound:

$$\frac{-gJ\Delta h^{t}}{T_{2}^{t}} = 0.931 \frac{(1400)^{2}}{1694} = 1077 \text{ sq ft/(sec}^{2})(^{\circ}R)$$

by equation (8)

From figure 4(a) at $-gJ\Delta h^{\dagger}/T_2^{\dagger}=1077$ sq ft/(sec²)(^{O}R) and $\eta=0.85$, the loss factor $e^{J\Delta s/R}=1.12$. Because an annular area ratio of 1.0 is desired, interpolation is necessary between isentropic annular area ratios of 0.8 and 0.9. The following values of $-gJ\Delta h^{\dagger}/U_t^2$ have been interpolated linearly from the tables for $r_h/r_t=0.614$.

			Table I(c)l	Table I(c)3
Ut air,2	$\left(\frac{A_2}{A_1}\right)_s$	$\frac{A_2}{A_1}$	$\left(\frac{-gJ\Delta h^{t}}{U_{t}^{2}}\right)_{I,V_{u,2}=0}$	$\left(\frac{-gJ\Delta h^{t}}{U_{t}^{2}}\right)_{M,V_{u,2}=0}$
0.76	0.8	0.896	0.97	0.96
	.9	1.008	.93	.92
0.78	0.8	0.896	0.96	0.95
	.9	1.008	.93	.91

Interpolated in the suggested manner for an annular area ratio of 1.0 and a blade-speed parameter of 0.768, the values of stage-work parameter are

$$\left(\frac{-gJ\Delta h^{t}}{U_{t}^{2}}\right)_{I,V_{u,2}=0} = 0.93$$

and

$$\left(\frac{-gJ\Delta h^{t}}{U_{t}^{2}}\right)_{M,V_{u,2}=0} = 0.92$$

From these results it can be seen that the turbine is limited by 0.8 relative entrance Mach number at the hub radius. A small amount of exit whirl can be used in order to produce the required stage-work parameter of 0.931.

Example 4

Multistage turbine. - Use of the charts is next extended to a multistage turbine, in order to show how the number of stages can be ascertained along with the division of work between the stages.

Turbine design requirements	Assigned variables
$-\Delta h^{\dagger}/\theta_{c}^{\dagger} = 130.0 \text{ Btu/lb}$	$A_2/A_1 = 1.0$
$w \sqrt{\theta_c^t}/A_F \delta_c^t = 25.0 lb/(sec)(sq ft)$	$\Delta \beta_{\rm h} \leq 120^{\rm O}$
$U_t / \sqrt{\theta_c^1} = 900 \text{ ft/sec}$	η = 0.85
$T_1^t = 2160^\circ R$	$M_{h} \leq 0.80$
$p_1^{!} = 17,000 \text{ lb/sq ft}$	$(v_{x}/a_{cr}^{t})_{2} = 0.70$
	k = 4/3
At sea level: $\theta_c^t = 1$, $\delta_c^t = 1$	$c_p = 0.2745 \text{ Btu/(lb)(}^{\circ}\text{R)}$

Calculation of parameters:

$$T_{2}^{r} = 2160 - \frac{130.0}{0.2745} = 1686^{\circ} R$$
 by equation (3)
$$p_{2}^{r} = 17,000 \left[1 - \left(\frac{2160 - 1686}{2160(0.85)} \right) \right]^{4} = 5160 \text{ lb/sq ft}$$
 by equation (4)
$$\rho_{2}^{r} = \frac{5160}{53.4(1686)} = 0.0575 \text{ lb/cu ft}$$
 by equation (B1)

Last

Last stage
$$a_{cr,2}^{i} = 44.3 \sqrt{1686} = 1818 \text{ ft/sec}$$
 by equation (B4)

$$\frac{U_{t}}{a_{cr,2}^{!}} = \frac{900}{1818} = 0.495$$
 by equation (5)

$$\hat{w}_2 = \frac{25.0}{0.0575(1818)} = 0.239$$
 by equation (6)

From figure 2 at $\hat{w}_2 = 0.239$ and $(v_x/a_{cr}^i)_2 = 0.7$, the hub-tip radius ratio $r_h/r_t = 0.759$.

$$\rho_1' = \frac{17,000}{53.4(2160)} = 0.1474 \text{ lb/cu ft} \qquad \text{by equation (Bl)}$$

$$a_{\text{cr,l}}' = 44.3 \sqrt{2160} = 2058 \text{ ft/sec} \qquad \text{by equation (B4)}$$

$$\frac{U_t}{a_{\text{cr,l}}'} = \frac{900}{2058} = 0.437 \qquad \text{by equation (5)}$$

$$\frac{\Lambda}{v_1} = \frac{25.0}{0.1474(2058)} = 0.0824 \qquad \text{by equation (6)}$$
From figure 3(b) at $M_h = 0.8$, $\frac{\Lambda}{v_1} = 0.0824$, and $U_t/a_{\text{cr,l}}' = 0.437$, the hub-tip radius ratio $r_h/r_t = 0.811$.

For the turbine, the over-all stage-work parameter required is

$$\left(\frac{-gJ\Delta h!}{U_t^2}\right)_{\text{req}} = \frac{25,000(130.0)}{(900)^2} = 4.015$$
 by equation (7)

Entry into charts. - Because a cursory examination of the stagework parameter in chart I reveals that a single stage cannot possibly suffice, a multistage turbine is required.

First stage:

Chart II(b)1
$$\begin{cases} \frac{-gJ\Delta h^{\dagger}}{U_{t}^{2}} = 2.865 & \text{at } \left(\frac{A_{2}}{A_{1}}\right)_{s} = 0.8\\ \frac{-gJ\Delta h^{\dagger}}{U_{t}^{2}} = 2.910 & \text{at } \left(\frac{A_{2}}{A_{1}}\right)_{s} = 1.0 \end{cases}$$

$$\begin{cases} \left(\frac{V_{u,1}}{V_{u,2}}\right)_{h} = -2.24 & \text{at } \left(\frac{A_{2}}{A_{1}}\right)_{s} = 0.8\\ \left(\frac{V_{u,1}}{V_{u,2}}\right)_{h} = -1.99 & \text{at } \left(\frac{A_{2}}{A_{1}}\right)_{s} = 1.0 \end{cases}$$
Chart II(b)2

Because an annular area ratio of 1.0 is desired, it is more nearly correct to use the value of $-\Delta h'$ obtained from $-gJ\Delta h'/U_t^2$ at an isentropic annular area ratio of 0.8. Hence,

$$\frac{-gJ\Delta h^{t}}{T_{1}^{t}} = 2.865 \frac{(900)^{2}}{2160} = 1074 \text{ sq ft/(sec}^{2})(^{\circ}R)$$

From figure 4(b) at $-gJ\Delta h^{\dagger}/T_1^{\dagger}=1074$ sq ft/(sec²)(^{O}R) and $\eta=0.85$, the loss factor $e^{J\Delta s/R}=1.142$. By equation (F6), $(A_2/A_1)_s=0.8$ and 1.0 correspond, respectively, to $A_2/A_1=0.914$ and 1.142 for the first stage. Therefore, interpolation for $A_2/A_1=1.0$ yields $-gJ\Delta h^{\dagger}/U_t^2=2.882$ and $(V_{u,1}/V_{u,2})_h=-2.130$. Sufficient information is now available for making the first-stage velocity diagram.

The value of the stage-work parameter required of the additional staging is

$$\left(\frac{-gJ\Delta h^{\dagger}}{U_{t}^{2}}\right)_{req} - \left(\frac{-gJ\Delta h^{\dagger}}{U_{t}^{2}}\right)_{lst stage} = 4.015 - 2.882 = 1.133$$

Entry into chart I will now indicate whether or not the remaining work requirement can be accomplished by one stage.

Last stage:

Chart I(c)1
$$\begin{cases} \left(\frac{-gJ\Delta h^{\dagger}}{U_{t}^{2}}\right)_{I,V_{u},2=0} = 1.426 & \text{at } \left(\frac{A_{2}}{A_{1}}\right)_{s} = 0.9 \\ \left(\frac{-gJ\Delta h^{\dagger}}{U_{t}^{2}}\right)_{I,V_{u},2=0} = 1.289 & \text{at } \left(\frac{A_{2}}{A_{1}}\right)_{s} = 1.0 \end{cases}$$

$$\begin{cases} \left(\frac{-gJ\Delta h^{\dagger}}{U_{t}^{2}}\right)_{M,V_{u},2=0} = 1.480 & \text{at } \left(\frac{A_{2}}{A_{1}}\right)_{s} = 0.9 \\ \left(\frac{-gJ\Delta h^{\dagger}}{U_{t}^{2}}\right)_{M,V_{u},2=0} = 1.353 & \text{at } \left(\frac{A_{2}}{A_{1}}\right)_{s} = 1.0 \end{cases}$$

Comparison of these values of stage-work parameter with the value 1.133 required of staging additional to the first indicates that one additional stage will suffice. Hence,

$$\frac{-gJ\Delta h^{t}}{T_{c}^{t}} = 1.133 \frac{(900)^{2}}{1686} = 544 \text{ sq ft/(sec}^{2})(^{\circ}R)$$

From figure 4(a) at $-gJ\Delta h^{t}/T_{2}^{t}=544$ sq ft/(sec²)(OR) and $\eta=0.85$, the loss factor $e^{J\Delta s/R}=1.058$. Use of equation (F6) and interpolation for $A_{2}/A_{1}=1.0$ yield

$$\left(\frac{-gJ\Delta h^{\dagger}}{U_{t}^{2}}\right)_{I,V_{u,2}=0} = 1.364 \text{ and } \left(\frac{-gJ\Delta h^{\dagger}}{U_{t}^{2}}\right)_{M,V_{u,2}=0} = 1.423$$

Since the values of these two parameters exceed the required value of stage-work parameter of 1.133, a two-stage turbine can meet the turbine design requirements. Lower values of $(v_u/u)_{1,h}$, of $(v_x/a_{cr}^i)_2$, or of $M_{1,h}$ can be employed in the second stage. The work division between the stages is 71.8 percent for the first stage and 28.2 percent for the second stage.

The occurrence of a static-pressure rise across the second stator is indeterminate until the manner of lowering the stage-work parameter to the required value of 1.133 has been selected, that is, whether $(V_u/U)_{1,h}$, $(V_x/a_{cr}^i)_2$, or $M_{1,h}$ is decreased. In any event, the choice of lowering the value of one of these parameters should be such that a static-pressure rise does not occur across the second stator. If the value of -gJ Δ h'/ U_t^2 required of the last stage were too greatly in excess of that obtainable from the designs of chart I to allow for a reasonably small amount of exit whirl, the charts would permit determining how many stages - three or four, for example - would be required.

CONCLUDING REMARKS

A method has been devised for the rapid determination of design characteristics of turbine stages within specified aerodynamic limits. For convenience, the information has been presented in two alternate forms, in charts and in tables. One set of charts and the corresponding set of tables are designed to pertain to a last turbine stage; the use of this set permits a determination of the proximity of a particular design to limits of zero change in the magnitude of relative velocity,

32

275

of specified entrance relative Mach number, and of exit whirl. A second set of charts and tables is designed for aiding in calculations involving a stage other than the last; Mach number and turning angle limits can be employed with this set. Using the two sets in combination makes possible the rapid determination of the number of turbine stages needed for a given application and a desirable work division among the stages. It is intended that this method be used primarily for the purpose of sketching out a turbine design with a minimum expenditure of time and effort. Based on the information so gained, a conventional detailed analysis can quickly be made with the expectation that the turbine design requirements can satisfactorily be met.

Lewis Flight Propulsion Laboratory
National Advisory Committee for Aeronautics
Cleveland, Ohio, December 9, 1952

APPENDIX A

SYMBOLS

The following list of symbols comprises those used in this paper:

A annular area, sq ft

turbine-tip frontal area, sq ft AF

sonic velocity, $\sqrt{\text{kgRT}}$, ft/sec a

 $\sqrt{\frac{2k}{k+1}}$ gRT', ft/sec a'cr

 $\sqrt{\frac{2k}{k+1}}$ gRT", ft/sec

specific heat at constant pressure, Btu/(lb)(OR) Cp

acceleration due to gravity, 32.2 ft/sec2 g

specific enthalpy, Btu/lb h

mechanical equivalent of heat, 778.2 ft-lb/Btu J

ratio of specific heats k

Mach number at hub radius when $M_{l,h} = M_{2,h}$ Mh

relative Mach number at hub radius (W/a)1,h M_{l,h}

absolute Mach number at hub radius (V/a)2.h M2,h

absolute pressure, lb/sq ft p

gas constant, 53.4 ft-lb/(lb)(OR) R

radius, ft r

 $r_h/r_m = 2(r_h/r_t)/(1 + r_h/r_t)$ r

entropy, Btu/(1b)(OR) S

absolute temperature, OR T

blade velocity, ft/sec U

V	absolute velocity of gas, ft/sec
W	relative velocity of gas, ft/sec
w	weight-flow rate of gas, lb/sec
ŵ	weight-flow parameter, w/AFp'acr
β	flow angle of relative velocity measured from tangential direction (fig. 1), deg
Δ	prefix to indicate change
δ	pressure-reduction ratio, p/2116
η	adiabatic efficiency
θ	temperature-reduction ratio, T/518.4
ρ	gas density, lb/cu ft
ω	angular velocity, radians/sec
Subscripts	:
С	compressor-inlet conditions
h	hub radius
I	limited by zero change in magnitude of relative velocity at hub radius
i	ideal
М	limited by entrance relative Mach number at hub radius
m	mean radius
req	required
s	isentropic
t	tip radius
u	tangential component
$V_{u,2} = 0$	without exit whirl
$v_{u,2} \neq 0$	with exit whirl

x	axial component
1	station upstream of rotor
2	station downstream of rotor
Supersc	ripts:

stagnation state relative to stator

" stagnation state relative to rotor

(B8)

APPENDIX B

THERMODYNAMIC RELATIONS USED THROUGHOUT ANALYSIS

The following general thermodynamic relations are used in the derivation of the charts, tables, and figures:

Equation of state:
$$p = \rho rt$$
 (B1)

Isentropic relation:
$$p\rho^{-k} = constant$$
 (B2)

Sonic velocity:
$$a = \sqrt{kgRT}$$
 (B3)

Absolute critical velocity:
$$a'_{cr} = \sqrt{\frac{2k}{k+1}} gRT'$$
 (B4)

Relative critical velocity:
$$a_{cr}'' = \sqrt{\frac{2k}{k+1}} gRT''$$
 (B5)

Free vortex:
$$rV_u = constant along a radial line$$
 (B6)

Free vortex and simplified radial equilibrium:

$$V_X$$
 = constant along a radial line (B7)

From velocity triangle:
$$V^2 = V_X^2 + V_u^2$$

$$W^2 = V_x^2 + (V_u - U)^2$$
 (B9)

$$\beta = \cot^{-1} \left(\frac{V_{u} - U}{V_{x}} \right)$$
 (Blo)

Absolute Mach number:
$$M_2 = \left(\frac{V}{a}\right)_2$$
 (B11)

Relative Mach number:
$$M_1 = \left(\frac{W}{a}\right)_1$$
 (B12)

Absolute stagnation temperature:
$$T' \equiv T + \frac{v^2}{2gJc_p}$$
 (B13)

Relative stagnation temperature:
$$T'' \equiv T + \frac{W^2}{2gJc_p}$$
 (B14)

Subtracting equation (Bl4) from (Bl3) and utilizing equations (B4), (B8), and (B9) yield

$$\frac{\mathbf{T''}}{\mathbf{T'}} = 1 - \frac{\mathbf{k-l}}{\mathbf{k+l}} \frac{\mathbf{U}}{\mathbf{a'_{cr}}} \left[2 \left(\frac{\mathbf{V_{u}}}{\mathbf{a'_{cr}}} \right) - \frac{\mathbf{U}}{\mathbf{a'_{cr}}} \right]$$
 (B15)

Equation (Bl3) can be restated with the use of equation (B3) as

$$\frac{T'}{T} = 1 + \frac{k-1}{2} \left(\frac{V}{a}\right)^2$$
 (B16)

Similarly, equation (Bl4) becomes

$$\frac{\mathbf{T''}}{\mathbf{T}} = 1 + \frac{\mathbf{k} - 1}{2} \left(\frac{\mathbf{W}}{\mathbf{a}} \right)^2 \tag{B17}$$

Equation (Bl3) can also be restated with the use of equations (B4) and (B8) as

$$\frac{T}{T'} = 1 - \frac{k-1}{k+1} \left(\frac{V_x}{a_{cr}^{\prime}} \right)^2 - \frac{k-1}{k+1} \left(\frac{V_u}{a_{cr}^{\prime}} \right)^2$$
(B18)

In like manner, (Bl4) can be rewritten by means of equations (B5), (B8), and (B9) as

$$\frac{T}{T''} = 1 - \frac{k-1}{k+1} \left(\frac{V_x}{a_{cr}''} \right)^2 - \frac{k-1}{k+1} \left(\frac{V_u}{a_{cr}''} - \frac{U}{a_{cr}''} \right)^2$$
 (B19)

APPENDIX C

DERIVATION OF EQUATIONS FOR CHART I, TABLE I, AND FIGURE 2 -

LAST STAGE OR SINGLE STAGE WITH ZERO EXIT WHIRL:

LIMITATION OF ZERO CHANGE IN MAGNITUDE OF

RELATIVE VELOCITY AT HUB RADIUS

The following four equations give the specifications for chart I,l and table I,l:

Work:

$$-\Delta h' = \left(\frac{r_1 V_{u,1} - r_2 V_{u,2}}{gJ}\right) \omega \tag{C1}$$

Zero change in magnitude of relative velocity across rotor at hub radius:

$$W_{1,h} = W_{2,h} \tag{C2}$$

Continuity at mean radius:

$$(\rho V_X A)_{\perp,m} = (\rho V_X A)_{2,m}$$
 (C3)

Zero exit whirl:

$$V_{u,2} = 0 \tag{C4}$$

In combining these equations, use is made of assumption (5), that is,

$$r_{1,h} = r_{2,h}$$
 $r_{1,m} = r_{2,m}$
(C5)

Equation (C1) combined with (C4) and (C5) yields

$$\left(\frac{-gJ\triangle h'}{U^2}\right)_{V_{u,2}=0} = \left(\frac{V_{u}}{U}\right)_{1}$$
(C6)

Combination of equation (C2) with (B9) yields

$$\left[\left(\frac{v_{u}}{U}\right)_{1,h} - 1\right]^{2} + \left(\frac{v_{x}}{U}\right)_{1,h}^{2} = \left[\left(\frac{v_{u}}{U}\right)_{2,h} - 1\right]^{2} + \left(\frac{v_{x}}{U}\right)_{2,h}^{2}$$
(C7)

Insertion of equations (C4) and (C5) into (C7) results in

$$\left[\left(\frac{\mathbf{v}_{\mathbf{u}}}{\mathbf{U}}\right)_{1,h} - 1\right]^{2} - 1 = \left(\frac{\mathbf{v}_{\mathbf{x}}}{\mathbf{a}_{cr}^{\dagger}}\right)_{2}^{2} \left(\frac{\mathbf{a}_{cr}^{\dagger}}{\mathbf{U}}\right)_{2,h}^{2} \left[1 - \left(\frac{\mathbf{v}_{\mathbf{x},1}}{\mathbf{v}_{\mathbf{x},2}}\right)^{2}\right]$$

which is solved for

$$\frac{\mathbf{v}_{x,1}}{\mathbf{v}_{x,2}} = \sqrt{1 + \left(\frac{\mathbf{u}}{\mathbf{a}_{cr}^{\dagger}}\right)^{2}_{2,h} \left(\frac{\mathbf{a}_{cr}^{\dagger}}{\mathbf{v}_{x}}\right)^{2}_{2} \left\{1 - \left[\left(\frac{\mathbf{v}_{u}}{\mathbf{u}}\right)_{1,h} - 1\right]^{2}\right\}}$$
(C8)

The continuity equation (C3) is next to be manipulated, with the use of equation (B1):

$$\frac{A_{2}V_{x,2}}{A_{1}V_{x,1}} = \left(\frac{\rho_{1}/\rho_{1}^{"}}{\rho_{2}/\rho_{2}^{"}} \frac{p_{1}^{"}/RT_{1}^{"}}{p_{2}^{"}/RT_{2}^{"}}\right)_{m}$$
(C9)

Relative to the blading, $T_{1,m}^{"} = T_{2,m}^{"}$. Therefore, equation (C9) becomes

$$\frac{A_2 V_{x,2}}{A_1 V_{x,1}} = \left(\frac{\rho_1 / \rho_1''}{\rho_2 / \rho_2''} \frac{p_1''}{p_2''}\right)_m \tag{C10}$$

which is

$$\frac{A_2}{A_1} \left(\frac{p_2''}{p_1''} \right)_{m} = \frac{V_{x,1}}{V_{x,2}} \left(\frac{\rho_1/\rho_1''}{\rho_2/\rho_2''} \right)_{m}$$
 (C11)

The left side of equation (Cll) is defined as the isentropic annular area ratio $(A_2/A_1)_s$, because, for constant entropy $(p_2''/p_1'')_m = 1$:

$$\left(\frac{A_{2}}{A_{1}}\right)_{s} \equiv \frac{A_{2}}{A_{1}} \left(\frac{p_{2}^{"}}{p_{1}^{"}}\right)_{m}$$
(C12)

Substitution of equations (B1), (B2), (B19), and (C12) transforms equation (C11) into

$$\left(\frac{A_{2}}{A_{1}}\right)_{s} = \frac{V_{x,1}}{V_{x,2}} \left\{ \frac{1 - \frac{k-1}{k+1} \left(\frac{V_{x}}{a_{cr}^{"}}\right)_{1}^{2} - \frac{k-1}{k+1} \left[\left(\frac{V_{u}}{a_{cr}^{"}}\right)_{1} - \left(\frac{U}{a_{cr}^{"}}\right)_{1}^{2}\right]^{2}}{1 - \frac{k-1}{k+1} \left(\frac{V_{x}}{a_{cr}^{"}}\right)_{2}^{2} - \frac{k-1}{k+1} \left[\left(\frac{V_{u}}{a_{cr}^{"}}\right)_{2} - \left(\frac{U}{a_{cr}^{"}}\right)_{2}^{2}\right]^{2}} \right\}_{m}^{L} (C13)$$

2754

which reduces to

$$\left(\frac{A_{2}}{A_{1}}\right)_{s} = \frac{V_{x,1}}{V_{x,2}} \left\{ \frac{1 - \frac{k-1}{k+1} \left(\frac{V_{x}}{a_{cr}^{"}}\right)_{1}^{2} - \frac{k-1}{k+1} \left[\left(\frac{V_{u}}{U}\right)_{1} - 1\right]^{2} \left(\frac{U}{a_{cr}^{"}}\right)_{1}^{2}}{1 - \frac{k-1}{k+1} \left(\frac{V_{x}}{a_{cr}^{"}}\right)_{2}^{2} - \frac{k-1}{k+1} \left(\frac{U}{a_{cr}^{"}}\right)_{2}^{2}} \right\}_{m}^{\frac{1}{k-1}} (C14)$$

by substitution of equation (C4). With the use of equations (B4) and (C10), equation (C14) becomes

$$\left(\frac{A_{2}}{A_{1}}\right)_{s} = \frac{V_{x,1}}{V_{x,2}} \left\{ \frac{\frac{k+1}{k-1} - \left(\frac{V_{x,1}}{V_{x,2}}\right)^{2} \left(\frac{V_{x}}{a_{cr}^{!}}\right)_{2}^{2} \left(\frac{T'}{T''}\right)_{2} - \left[\left(\frac{V_{u}}{U}\right)_{1} - 1\right]^{2} \left(\frac{U}{a_{cr}^{!}}\right)_{2}^{2} \left(\frac{T'}{T''}\right)_{2}}{\frac{k+1}{k-1} - \left(\frac{V_{x}}{a_{cr}^{!}}\right)_{2}^{2} \left(\frac{T'}{T''}\right)_{2} - \left(\frac{U}{a_{cr}^{!}}\right)_{2}^{2} \left(\frac{T'}{T''}\right)_{2}} \right\}_{m}^{\frac{1}{k-1}}$$
(C15)

Let

$$\bar{r} = \frac{r_h}{r_m} = \frac{2 \frac{r_h}{r_t}}{1 + \frac{r_h}{r_t}}$$
 (C16)

In accordance with assumption (5),

$$\overline{r}_1 = \overline{r}_2 = \overline{r}$$
 (C17)

Conversion of equation (Cl5) to a function of hub velocities with the aid of equations (B6), (B7), (B15), (Cl6), and (Cl7) yields

$$\left(\frac{A_{2}}{A_{1}}\right)_{s} = \frac{V_{x,1}}{V_{x,2}} \left\{ \frac{\frac{k+1}{k-1} + \left(\frac{U}{a_{cr}^{!}}\right)^{2}, h^{\left(\frac{1}{\overline{r}}\right)^{2}} \left\{1 - \left(\frac{V_{u}}{U}\right)_{1,h}^{\overline{r}^{2}} - 1\right]^{2} - \left(\frac{V_{x,1}}{V_{x,2}}\right)^{2} \left(\frac{V_{x}}{a_{cr}^{!}}\right)^{2}}{\frac{k+1}{k-1} - \left(\frac{V_{x}}{a_{cr}^{!}}\right)^{2}} \right\}^{\frac{1}{k-1}}$$

2754

(C18)

which finally becomes

$$\left(\frac{Az}{A_{1}}\right)_{s} = \frac{V_{x,1}}{V_{x,2}} \left\{ \frac{\frac{k+1}{k-1} + \left(\frac{U}{a_{cr}^{\prime}}\right)^{2}, h^{\left(\frac{V_{u}}{U}\right)_{1,h}} \left[2 - \left(\frac{V_{u}}{U}\right)_{1,h} \vec{r}^{2}\right] - \left(\frac{V_{x,1}}{V_{x,2}}\right)^{2} \left(\frac{V_{x}}{a_{cr}^{\prime}}\right)^{2}}{\frac{k+1}{k-1} - \left(\frac{V_{x}}{a_{cr}^{\prime}}\right)^{2}} \right\} \xrightarrow{\frac{1}{k-1}} \frac{1}{k-1} \left(\frac{V_{x}}{a_{cr}^{\prime}}\right)^{2} \left(\frac{V_{x}}{a_{cr}^{\prime$$

Solution of equation (C18) is completed upon insertion of (C8).

So that chart I can be presented in terms of blade-tip velocity, equation (C6) is altered by equation (B6) to read

$$\left(\frac{-gJ\triangle h'}{U_{t}^{2}}\right)_{V_{u,2}=0} = \left(\frac{V_{u}}{U}\right)_{1,h} \left(\frac{r_{h}}{r_{t}}\right)^{2} \tag{C19}$$

for the stage-work parameter.

Derivation of equation for exit weight-flow parameter (fig. 2). The exit weight-flow parameter is defined as

$$\hat{\mathbf{w}}_{2} = \frac{\mathbf{w}}{\mathbf{A}_{\mathbf{F}}(\rho^{\dagger}\mathbf{a}_{\mathbf{Cr}}^{\dagger})_{2}} \tag{C20}$$

where

$$W = (\rho AV_x)_{2,m}$$
 (C21)

Equations (C20) and (C21) can be combined to give

$$\hat{\mathbf{w}}_{2} = \left(\frac{\rho}{\rho'}\right)_{2,m} \left(\frac{\mathbf{v}_{x}}{\mathbf{a}_{cr}'}\right)_{2} \left[1 - \left(\frac{\mathbf{r}_{h}}{\mathbf{r}_{t}}\right)^{2}\right]$$
 (C22)

By means of equations (B2) and (B18), equation (C22) reads

$$\hat{\mathbf{w}}_{2} = \left[1 - \frac{\mathbf{k} - \mathbf{l}}{\mathbf{k} + \mathbf{l}} \left(\frac{\mathbf{v}_{x}}{\mathbf{a}_{cr}^{\dagger}}\right)_{2}^{2} - \frac{\mathbf{k} - \mathbf{l}}{\mathbf{k} + \mathbf{l}} \left(\frac{\mathbf{v}_{u}}{\mathbf{U}}\right)_{2}^{2} \left(\frac{\mathbf{U}}{\mathbf{a}_{cr}^{\dagger}}\right)_{2}^{2}\right]_{m}^{\frac{1}{\mathbf{k} - \mathbf{l}}} \left(\frac{\mathbf{v}_{x}}{\mathbf{a}_{cr}^{\dagger}}\right)_{2} \left[1 - \left(\frac{\mathbf{r}_{h}}{\mathbf{r}_{t}}\right)^{2}\right]$$
(C23)

Upon substitution of equation (C4), equation (C23) finally becomes

$$\hat{\mathbf{w}}_{2} = \left[1 - \frac{\mathbf{k} - 1}{\mathbf{k} + 1} \left(\frac{\mathbf{v}_{x}}{\mathbf{a}_{cr}^{\dagger}}\right)^{2}\right]^{\frac{1}{\mathbf{k} - 1}} \left(\frac{\mathbf{v}_{x}}{\mathbf{a}_{cr}^{\dagger}}\right)^{2} \left[1 - \left(\frac{\mathbf{r}_{h}}{\mathbf{r}_{t}}\right)^{2}\right]$$
(C24)

which is plotted directly in figure 2.

2754

APPENDIX D

DERIVATION OF EQUATIONS FOR CHART I, TABLE I, AND FIGURE 2 -

LAST STAGE OR SINGLE STAGE WITH ZERO EXIT WHIRL:

LIMITATION OF SPECIFIED ENTRANCE RELATIVE MACH

NUMBER AT HUB RADIUS

The specifications for chart I,2,3,4, table I,2,3,4, and figure 2 are established by equations (C1), (C3), and (C4) along with

$$M_{l,h} = \left(\frac{W}{a}\right)_{l,h}$$
 (D1)

Equation (B9) can be rewritten and applied at the hub inlet as

$$\left(\frac{\mathbf{W}}{\mathbf{U}}\right)_{1,h}^{2} = \left(\frac{\mathbf{V}_{\mathbf{X}}}{\mathbf{U}}\right)_{1,h}^{2} \quad \left[\left(\frac{\mathbf{V}_{\mathbf{U}}}{\mathbf{U}}\right)_{1,h} - 1\right]^{2} \tag{D2}$$

The term on the left side of equation (D2) can be expanded to

$$\left(\frac{\mathbf{W}}{\mathbf{U}}\right)_{1,h}^{2} = \left(\frac{\mathbf{W}}{\mathbf{a}}\right)_{1,h}^{2} \left(\frac{\mathbf{a}}{\mathbf{a}_{cr}^{\prime}}\right)_{1,h}^{2} \left(\frac{\mathbf{a}_{cr,1}^{\prime}}{\mathbf{a}_{cr,2}^{\prime}}\right)^{2} \left(\frac{\mathbf{a}_{cr}^{\prime}}{\mathbf{U}}\right)_{2,h}^{2}$$

which by equations (B3), (B4), (ClO), and (D1) can be written as

$$\left(\frac{\mathbf{W}}{\mathbf{U}}\right)_{1,h}^{2} = \frac{\mathbf{k+1}}{2} \, \mathbf{M}_{1,h}^{2} \left(\frac{\mathbf{T}}{\mathbf{T}''}\right)_{1,h} \left(\frac{\mathbf{T}''}{\mathbf{T}'}\right)_{2,h} \left(\frac{\mathbf{a}_{cr}^{*}}{\mathbf{U}}\right)_{2,h}^{2} \tag{D3}$$

Equation (D3) reduces to

$$\left(\frac{W}{U}\right)_{1,h}^{2} = \frac{k+1}{2} M_{1,h}^{2} \left[\frac{1 + \frac{k-1}{k+1} \left(\frac{U}{a_{cr}^{\prime}}\right)_{2,h}^{2}}{\left(\frac{U}{a_{cr}^{\prime}}\right)_{2,h}^{2} \left(1 + \frac{k-1}{2} M_{1,h}^{2}\right)} \right]$$
(D4)

by virtue of equations (B15) and (B16). Equating the right sides of equations (D2) and (D4) and solving for $V_{x,1}/V_{x,2}$ yield

$$\frac{v_{x,1}}{v_{x,2}}$$

$$= \left[\frac{\left(\frac{\mathbf{U}}{\mathbf{a}_{cr}^{\dagger}}\right)_{2,h}}{\left(\frac{\mathbf{V}_{x}}{\mathbf{a}_{cr}^{\dagger}}\right)_{2}} \right] \sqrt{\frac{\mathbf{k}+1}{2}} \, \mathbf{M}_{1,h}^{2} \left[\frac{1 + \frac{\mathbf{k}-1}{\mathbf{k}+1} \left(\frac{\mathbf{U}}{\mathbf{a}_{cr}^{\dagger}}\right)_{2,h}^{2}}{\left(\frac{\mathbf{U}}{\mathbf{a}_{cr}^{\dagger}}\right)_{2,h}^{2} \left(1 + \frac{\mathbf{k}-1}{2} \, \mathbf{M}_{1,h}^{2}\right)} - \left[\left(\frac{\mathbf{V}_{u}}{\mathbf{U}}\right)_{1,h}^{2} - 1\right]^{2}$$
(D5)

The isentropic annular area ratio $(A_2/A_1)_s$ can now be obtained by insertion of equation (D5) into (C18).

The stage-work parameter for this set is again calculated from equation (C19).

The ratio W_1/W_2 at the hub radius can be calculated by altering equation (D4) slightly. From this equation

Equation (B9) can be reduced by equation (C4) to

$$\left(\frac{W}{a_{cr}^{\dagger}}\right)_{2,h}^{2} = \left(\frac{U}{a_{cr}^{\dagger}}\right)_{2,h}^{2} + \left(\frac{V_{x}}{a_{cr}^{\dagger}}\right)_{2}^{2}$$
 (D7)

Substitution of equation (D7) into (D6) yields

$$\left(\frac{W_{1}}{W_{2}}\right)_{h}^{2} = \frac{k+1}{2} \left[\frac{M_{1,h}^{2}}{\left(\frac{U}{a_{cr}^{2}}\right)_{2,h}^{2} + \left(\frac{V_{x}}{a_{cr}^{2}}\right)_{2}^{2}} \right] \left[\frac{1 + \frac{k-1}{k+1} \left(\frac{U}{a_{cr}^{1}}\right)_{2,h}^{2}}{1 + \frac{k-1}{2} M_{1,h}^{2}} \right]$$
(D8)

This relation was used to plot the dotted lines on the set of chart ${\tt I}$ limited by Mach number.

Equation (C24) once again holds true for the exit weight-flow parameter.

DERIVATION OF EQUATIONS FOR CHART II, TABLE II, AND FIGURE 3 -

STAGE OTHER THAN LAST LIMITED BY HUB-RADIUS MACH NUMBERS

RELATIVE TO ROTOR ENTRANCE AND RELATIVE TO FOLLOWING

STATOR AND BY AMOUNT OF TURNING IN ROTOR

The work equation (C1) with the use of equation (C5) can be written

$$\frac{-gJ\triangle h'}{U^2} = \left(\frac{V_u}{U}\right)_1 - \left(\frac{V_u}{U}\right)_2$$
 (E1)

The specification on Mach number at the hub radius is

$$\left(\frac{W}{a}\right)_{l,h} = \left(\frac{V}{a}\right)_{2,h} = M_{h}$$
 (E2)

Once again, equation (C3) holds true.

Equation (E2) can be expanded by means of equation (B9) to

$$\left(\frac{V_{u}}{a} - \frac{U}{a}\right)_{1,h}^{2} + \left(\frac{V_{x}}{a}\right)_{1,h}^{2} = M_{h}^{2}$$
 (E3)

and by means of equation (B8) to

$$\left(\frac{V_{u}}{a}\right)_{2,h}^{2} + \left(\frac{V_{x}}{a}\right)_{2,h}^{2} = M_{h}^{2}$$
 (E4)

Expansion of equation (E3) yields

$$\left[\left(\frac{\mathbf{v}_{\mathbf{u}}}{\mathbf{U}}\right)_{1,h} - 1\right]^{2} \left(\frac{\mathbf{u}}{\mathbf{a}_{\mathbf{cr}}^{\prime}}\right)_{1,h}^{2} \left(\frac{\mathbf{a}_{\mathbf{cr}}^{\prime}}{\mathbf{a}}\right)_{1,h}^{2} + \left(\frac{\mathbf{v}_{\mathbf{x}}}{\mathbf{a}_{\mathbf{cr}}^{\prime}}\right)_{1}^{2} \left(\frac{\mathbf{a}_{\mathbf{cr}}^{\prime}}{\mathbf{a}}\right)_{1,h}^{2} = \mathbf{M}_{h}^{2}$$

which by equations (B3) and (B4) gives

$$\left[\left(\frac{\mathbf{V}_{\mathbf{u}}}{\mathbf{U}}\right)_{1,\mathbf{h}} - 1\right]^{2} \left(\frac{\mathbf{U}}{\mathbf{a}_{\mathbf{c}\mathbf{r}}^{\mathbf{t}}}\right)_{1,\mathbf{h}}^{2} + \left(\frac{\mathbf{V}_{\mathbf{x}}}{\mathbf{a}_{\mathbf{c}\mathbf{r}}^{\mathbf{t}}}\right)_{1}^{2} = \left(\frac{\mathbf{T}}{\mathbf{T}^{\mathbf{u}}}\right)_{1,\mathbf{h}} \left(\frac{\mathbf{T}^{\mathbf{u}}}{\mathbf{T}^{\mathbf{t}}}\right)_{1,\mathbf{h}} \mathbf{M}_{\mathbf{h}}^{2} \frac{\mathbf{k}+1}{2}$$

which in turn results in

$$\left[\left(\frac{v_{u}}{U}\right)_{1,h} - 1\right]^{2} \left(\frac{U}{a_{cr}^{\prime}}\right)_{1,h}^{2} + \left(\frac{v_{x}}{a_{cr}^{\prime}}\right)_{1}^{2}$$

$$= \frac{\frac{k+1}{2} M_{h}^{2}}{1 + \frac{k-1}{2} M_{h}^{2}} \left\{ 1 - \frac{k-1}{k+1} \left(\frac{U}{a \dot{c} r} \right)_{1,h}^{2} \left[2 \left(\frac{V_{u}}{U} \right)_{1,h} - 1 \right] \right\}$$
(E5)

In like manner, equation (E4) can be expressed as

$$\left(\frac{v_{u}}{v}\right)_{2,h}^{2} \left(\frac{v_{x,2}}{v_{x,1}}\right)_{1,h}^{2} + \left(\frac{v_{x,2}}{v_{x,1}}\right)^{2} \left(\frac{v_{x}}{v_{x,1}}\right)_{1}^{2} = \frac{k+1}{2} M_{h}^{2} \frac{T_{2}'}{T_{1}'} \left(\frac{T_{2}}{T_{2}'}\right)_{h}$$
(E6)

The work equation can be expressed in the form

$$\frac{k}{k-1} \frac{R}{J} T_{1}^{i} \left(1 - \frac{T_{2}^{i}}{T_{1}^{i}} \right) = \frac{U \left(V_{u,1} - V_{u,2} \right)}{gJ}$$
 (E7)

which in combination with equation (B4) yields

$$\frac{\mathbb{T}_{2}^{\prime}}{\mathbb{T}_{1}^{\prime}} = 1 - 2 \frac{k-1}{k+1} \left(\frac{\mathbb{U}}{a_{cr}^{\prime}} \right)_{1,h}^{2} \left[\left(\frac{\mathbb{V}_{u}}{\mathbb{U}} \right)_{1,h} - \left(\frac{\mathbb{V}_{u}}{\mathbb{U}} \right)_{2,h} \right]$$
(E8)

When equations (B16) and (E8) are substituted for the temperature-ratio factors, equation (E6) becomes

$$\left(\frac{\mathbf{v}_{\mathbf{u}}}{\mathbf{U}}\right)_{2,h}^{2} \left(\frac{\mathbf{U}}{\mathbf{a}_{cr}^{\dagger}}\right)_{1,h}^{2} + \left(\frac{\mathbf{v}_{\mathbf{x},2}}{\mathbf{v}_{\mathbf{x},1}}\right)^{2} \left(\frac{\mathbf{v}_{\mathbf{x}}}{\mathbf{a}_{cr}^{\dagger}}\right)_{1}^{2}$$

$$= \frac{\frac{\mathbf{k}+1}{2} M_{h}^{2}}{1 + \frac{\mathbf{k}-1}{2} M_{h}^{2}} \left\{1 - 2 \frac{\mathbf{k}-1}{\mathbf{k}+1} \left(\frac{\mathbf{U}}{\mathbf{a}_{cr}^{\dagger}}\right)_{1,h}^{2} \left(\frac{\mathbf{v}_{\mathbf{u}}}{\mathbf{U}}\right)_{1,h} - \left(\frac{\mathbf{v}_{\mathbf{u}}}{\mathbf{U}}\right)_{2,h}\right\} \tag{E9}$$

Equation (E9) can be solved for

$$\left(\frac{v_{x,2}}{v_{x,1}}\right)^2$$

$$= \frac{1}{\left(\frac{\mathbf{v}_{x}}{\mathbf{a}_{cr}^{\prime}}\right)^{2}} \left(\frac{\frac{\mathbf{k}+1}{2} \, \mathbf{M}_{h}^{2}}{1 + \frac{\mathbf{k}-1}{2} \, \mathbf{M}_{h}^{2}} \left\{1 - 2 \, \frac{\mathbf{k}-1}{\mathbf{k}+1} \left(\frac{\mathbf{u}}{\mathbf{a}_{cr}^{\prime}}\right)^{2}_{1,h} \left[\left(\frac{\mathbf{v}_{u}}{\mathbf{u}}\right)_{1,h} - \left(\frac{\mathbf{v}_{u}}{\mathbf{u}}\right)_{2,h}\right]\right\} - \left(\frac{\mathbf{u}}{\mathbf{a}_{cr}^{\prime}}\right)^{2}_{1,h} \left(\frac{\mathbf{v}_{u}}{\mathbf{u}}\right)^{2}_{2,h}\right)$$
(E10)

where the factor $(V_x/a_{cr}^i)_1^2$ is found by solving equation (E5) for

Thus, equation (E10) embodies the specification of equation (E2).

The equation for isentropic annular area ratio (eq. (C13)) once more applies and can be written as

(E12)

which is, by equations (B4) and (ClO)

$$\left(\frac{A_{2}}{A_{1}}\right)_{s} = \frac{V_{x,1}}{V_{x,2}} \left\{ \frac{\frac{k+1}{k-1} \left(\frac{T''}{T'}\right)_{1} - \left(\frac{V_{x}}{a_{cr}'}\right)_{1}^{2} - \left[\left(\frac{V_{u}}{U}\right)_{1} - 1\right]^{2} \left(\frac{U}{a_{cr}'}\right)_{1}^{2}}{\frac{k+1}{k-1} \left(\frac{T''}{T'}\right)_{1} - \left(\frac{V_{x,2}}{V_{x,1}}\right)^{2} \left(\frac{V_{x}}{a_{cr}'}\right)_{1}^{2} - \left[\left(\frac{V_{u}}{U}\right)_{2} - 1\right]^{2} \left(\frac{U}{a_{cr}'}\right)_{1}^{2}} \right\}_{m}^{\frac{1}{k-1}} \tag{E13}$$

By equations (B6), (B7), (B15), (C15), and (C16), this last equation (E13) is written in terms of hub velocities

$$\left(\frac{A_2}{A_1}\right)_s$$

$$= \frac{V_{x,1}}{V_{x,2}} \left\{ \frac{\frac{k+1}{k-1} - \left(\frac{V_{x}}{a_{cr}^{\prime}}\right)_{1}^{2} - \left(\frac{V_{u}}{U}\right)_{1,h}^{2} \left(\frac{U}{a_{cr}^{\prime}}\right)_{1,h}^{2}}{\frac{k+1}{k-1} - \left(\frac{U}{a_{cr}^{\prime}}\right)_{1,h}^{2} \left[2\left(\frac{V_{u}}{U}\right)_{1,h} + \left(\frac{V_{u}}{U}\right)_{2,h}^{2} - 2\left(\frac{V_{u}}{U}\right)_{2,h}^{2}\right] - \left(\frac{V_{x,2}}{V_{x,1}}\right)^{2} \left(\frac{V_{x}}{a_{cr}^{\prime}}\right)_{1}^{2}} \right\}^{\frac{1}{k-1}}$$
(E14)

From a consideration of the velocity diagram, the turning angle can be expressed as

$$\Delta \beta_{h} = \beta_{2,h} - \beta_{1,h} = -\cot^{-1} \left\{ \frac{\left[\left(\frac{V_{u}}{U} \right)_{1,h} - 1 \right] \left(\frac{U}{a_{cr}^{\dagger}} \right)_{1,h}}{\left(\frac{V_{x}}{a_{cr}^{\dagger}} \right)_{1}} \right\} - \cot^{-1} \left\{ \frac{\left[\left(\frac{V_{u}}{U} \right)_{2,h} - 1 \right] \left(\frac{U}{a_{cr}^{\dagger}} \right)_{1,h}}{\frac{V_{x,2}}{V_{x,1}} \left(\frac{V_{x}}{a_{cr}^{\dagger}} \right)_{1}} \right\}$$
(E15)

The stage-work parameter of equation (El) is expressed in terms of blade-tip velocity as

$$\frac{-gJ\Delta h'}{U_{t}^{2}} = \left[\left(\frac{V_{u}}{U} \right)_{1,h} - \left(\frac{V_{u}}{U} \right)_{2,h} \right] \left(\frac{r_{h}}{r_{t}} \right)^{2}$$
 (E16)

Derivation of equation for entrance weight-flow parameter (fig. 3). - The entrance weight-flow parameter is defined as

$$\widehat{\mathbf{w}}_{1} \equiv \frac{\mathbf{w}}{\mathbf{A}_{\mathbf{F}}(\rho' \mathbf{a}_{\mathbf{cr}}')_{1}}$$
 (E17)

where

$$w = (\rho AV_{x})_{1,m}$$
 (E18)

Combination of equations (E17) and (E18) yields

$$\widehat{\mathbf{w}}_{1} = \left(\frac{\rho}{\rho'}\right)_{1,m} \left(\frac{\mathbf{v}_{x}}{\mathbf{a}_{cr}'}\right)_{1} \left[1 - \left(\frac{\mathbf{r}_{h}}{\mathbf{r}_{t}}\right)^{2}\right] \tag{E19}$$

which by means of equations (B2) and (B18) becomes

$$\widehat{\mathbf{w}}_{1} = \left[1 - \frac{\mathbf{k} - \mathbf{l}}{\mathbf{k} + \mathbf{l}} \left(\frac{\mathbf{v}_{x}}{\mathbf{a}_{cr}^{!}}\right)_{1}^{2} - \frac{\mathbf{k} - \mathbf{l}}{\mathbf{k} + \mathbf{l}} \left(\frac{\mathbf{v}_{u}}{\mathbf{u}}\right)_{1}^{2} \left(\frac{\mathbf{u}}{\mathbf{a}_{cr}^{!}}\right)_{1}^{2}\right]_{m}^{\frac{1}{\mathbf{k} - \mathbf{l}}} \left[\mathbf{v}_{x} - \frac{\mathbf{v}_{x}}{\mathbf{a}_{cr}^{!}}\right]_{1}^{2}$$

(E20)

Equations (B6), (B7), (C16), and (C17) yield the final form of equation (E20) as

$$\widehat{\mathbf{w}}_{1} = \left\{ 1 - \frac{\mathbf{k} - 1}{\mathbf{k} + 1} \left[\left(\frac{\mathbf{v}_{x}}{\mathbf{a}_{cr}^{\dagger}} \right)_{1}^{2} + \left(\frac{\mathbf{v}_{u}}{\mathbf{U}} \right)_{1,h}^{2} \left(\frac{\mathbf{u}}{\mathbf{a}_{cr}^{\dagger}} \right)_{1,h}^{2} - \frac{\mathbf{z}}{\mathbf{r}^{2}} \right] \right\}^{\frac{1}{\mathbf{k} - 1}} \left(\frac{\mathbf{v}_{x}}{\mathbf{a}_{cr}^{\dagger}} \right)_{1} \left[1 - \left(\frac{\mathbf{r}_{h}}{\mathbf{r}_{t}} \right)^{2} \right]$$
(E21)

where the factor $(V_x/a'_{cr})_1$ is solved from equation (Ell). Equation (E21) is plotted in figure 3.

APPENDIX F

DERIVATION OF EQUATIONS FOR LOSS FACTOR OF FIGURE 4

General Relations

Loss through a turbine stage as a consequence of nonisentropic flow is shown by equation (Cll) to be contained in the stage relative stagnation-pressure ratio $(p_1''/p_2'')_m$. This factor can be expressed in terms of the entropy increase across the stage by

$$\triangle s = -\frac{R}{J} \ln \left(\frac{p_2''}{p_1''} \right)_m$$
 (F1)

in view of equation (ClO) at temperature level $T_{l,m}^{"}$. If isentropic expansion of flow through the turbine stage is assumed, an ideal exit stagnation pressure $p_{2,i}^{"}$ corresponding to the actual exit stagnation temperature would be realized instead of the actual exit stagnation pressure $p_{2}^{"}$. The same increase in entropy as shown in equation (F1) can be calculated as

$$\Delta s = -\frac{R}{J} \ln \frac{p_2'}{p_{2,i}'}$$
 (F2)

at temperature level T_2' . Equating equations (F1) and (F2) yields

Also

$$\begin{pmatrix} p_{1} \\ p_{2}^{"} \end{pmatrix}_{m} = e^{\frac{J \triangle s}{R}}$$
(F4)

by equation (F1).

The actual annular area ratio is thus

$$\frac{A_{2}}{A_{1}} = \frac{A_{2}}{A_{1}} \left(\frac{p_{2}^{"}}{p_{1}^{"}} \right)_{m} e^{\frac{J\Delta s}{R}}$$
(F5)

because the product of the second and third factors on the right side is unity (see eq. (F4)). By the definition of isentropic annular area ratio (eq. (C12)), equation (F5) becomes

$$\frac{A_2}{A_1} = \left(\frac{A_2}{A_1}\right)_S e^{\frac{J\Delta s}{R}}$$
 (F6)

The actual drop in enthalpy across a turbine stage per pound of gas flow is

$$-\Delta h' = c_p \left(T_L' - T_Z' \right) \tag{F7}$$

which in terms of the ideal exit stagnation pressure from the stage is

$$-\Delta h' = c_p T_{\perp}^{!} \left[1 - \left(\frac{p_{2,i}^{!}}{p_{\perp}^{!}} \right)^{\frac{k-1}{k}} \right]$$
 (F8)

upon application of equation (B2). Equation (F7) can also be expressed in terms of the actual stagnation-pressure ratio as

$$-\Delta h' = c_p T_l' \eta \left[1 - \left(\frac{p_2'}{p_l'} \right)^{\frac{k-1}{k}} \right]$$
 (F9)

in which η is the adiabatic efficiency.

Determination of Loss Factor for Use with Chart I and Table I

Because chart I and table I are presented in terms of the exit stagnation thermodynamic state relative to the stator, an exit-stage-enthalpy parameter is defined for use with this chart and table. This parameter is $-gJ\Delta h'/T_2'$. Equation (F9) can be modified to read

$$-\Delta h' = c_p T_2^i \eta \left[1 - \left(\frac{p_2^i}{p_1^i} \right)^{\frac{k-1}{k}} \right] \frac{T_1^i}{T_2^i}$$
 (F10)

The ratio T_1'/T_1' can be solved from equation (F7) as

$$\frac{T_1'}{T_2'} = 1 + \frac{k-1}{kgR} \frac{-gJ\Delta h'}{T_2'}$$
 (F11)

With the substitution of equation (F11) into (F10),

$$\frac{-gJ\triangle h'}{T'_{2}} = \frac{kgR}{k-1} \eta \left[1 - \left(\frac{p'_{2}}{p'_{1}} \right)^{\frac{k-1}{k}} \right] \left(1 + \frac{k-1}{kgR} - \frac{-gJ\triangle h'}{T'_{2}} \right)$$
 (F12)

which expression can be solved for

$$\left(\frac{p_{2}^{\prime}}{p_{1}^{\prime}}\right)^{k} = \frac{1 - \frac{k-1}{kgR} \frac{1-\eta}{\eta} \frac{-gJ\Delta h^{\prime}}{T_{2}^{\prime}}}{1 + \frac{k-1}{kgR} \frac{-gJ\Delta h^{\prime}}{T_{2}^{\prime}}}$$
(F13)

In the same manner that equation (F8) was obtained from equation (F7), expression (F7) can be written

$$-\Delta h' = c_p T_2' \left[\left(\frac{p_1'}{p_2', i} \right)^{\frac{k-1}{k}} - 1 \right]$$

which is easily altered to

$$\frac{-gJ\triangle h'}{T_{2}'} = \frac{kgR}{k-1} \left[\left(\frac{p_{1}'}{p_{2}'} \right)^{\frac{k-1}{k}} \left(\frac{p_{2}'}{p_{2,1}'} \right)^{\frac{k-1}{k}} - 1 \right]$$
 (F14)

Equation (F14) becomes expanded to

$$\frac{-gJ\Delta h'}{T_{2}'} = \frac{kgR}{k-1} \left(\frac{1 + \frac{k-1}{kgR} \frac{-gJ\Delta h'}{T_{2}'}}{1 - \frac{k-1}{kgR} \frac{1-\eta}{\eta} \frac{-gJ\Delta h'}{T_{2}'}} e^{-\frac{k-1}{k} \frac{J\Delta s}{R}} - 1 \right)$$
(F15)

upon insertion of equations (F3), (F4), and (F13). Finally, equation (F15) is solved for the loss factor:

$$e^{\frac{J\triangle s}{R}} = \left(1 - \frac{k-1}{kgR} \frac{1-\eta}{\eta} \frac{-gJ\triangle h'}{T_2'}\right)^{-\frac{k}{k-1}}$$
(F16)

The relation expressed by equation (F16) is plotted in figure 4(a) for a range of adiabatic efficiencies from 0.75 to 1.00.

The actual annular area ratio is calculated from equation (F6) with the value of the loss factor obtained from figure 4(a).

Determination of Loss Factor for Use With

Chart II and Table II

Since chart II and table II are presented in terms of the entrance stagnation state relative to the stator, an entrance stage-enthalpy parameter $-gJ\triangle h'/T_1'$ is defined for use in the determination of the loss factor. This parameter is assembled from equation (F8) as

$$\frac{-gJ\Delta h'}{T'_{1}} = \frac{kgR}{k-1} \left[1 - \left(\frac{p'_{2}, i}{p'_{2}}\right)^{\frac{k-1}{k}} \left(\frac{p'_{2}}{p'_{1}}\right)^{\frac{k-1}{k}} \right]$$
 (F17)

from the relation $c_p = \frac{k}{k-1} \frac{R}{J}$. The actual stagnation-pressure ratio across the stage can be calculated from equation (F9), in which the adiabatic efficiency is defined:

$$\frac{p_{2}^{\prime}}{p_{1}^{\prime}} = \left(1 - \frac{k-1}{kgR} \frac{1}{\eta} \frac{-gJ\triangle h^{\prime}}{T_{1}^{\prime}}\right)^{\frac{k}{k-1}}$$
(F18)

Insertion of equation (F18) into (F17) yields

$$\frac{-gJ\triangle h'}{T_{\perp}^{\prime}} = \frac{kgR}{k-1} \left[1 - e^{\frac{k-1}{k}} \frac{J\triangle s}{R} \left(1 - \frac{k-1}{kgR} \frac{1}{\eta} \frac{-gJ\triangle h'}{T_{\perp}^{\prime}} \right) \right]$$
 (F19)

with the aid of equations (F3) and (F4). This last expression is finally solved for the loss factor:

$$e^{\frac{J\Delta s}{R}} = \begin{bmatrix} \frac{-gJ\Delta h^{\dagger}}{T_{1}^{\dagger}} - \frac{kgR}{k-1} \\ \frac{1}{\eta} \left(\frac{-gJ\Delta h^{\dagger}}{T_{1}^{\dagger}} \right) - \frac{kgR}{k-1} \end{bmatrix}^{\frac{k}{k-1}}$$
(F20)

The relation expressed by equation (F20) is plotted in figure 4(b) for a range of adiabatic efficiencies from 0.75 to 1.00.

The actual annular area ratio is calculated from equation (F6) with the value of loss factor obtained from figure 4(b).

REFERENCE

1. Alpert, Sumner, and Litrenta, Rose M.: Construction and Use of Charts in Design Studies of Gas Turbines. NACA TN 2402, 1951.

TABLE I. - LAST STAGE OR SINGLE STAGE WITH ZERO EXIT WHIRL (a) Exit axial velocity ratio $(V_X/a_{\rm cr}^i)_2 = 0.5$.

- 1. Limitation of zero change in magnitude of relative relative to rotor at velocity across hub radius.

 2. Limitation of 0.6 entrance Mach number relative to rotor at hub radius.

 3. Limitation of 0.8 entrance Mach number relative to rotor at hub radius.

Pult blod-	Tantant		adius		namet	en				g.	1900-4	ork n	aramet	ter	(-g.TA	р₁/π2)				
speed parameter,	Isentropic annular area ratio,	(-	ge-wor gJΔh',	/Ut) I	, Vu.2	=0				5	vake-W	ork pa	ar-ame	oct,	-80A	· / Ut	M, Vu,	2=0			
Ut/adr,2	(A2/A1)8				-,-							atio,									
		0.5	0.6	0.7	0.8	0.9	0.5	0.6			0.9		0.6		0.8	0.9	0.5	0.6	0.7	0.8	0.
0.40	0.8	0.74	0.98	1.25	1.55	1.88	0.89		1.38			1.16	1.46	1.74	2.07	2.40	1.40	1.73	2.07	2.43	2.
	1.0 1.1	.67		1.05	1.46	1.79 1.65 1.48	.84 .76	.97	1.29 1.20 1.07		1.72	1.07	1.41 1.35 1.27	1.61	1.92	2.21	1.32	1.63	2.02 1.95 1.86	2.27	12.
0.42	0.8	0.73	0.96	1.23	1.53	1.87	0.86	1.10	1.33	1.61	1.88	1.11	1.41	1.68	2.01	2.32	1.34	1.66	2.00	2.35	2.
	1.0 1.1	.66	.89 .79 .61	1.05	1.34	1.78 1.65 1.50	.81 .74 .65	.95	1.26 1.18 1.05	1.42	1.68	1.04	1.37 1.31 1.23	1.56	1.87	2.15	1.27	1.57	1.88	2.20	2.
0.44	0.8	0.71	0.95	1.22	1.51	1.85	0.83	1.07	1.30	1.57	1.84	1.08	1.36	1.63	1.95	2.26	1.29	1.61	1.93	2.28	2
	1.0 1.1	.57	.79	1.05	1.34	1.65	.72	.93	1.15	1.39	1.65	1.00	1.27	1.52	1.82	2.10	1.22	1.52	1.82	2.14	2
0.46	0.8		0.93	1.20	1.50	1.83	0.81		1.27				1.32						1.87		
	1.0 1.1	.65 .56	.79	1.05	1.34	1.76 1.65 1.53	.77 .71 .63	.91	1.21 1.13 1.02	1.37	1.63	.97	1.28 1.23 1.16	1,48	1.77	2.05	1.19	1.48	1.77	2.08	2
0.48	0.8		0.92	1.19	1.49	1.82	0.79	1.01	1.24	1.50	1.77	1.01	1.28	1.54	1.85	2.15	1.21	1.51	1.82	2.15	2.
	.9 1.0 1.1	.64 .56 .43	.87 .79 .67	1.05	1.34	1.75 1.65 1.54	.75 .69	.89	1.18	1.35	1.60	.95	1.24 1.20 1.13	1.44	1.73	2.01	1.15	1.43	1.78 1.72 1.66	2.03	2
0.50	0.8		0.91	1.18	1.48	1.81	-	0.98	1.21	1.47	1.74	0.99	1.24	1.50	1.80	2.10	1.18	1.47	1.77	2.09	2
	1.0	.63 .56 .45	.86	1.12	1.42	1.74 1.65 1.55	.73 .68	.94	1.16 1.09 1.00	1.41	1.67	.92	1.21 1.17 1.11	1.41	1.69	1.97	1.12	1.40	1.73 1.68 1.62	1.98	2
0.52	0.8		0.90				-		1.19			0.96	1.21	1.47	1.76	2.06	1.14	1.43	1.72	2.03	2
0.05	.9 1.0 1.1	.63 .56	.85	1.12	1.41	1.73 1.65 1.56	.72 .67	.92	1.14	1.38	1.64	.93	1.18 1.14 1.08	1.44	1.71	2.00	1.12	1.39	1.69 1.64 1.58	1.99	2
0.54	0.8			-		1.78			1.17			0.93	1.18	1.44	1.72	2.02	1.11	1.39	1.68	1.99	2
0.04	1.0	.62	.85	1.11	1.40	1.73	.70	.90	1.12	1.36	1.62	.91	1.15	1.41	1.68	1.97	1.09	1.36	1.65	1.95	2
	1.1	.47	.70	.96	1.25	1.57	.59	.78	.98	1.21	1.44	.84	1.06	1.30	1.55	1.82			1.55		
0.56	0.8	0.65				1.77	0.72		1.15			.89	1.15	1.38	1.64	1.93	1.06	1.33	1.64	1.91	2
	1.0	.56	.79	1.05	1.34	1.65	.64	.83	1.05	1.28	1.52	.86	1.09	1.33	1.59	1.87	1.04	1.30	1.57	1.85	5
0.58	0.8	0.65	0.87	1.14	1.44	1.77	0.70	0.91	1.13	1.37	1.63		1.12						1.61		
	1.0 1.1	.61 .56 .49	.79	1.05	1.34	1.72 1.65 1.58	.67 .63 .57	.82	1.09	1.32	1.51	.84	1.10	1.31	1.56	1.84	1.01	1.27	1.58 1.54 1.49	1.82	2
0.60	0.8	0.64	0.87	1.13	1.43	1.76	0.69		1.11			0.87	1.10	1.35	1.62	1.91	1.03	1.30	1.58	1.87	2
	1.0 1.1	.61 .56	.83 .79	1.05	1.34	1.71 1.65 1.59	.66 .62	.85	1.07	1.25	1.49	.82	1.08 1.05 1.01	1.29	1.54	1.82	.99	1:24	1.55 1.51 1.46	1.79	2
0.62	0.8	0.63	0.86	1.12	1.43	1.75	0.68	0.88	1.09	1.33	1.59	0.85	1.08	1.33	1.60	1.88	1.00	1.27	1.54	1.83	2
	1.0 1.1	.60 .56	.83 .79 .73	1.04	1.34	1.71 1.65 1.59	.65 .62	.84 .80 .75	1.01	1.29 1.24 1.17	1.48	.83 .81 .78	1.06 1.03 .99	1.26	1.52	1.79	.97	1.22	1.51 1.48 1.44	1.76	5
0.64	0.8	0.63	0.85	1.12	1.42	1.75	0.67	0.86	1.08	1.31	1.57	0.83	1.06	1.31	1.57	1.86	0.98	1.24	1.51	1.80	2
	1.0	.60	.79	1.04	1.34	1.70	.64 .61 .56		1.04		1.52	.82 .80	1.04	1.28	1.50	1.77	.95	1.20	1.48 1.45 1.41	1.73	5
0.66	0.8	0.62		-	-	1.60	0.65		1.06		_		1.04	_		-			1.48		+-
0.00	.9	.60	.82	1.08	1.38	1.70	.63	.82	1.03	1.26	1.51	.80	1.03	1.26	1.52	1.79	.95	1.20	1.46	1.74	1
	1.1	.51	.74	1.00	1.28	1.60	.55	.74	.93	1.15	1.39	.75	.96	1.19	1.43	1.69	.91	1.14	1.39	1.66	1
0.68	0.8	0.62	0.84	1.11	1.41	1.73	0.64	.81	1.05	1.25	1.49	.79	1.03	1.24	1.50	1.77	.93	1.17	1.46	1.71	2
	1.0	.56	.79	1.04	1.33	1.65	.59 .55	.77	.98	1.20	1.44	.77	.98	1.21	1.46	1.73	.91	1.15	1.41	1.68	1
0.70	0.8					1.73	0.63	0.83	1.04	1.27	1.52		1.01	1.25	1.50	1.78			1.43		
	1.0 1.1	.59 .56	.78	1.04	1.33	1.70 1.65 1.61	.61 .58 .54	.80 .77 .73	1.01	1.23	1.43	.77 .75 .73	.97	1.19	1.44	1.71	.89	1.13	1.38	1.65	1
0.72	0.8	0.61	0.84	1.10	1.40	1.72	0.62	0.82	1.02	1.25	1.50	0.77	0.99	1.23	1.48	1.76	0.91	1.15	1.41	1.69	1
	1.0	.59	.78	1.04	1.33	1.69	.60	.76	1.00	1.18	1.42	.76	.95	1.21	1.43	1.69	.88	1.11	1.39	1.63	1.
	1.1	.52	.75	1.00	1.29	1.61	.54	.72	1.01	1.13		.72	.93	1.15					1.33	-	+-
0.74	0.8	.58	.81	1.07	1.37	1.72	0.62	.79	.99	1.21	1.46	.75	.96	1.19	1.44	1.71	.88	1.11	1.37	1.64	1
	1.0	.56	.75	1.01	1.30	1.65	.57	.75	.91	1.17	1.36	.73	.91	1.17	1.37	1.63	.85	1.07	1.32	1.57	1.
0.76	0.8	0.60	.81	1.07	1.36	1.72	.59	0.80	1.00	1.20	1.44	.74	0.96	1.18	1.43	1.69	.86	1.10	1.37	1.62	1
	1.0	.56	.78	1.04	1.33	1.65	.56	.74	.95	1.16	1.40	.72	.93	1.15	1.40	1.66	.85	1.08	1.32	1.59	1
0.78	0.8	0.60	0.82	1.09	1.38	1.71	0.60	0.79	0.99	1.22	1.46	0.74	0.95	1.18	1.43	1.70	0.86	1.09	1.35	1.61	1.
	1.0	.58	.78	1.04	1.33	1.65	.58	.74	.94	1.19	1.40	.72	.91	1.16 1.14 1.11	1.38	1.64	.84	1.06	1.31	1.57	1.
0.80	0.8	0.60	0.82	1.08	1.38	1.62	0.59		0.98	1.21	1.45	0.73	0.94	1.17	1.41	1.68	0.85	1.08	1.33	1.59	1.
	.9	.58	.80	1.07	1.36	1.68	.58	.77	.96	1.18	1.42	.71	.92	1.15	1.39	1.66	.84	1.07	1.31	1.58	1.
	1.1	.53	.75	1.01	1.30	1.62	.52	.70	.90	1.11	1.35	.68	.88	1.10	1.33	1.63 1.59	.81	1.03	1.27	1.52	1.

TABLE I. - LAST STAGE OR SINGLE STAGE WITH ZERO EXIT WHIRL - Continued (b) Exit axial velocity ratio $(V_{x}/a_{cr}^{i})_{2} = 0.6$.

- 1. Limitation of zero change in magnitude of relative relative to rotor at hub radius.

 2. Limitation of 0.6 antrance Mach number that of relative to rotor at hub radius.

 3. Limitation of 0.8 entrance Mach number relative to rotor at hub radius.

 4. Limitation of 1.0 entrance Mach number relative to rotor at hub radius.

N	r	eloci otor adius	at hu			hub radius. hub radius. Stage-work parameter, $(-gJ\Delta h^1/U_{\overline{b}}^2)$											hub radius.					
Exit blade- speed parameter,	annular area ratio,	Sta (-	ge-wo gJ∆h¹	rk pa	ramet	er, =0									(-gJΔ	h'/σ²)	M, Vu,	2=0				
Ut/acr,2	(A ₂ /A ₁) ₈							H	lub-ti	lp rad	ius r	atio,	rh/rt									
		0.5	0.6	0.7	0.8	0.9	0.5	0.6	0.7	0.8	0.9	0.5	0.6	0.7	0.8	0.9	0.5	0.6	0.7	0.8	0.	
0.40	0.8	.74	.83	1.24	1.54	1.85	0.83 .74 .60	.95	1.00	1.41	1.68	1.06		1.59	1.89	2.18	1.31	1.61	2.00 1.92 1.81	2.09	2.	
0.42	0.8	.73	1.05	1.33	1.63	1.84	0.80	.93	1.26	1.52	1.65	1.07	1.36 1.28	1.63 1.55	1.93	2.23	1.31	1.62	1.65 1.93 1.86	2.27	2.	
0.44	0.8		1.03	1.30	1.13	1.44	0.78		1.23	1.48	1.07	1.04	1.20 1.06	1.29	1.53	2.18	1.11	1.36	1.76 1.61	2.20	2.	
0.46	.9 1.0 1.1	.71	.95 .83 .57	1.08	1.37	1.46	.70	.91	1.13	.85	1.44	.92	1.24	1.41	1.67	1.94	1.16	1.43	1.80 1.71 1.58	1.99	2.	
0.40	1.0	.70	.94	1.20	1.49	1.81	0.76 .69 .58	.89	1.20 1.11 .97 .65	1.34	1.59	.96	1.28 1.21 1.13 1.02	1.46	1.75	2.03	1.18	1.46	1.82 1.75 1.66 1.55	2.05	2.	
0.48	0.8 .9 1.0 1.1	0.76 .69 .60	.93	1.27 1.19 1.08	1.48	1.80	0.74 .68 .57	0.95 .87 .75	1.17 1.09 .96	1.32	1.57	,93	1.24 1.18 1.10 1.00	1.43	1.71	1.98	1.18 1.14 1.09	1.47 1.42 1.36	1.77	2.09 2.00 1.90	2.2.	
0.50	0.8 .9 1.0	0.75 .69 .60	.92	1.25 1.18 1.08	1.55 1.47 1.36	1.88	0.72 .66 .56	.86		1.40 1.30 1.17	1.65 1.55 1.41	0.95 .91 .86	1.20 1.15 1.08	1.46 1.40 1.32	1.74 1.67 1.57	2.03 1.95 1.84	1.15 1.11 1.06	1.43 1.38 1.32	1.72 1.66 1.58	2.03 1.96 1.86	2.2.	
0.52	0.8 .9 1.0	0.73 .68 .60	0.97	1.24 1.17 1.08	1.54 1.46 1.36	1.86 1.78 1.67	0.71 .65 .56	0.91 .84 .74	1.13 1.06 .95	1.37 1.28 1.17	1.40	.89	1.17 1.12 1.06	1.37	1.70 1.64 1.55	1.99 1.91 1.81	1.11 1.08 1.04	1.39 1.35 1.29	1.49 1.68 1.63 1.55	1.98 1.91 1.82	2.	
0.54	0.8 .9 1.0	0.72 .67 .60	0.96	1.23 1.16 1.08	1.52 1.45 1.36	1.67	0.69 .64 .55	0.90 .83 .74	1.11 1.04 .94	1.35 1.27 1.16	1.52	.87	1.14 1.09 1.04	1.34	1.67 1.61 1.52	1.96 1.88 1.79	1.08 1.06 1.01	1.36 1.32 1.27	1.46 1.64 1.59 1.52	1.71 1.94 1.87 1.79	2.	
0.56	1.1 0.8 .9 1.0	0.71 .66 .59	0.95	1.21 1.15	1.24	1.54 1.84 1.77	0.68 .63 .55	.53	.75 1.09 1.03 .93	.98 1.33 1.25	1.21	.75 0.89 .85	.96	1.18 1.37 1.32	1.42 1.64 1.58	1.66 1.93 1.85	1.06	1.19 1.33 1.28	1.44 1.60 1.55	1.69	2.	
0.58	1.1 0.8 .9 1.0	0.70 .66 .59	.70 0.94 .89	1.20 1.15	1.25	1.55 1.83 1.76	0.67 .62 .54	0.86 .81 .72	.77	1.31 1.24	1.22	.74 0.87 .83	1.09	1.17	1.41	1.65 1.89 1.83	1.03	1.17	1.41 1.57 1.52	1.66	2.	
0.60	0.8	0.70 .65	0.93	1.19 1.14	1.49 1.43	1.56 1.82 1.75	0.66 .61	.56 0.85 .80	1.06 1.00	1.00 1.30 1.23	1.23 1.55 1.48	.73 0.85 .82	.93 1.07 1.03	1.15 1.32 1.28	1.58 1.53	1.64 1.86 1.80	1.01 .98	1.15 1.27 1.23	1.39 1.54 1.50	1.64 1.82 1.77	2.	
0.62	1.0 1.1 0.8 .9	.59 .49 0.69	0.92		1.48	1.57	.54 .38 0.64 .60	.72 .58	1.05		1.24	.77 .72 0.83 .80	.92	1.22	1.38	1.62	0.98	1.13	1.44 1.37 1.51 1.47	1.62	2.	
0.64	1.0	.59	.82	1.08	1.36		.54	.79 .72 .59	.92		1.37	.76	.97	1.20	1.44	1.70	.93	1.17	1.42 1.35	1.68	1.	
	.9 1.0 1.1	.64 .59	.87	1.13 1.08 1.00	1.42	1.74	.59 .53 .41	.78 .71 .60	.98	1.21 1.13 1.02	1.45		1.00		1.48	1.76	.94	1.19	1.44 1.40 1.33	1.72	2.	
0.66	0.8 .9 1.0 1.1	0.67 .64 .59	.87		1.42	1.79 1.74 1.67 1.59	0.62 .59 .53	0.81 .77 .71 .60	.97	1.25 1.20 1.12 1.02	1.44	0.80 .77 .74 .69	.94	1.22	1.47	1.74	.92	1.16	1.46 1.42 1.38 1.32	1.69	1	
0.68	0.8 .9 1.0 1.1	0.67 .63 .59	0.90 .86 .82	1.16 1.12 1.07 1.01	1.46 1.41 1.36	1.78 1.73 1.67	0.62 .58 .53 .43	0.80	1.01 .97 .90	1.24 1.19 1.12 1.03	1.48 1.43 1.35	0.78 .76 .72	1.00 .97 .93	1.23 1.20 1.16 1.10	1.49 1.45 1.40	1.76 1.72 1.65	0.92	1.17	1.43 1.40 1.36 1.30	1.71	1	
0.70	0.8 .9 1.0		0.89 .86 .81	_	1.45 1.41 1.36	1.77 1.73 1.67	0.61 .57 .52 .43	0.79 .75 .70	1.00 .96 .90	1.23 1.18 1.11 1.03	1.46 1.42 1.35	0.77 .75 .71	0.98 .95 .92	1.22 1.19 1.14 1.09	1.47 1.43 1.38	1.74 1.70 1.64	0.91 .89 .86	1.15 1.13 1.09	1.41 1.38 1.34 1.29	1.68 1.64 1.59	1.1	
0.72	0.8 .9 1.0		0.89 .85 .81	1.15 1.11 1.07	1.44	1.77	0.60 .57 .52	0.78 .75 .70	0.99 .95 .89		1.45 1.41 1.34	0.76 .73 .70	0.96 .94 .91		1.45 1.42 1.37	1.72 1.68 1.62	0.89	1.13	1.39 1.36 1.32 1.27	1.66	1.	
0.74	0.8 .9 1.0 1.1		0.88 .85 .81	1.14	1.44 1.40 1.36	1.76 1.72 1.67 1.61		0.78 .74 .69	0.98 .94 .89	1.21 1.16 1.10 1.03	1.44 1.40 1.34		0.95 .93 .90		1.43 1.40 1.36	1.70 1.66 1.61	0.88	1.11	1.37 1.34 1.30 1.26	1.63	1.	
0.76	0.8 .9 1.0 1.1		0.87 .84 .81	_	1.43 1.40 1.36	1.76 1.72 1.67	0.58 .56 .51	0.77 .74 .69	0.97	1.20 1.16 1.10 1.03	1.43 1.39 1.33		0.94	1.17 1.14 1.11	1.42 1.39 1.35	1.68	0.86 .84 .82	1.10 1.07 1.05	1.35 1.32 1.29 1.24	1.61 1.58 1.54	1.	
0.78	0.8 .9 1.0 1.1	1000	0.87 .84 .81	1.13 1.11 1.07	1.42 1.40 1.36	1.75	0.58 .55 .51	-	0.96 .93 .88	1.19 1.15 1.09 1.03	1.42 1.38 1.33		0.93 .91 .88		1.40 1.37 1.33	1.67 1.63 1.59	0.85 .83	1.08 1.06 1.03	1.33 1.30 1.27 1.23	1.59 1.56 1.52	1 1 1	
0.80	0.8 .9 1.0		0.86 .84 .81	1.13 1.10 1.07	1.42 1.40 1.36	1.75	0.57 .54 .51	0.75 .73 .68	0.96	1.18 1.14 1.09 1.03	1.41 1.37 1.33		0.93 .90 .87	1.15 1.11 1.09	1.39 1.36 1.32	1.65	0.84 .82 .80	1.06 1.04 1.02	1.31 1.29 1.26 1.22	1.57 1.54 1.51	1.1.1	

TABLE I. - LAST STAGE OR SINGLE STAGE WITH ZERO EXIT WHIRL - Concluded (c) Exit axial velocity ratio $(V_{x}/a_{cr}^{i})_{2} = 0.7$.

1. Limitation of zero change in magnitude of relative relative to rotor at hub radius.

2. Limitation of 0.6 entrance Mach number relative to rotor at hub radius.

3. Limitation of 0.8 entrance Mach number relative to rotor at hub radius.

4. Limitation of 1.0 entrance Mach number relative to rotor at hub radius.

NA.	CA	r	eloci otor adius	at hu	D			ub ra					ıb ra					ub ra		4	
Exit blade- speed	annular	Sta (-	ge-wor	rk par	vamet	er, =0				S	tage-v	ork pa	arame	ter,	-gJ∆l	1'/u{)	M, Vu,	2=0			
Ut/acr,2	area ratio, (A ₂ /A ₁) _s				-,-							atio,									
,.		0.5	0.6	0.7	0.8	0.9	0.5	0.6	0.7		0.9	0.5	0.6	-	0.8	0.9	0.5	0.6	0.7	0.8	0.
0.40	0.8 .9 1.0	100	1.18		1.77	2.11	0.76	0.97	1.19	1.45	1.72	1.07 .99 .86	1.34	1.61 1.48 1.31	1.89	2.21	1.32		1.94 1.82	2.12	
0.42	0.8	0.90	1.15	1.44	1.74	2.07	0.74	0.95	1.17	1.42	1.68	1.03	1.30	1.00 1.56 1.44	1.21	1.44		1.18	1.40	2.19	2.
	1.0 1.1	.81	.88	1.31	1.02	1.69	.61	.80	1.00		1.06	.95 .84 .59	. 79	1.28	1.52	1.79	1.11	1.36	1.62	1.87	2.
0.44	0.8 .9 1.0 1.1	0.88 .79 .65	1.03	1.41 1.30 1.13 .77	1.58	2.04 1.89 1.69 1.38	0.72	0.93	1.15	1.22	1.65 1.46 1.11	.93	1.17	1.51 1.41 1.26 1.02	1.67	1.95			1.82 1.72 1.58 1.37	2.01	2.
0.46	0.8 .9 1.0 1.1	0.86 .78 .65	1.11	1.13	1.57	2.01 1.87 1.69 1.42	0.70	0.91	1.12	1.21	1.62 1.45 1.14	0.97 .90 .80	1.14	1.47 1.38 1.24 1.02	1.64	1.91	1.13	1.47 1.40 1.30 1.13	1.68	2.07 1.96 1.80 1.57	2.
0.48	0.8 .9 1.0	0.84 .76 .64	1.09	1.36 1.27 1.13	1.66 1.55 1.40	1.99 1.86 1.69	0.69	0.89	1.10	1.20	1.60 1.44 1.16	0.94 .88 .79 .61	1.19 1.11 1.00	1.44 1.35 1.22 1.03	1.72 1.61 1.46	2.00 1.88 1.71	1.10	1.36	1.64	2.02 1.91 1.77 1.56	2.
0.50	0.8 .9 1.0	0.82 .75			1.54	1.97 1.85 1.69	0.68		1.09	1.32		0.92 .86 .77	1.16 1.09 .98	1.41 1.32 1.21	1.68 1.58 1.45	1.96 1.85 1.69	1.12	1.39 1.33 1.24	1.68 1.60 1.49	1.97 1.87 1.74	2.
0.52	0.8 .9 1.0	0.81 .74 .64	.62	.91 1.32 1.24 1.13	1.19	1.48 1.95 1.84	0.66	0.86 .76	1.07 .96 .74	1.31	1.55 1.42 1.20	0.90 .84 .76	1.13	1.38 1.30 1.19	1.65	1.93 1.82	1.09	1.36 1.30 1.21	1.64 1.56 1.46	1.55 1.93 1.84 1.71	2.
0.54	0.8 .9 1.0	0.79 .73 .64	.65		1.61 1.52 1.40	1.50 1.93 1.83	0.65	0.85 .75 .54	1.06 .95 .76	1.29	1.54 1.41 1.21	.61 0.88 .82 .75	1.11	1.28	1.61 1.53 1.42		1.06	1.32 1.27 1.19	1.60 1.53 1.44	1.54 1.89 1.80 1.68	2.
0.56	0.8 .9 1.0	0.78 .72 .64	1.03	.95	1.23 1.59 1.51 1.40	1.52 1.91 1.82	0.64	0.83 .74 .55	1.04 .95 .77	1.27	1.52 1.40 1.22	0.86 .81 .74	1.09 1.03 .94	1.03 1.33 1.26		1.48 1.87 1.77 1.65	1.03 .99 .94	1.29 1.24 1.17	1.57 1.50 1.41	1.53 1.85 1.77 1.66	2.
0.58	1.1 . 0.8 .9 1.0	.43 0.77 .72	1.01 .95	.97 1.28 1.21	1.24 1.58 1.50	1.53 1.90 1.81	0.63 .55 .36	0.82 .74 .57	1.03 .94 .78	1.26	1.50	0.84 .79 .73	1.07 1.01 .93	1.03 1.30 1.24 1.15	1.56	1.48 1.84 1.75 1.63	1.01 .97 .92	1.26	1.54	1.52 1.81 1.74 1.64	2.
0.60	0.8	0.76 .71	.94	1.26	1.26 1.56 1.49	1.54 1.88 1.80	0.62	0.81	1.02	1.25	1.49	.61 0.82 .78	.81 1.05 .99	1.03 1.28 1.22	1.24 1.53 1.47	1.48 1.81 1.73	0.99 .95	1.05 1.24 1.19	1.28 1.51 1.45	1.51 1.78 1.71	2.
0.62	1.0 1.1	.63 .49	.86 .73	1.12	1.27	1.56	0.61	0.80				.72 .61	1.03	1.02	1.24	1.48	.90 .83	1.04	1.27	1.62 1.50	2.
	.9 1.0 1.1	.70 .63 .50	.86	1.20 1.12 1.00	1.40	1.69	.54	.73		1.15	.95	.76 .71 .61		1.13	1.24		.93 .89 .82	1.11	1.35	1.69 1.60 1.49	1.
0.64	0.8 .9 1.0 1.1	0.74 .69 .63	.93	1.24 1.19 1.12 1.01	1.48	1.79	0.60 .54 .41	0.79 .72 .60	.92	1.22	1.37	0.79 .75 .70 .61	1.01 .96 .90	1.24 1.19 1.12 1.02	1.43	1.69	.91 .87 .81	1.15 1.10 1.02	1.40 1.33 1.25	1.66 1.58 1.48	1.
0.66	0.8 .9 1.0	0.73 .69 .63	.92	1.23 1.18 1.11 1.02	1.47	1.78	0.59 .53 .42	0.78 .72 .60	0.99 .92 .81	1.21 1.13 1.02	1.37	0.78 .74 .69	.95	1.22 1.18 1.11 1.02	1.42	1.67	.90	1.13	1.38	1.70 1.64 1.56 1.47	1.
0.68	0.8 .9 1.0 1.1	0.72 .68 .63	.92	1.22 1.18 1.11 1.03	1.46	1.69	0.59 .53 .42	0.77 .71 .61	0.98 .91 .81	1.20 1.13 1.03 .81	1.44 1.36 1.26 1.07	0.76 .73 .68	.88	1.21 1.16 1.10 1.01	1.40	1.58	0.91 .88 .84 .79	1.11	1.36	1.67 1.62 1.55 1.46	1.
0.70	0.8 .9 1.0 1.1	0.71 .68 .63	0.95 .91 .85	1.21 1.17 1.11	1.50 1.46 1.39	1.83	0.58 .53 .43	0.76 .71 .61	.91	1.03	1.43 1.36 1.26 1.10	0.75 .72 .67	.93		1.39	1.64	0.89 .87 .83 .78	1.10	1.34	1.65 1.60 1.53 1.45	1.
0.72	0.8 .9 1.0 1.1		0.94 .90 .85	1.20 1.17 1.11	1.49 1.45 1.39			0.76 .70 .62	0.96 .90 .81		1.42 1.35 1.26	0.74 .71 .66	0.95	1.18 1.13 1.08	1.42	1.68 1.63 1.56	. 85	1.08	1.32	1.63 1.58 1.51 1.44	1.
0.74	0.8 .9 1.0 1.1	0.70 .67 .62	0.94 .90 .85	1.20 1.16 1.11	1.48 1.45 1.39	1.81 1.76 1.69 1.61	0.57 .52 .44	.70	0.95	1.17 1.11 1.03	1.41	0.73 .70 .66 .60	.90	1.16 1.12 1.07 1.00	1.36	1.62	.84 .81 .76	1.06 1.02 .97	1.30 1.26 1.20	1.62 1.56 1.50 1.43	1.
0.76	0.8 .9 1.0	0.69 .66 .62	0.93	1.19	1.48 1.44 1.39	1.80	0.56 .52 .44	.70	0.94	1.16	1.40	0.72 .69 .65	.89	1.15 1.11 1.06 1.00	1.35	1.60	.83 .79 .75	1.05 1.01 .96	1.29 1.24 1.19	1.59 1.54 1.49 1.42	1.
0.78	0.8 .9 1.0 1.1	0.68 .66 .62	0.92 .89 .85	1.18 1.15 1.10	1.47 1.44 1.39	1.80 1.75 1.69 1.61	0.56 .51 .45	.69	0.93	1.15 1.10 1.03	1.39	0.71 .68 .64 .59	.88	1.14 1.10 1.05 .99	1.34	1.59	.81	1.04	1.27	1.57 1.53 1.48 1.42	1.
0.80	0.8 .9 1.0	0.68 .65 .62	0.91 .89 .85	1.18 1.15 1.10	1.47 1.43 1.39	1.79	0.55 .51 .45	.69	0.93 .89 .82	1.10	1.33	0.70 .67 .64	.87	1.13 1.09 1.05	1.33	1.58	.80	1.02	1.26	1.55 1.51 1.46 1.41	1.

2

75

TABLE II. - STAGE OTHER THAN LAST WITH SPECIFIED MACH NUMBER AND 120° TURNING ANGLE AT HUB RADIUS (a) $M_{1,h} = M_{2,h} = 0.6$. (b) $M_{1,h} = M_{2,h} = 0.8$.

Ratio of tangen-tial velocities. 1. Stage-work 2. Ratio of tangen-1. Stage-work NACA parameter. parameter. tial velocities. Isentropic Stage-work Exit blade-Ratio of tangential Stage-work Ratio of tangential parameter. -gJΔh'/U²t parameter, -gJΔh'/Uξ speed annular area ratio, velocities, velocities, -(Vu,1/Vu,2)h parameter, $-(v_{u,1}/v_{u,2})_h$ Ut/acr,2 $(A_2/A_1)_s$ Hub-tip radius ratio, rh/rt Hub-tip radius ratio, rh/rt 0.6 0.7 0.8 0.9 0.6 0.7 0.8 0.9 0.6 0.7 0.8 0.9 0.6 0.7 0.8 0.9 1.82 2.15 2.50 2.85 1.84 2.19 2.52 2.90 1.92 2.05 2.23 2.40 2.27 2.66 3.08 3.50 2.29 2.71 3.11 3.53 2.31 2.72 3.13 3.54 0.40 0.8 1.78 1.91 2.06 2.22 1.0 1.71 1.82 1.97 1.55 1.65 1.78 1.92 2.20 2.54 2.91 2.17 2.55 2.94 3.35 2.19 2.59 2.97 3.39 2.21 2.60 3.00 3.41 0.42 0.8 1.74 2.05 2.40 2.74 1.97 2.13 2.32 2.51 1.76 2.10 2.42 2.78 1.76 2.11 2.44 2.80 1.0 1.75 1.87 2.04 2.20 1.59 1.70 1.84 1.98 1.64 1.76 1.91 1.49 1.62 1.75 1.2 1.67 1.97 2.30 2.62 1.69 2.01 2.32 2.67 2.02 2.21 2.42 2.63 1.79 1.93 2.11 2.29 2.07 2.44 2.82 3.20 2.10 2.47 2.85 3.25 2.11 2.48 2.88 3.28 0.44 0.8 1.0 1.68 | 1.82 | 1.97 1.69 2.03 2.35 2.70 1.63 1.76 1.90 2.06 0.8 1.60 1.90 2.21 2.52 2.08 2.30 2.53 2.76 1.99 2.33 2.70 3.07 0.46 1.62 1.93 2.24 2.57 1.62 1.95 2.26 2.60 1.0 1.83 1.99 2.19 2.38 2.36 2.73 2.01 2.36 2.73 3.12 2.02 2.38 2.76 3.16 1.72 1.87 1.67 1.82 1.97 2.13 1.57 1.71 1.86 1.54 1.83 2.12 2.43 1.57 1.85 2.16 2.47 2.15 2.38 2.64 2.89 1.88 2.05 2.27 2.48 0.48 0.8 1.90 2.24 2.59 2.94 1.57 | 1.85 | 2.16 | 2.47 | 1.57 | 1.88 | 2.18 | 2.51 1.93 2.27 2.63 3.00 1.93 2.28 2.66 3.04 1.0 1.77 1.93 2.11 2.27 1.62 1.76 1.92 2.06 1.2 1.71 1.87 2.03 2.21 1.48 1.76 2.05 2.34 1.51 1.79 2.08 2.39 0.50 2.21 2.47 2.76 3.03 1.93 2.12 2.36 2.58 0.8 1.83 2.16 2.49 2.83 1.0 1.86 2.19 2.53 2.89 1.82 2.00 2.18 2.36 1.2 1.81 2.11 2.42 1.86 2.20 2.56 2.93 1.75 | 1.94 | 2.11 | 2.30 0.52 0.8 1.43 1.70 1.97 2.26 2.28 2.56 2.88 3.19 1.76 2.08 2.39 2.73 1.98 2.19 2.45 2.69 1.80 1.99 2.18 2.39 1.0 1.45 1.73 2.01 2.31 1.45 1.75 2.04 2.34 2.06 1.79 2.11 2.44 2.78 1.79 2.12 2.47 2.82 1.87 1.38 1.64 1.91 2.18 0.54 0.8 2.35 2.66 3.01 3.36 1.70 2.00 2.31 2.63 1.73 2.03 2.35 2.69 1.40 1.67 1.95 2.24 1.40 1.69 1.98 2.26 2.03 2.26 2.55 2.81 1.85 2.06 2.25 2.49 1.0 1.2 1.73 2.04 2.38 2.72 0.56 0.8 1.65 1.93 2.23 2.54

1.59 | 1.70 | 1.85 | 1.96 1.46 | 1.57 | 1.70 | 1.80 1.83 1.98 2.14 2.30 1.88 2.05 2.22 2.40 1.53 | 1.66 | 1.80 | 1.93 1.93 2.13 2.30 2.49 1.99 2.20 2.40 2.60 2.05 2.26 2.50 2.71 1.66 | 1.81 | 1.97 | 2.14 2.10 2.36 2.60 2.84 1.70 | 1.87 | 2.04 | 2.22 2.16 2.45 2.70 2.97 1.92 2.13 2.35 2.55 1.75 1.92 2.10 2.30 1.34 1.59 1.85 2.11 1.36 1.62 1.89 2.17 2.42 2.76 3.15 3.56 2.09 2.35 2.65 2.94 2.23 2.54 2.82 3.12 1.0 1.67 | 1.97 | 2.27 | 2.60 | 1.67 | 1.99 | 2.30 | 2.63 1.97 2.20 2.44 2.67 1.80 1.98 2.17 2.39 1.2 1.36 1.64 1.91 2.20 1.90 2.12 2.34 2.59 1.30 1.54 1.79 2.05 0.58 0.8 2.50 2.87 3.31 3.80 1.59 1.87 2.16 2.45 2.30 2.64 2.95 3.28 1.32 1.57 1.83 2.11 2.15 2.43 2.76 3.09 1.94 2.19 2.43 2.70 1.61 1.91 2.20 2.51 1.62 1.93 2.23 2.54 2.02 2.27 1.84 2.04 2.54 2.80 2.25 2.49 1.0 1.2 1.32 | 1.59 | 1.85 | 2.13 1.26 1.49 1.74 1.99 1.28 1.53 1.78 2.04 0.60 0.8 2.58 2.99 3.47 4.05 1.54 1.80 2.09 2.37 2.37 2.74 3.08 3.48 2.21 2.52 2.00 2.26 1.56 | 1.85 | 2.13 | 2.43 | 1.57 | 1.87 | 2.16 | 2.46 2.08 2.35 2.64 2.95 1.89 2.11 2.34 2.58 1.0 2.88 3.25 1.2 1.29 1.55 1.80 2.07 2.52 2.82 0.62 0.8 1.22 1.45 1.68 1.93 2.67 3.10 3.66 4.35 1.49 1.75 2.02 2.29 2.45 2.85 3.22 3.70 1.0 2.27 2.62 3.01 3.43 2.05 2.33 2.61 2.95 1.24 | 1.48 | 1.73 1.98 1.51 1.79 2.07 2.35 2.15 2.44 1.25 1.50 1.75 1.53 | 1.81 | 2.10 | 2.39 1.94 2.18 2.42 2.52 2.97 3.39 3.94 2.21 2.52 2.87 3.25 0.64 0.8 1.19 1.41 1.64 1.87 2.77 3.24 3.87 4.67 1.45 1.69 1.96 2.22 1.0 1.44 1.68 1.21 1.74 2.00 2.28 1.22 1.46 1.71 1.97 1.2 2.11 2.40 2.72 3.07 1.49 1.76 2.02 2.32 2.00 2.25 2.51 2.80 1.15 1.37 1.59 1.82 1.18 1.40 1.63 1.87 2.87 3.38 4.11 5.02 1.40 1.64 1.90 2.15 0.66 0.8 2.62 3.10 3.58 4.23 1.0 2.62 3.00 2.42 2.83 3.29 3.84 2.17 2.48 2.83 3.22 1.42 1.68 1.94 2.21 2.27 1.19 1.42 1.66 1.92 1.44 1.70 1.98 2.25 2.05 2.33 2.63 1.2 2.93 1.12 1.33 1.55 1.77 1.15 1.37 1.59 1.83 0.68 0.8 2.98 3.54 4.39 5.41 1.36 1.59 1.86 2.08 3.24 3.80 2.72 1.0 2.50 2.95 3.45 4.08 1.38 | 1.64 | 1.89 | 2.15 | 1.40 | 1.66 | 1.93 | 2.19 2.35 2.72 3.14 3.63 2.11 2.40 2.74 3.08 1.2 1.16 | 1.39 | 1.62 | 1.87 2.23 2.56 2.95 3.38 1.09 1.30 1.51 1.73 3.10 3.71 4.70 5.90 2.83 3.38 4.04 4.87 2.42 2.83 3.30 3.85 0.70 0.8 1.32 1.55 1.79 2.02 1.33 1.55 2.58 1.13 1.35 1.58 1.82 1.2 2.30 | 2.64 | 3.09 | 3.54 1.37 1.62 1.88 2.13 2.16 2.49 2.85 3.26 3.23 3.93 5.05 6.49 2.67 3.19 3.84 4.66 0.72 0.8 1.07 1.27 1.47 1.68 1.28 1.50 1.74 1.97 2.95 3.54 4.31 5.31 2.50 2.95 3.48 4.10 1.09 1.30 1.51 1.73 1.10 1.32 1.54 1.78 1.31 1.55 1.78 2.03 1.33 1.57 1.83 2.07 1.2 2.36 2.73 3.24 3.73 2.23 2.58 2.98 0.74 0.8 1.04 1.23 1.43 1.64 3.38 4.16 5.42 7.21 3.07 3.72 4.61 5.81 2.58 3.07 3.69 4.80 2.29 2.67 3.12 3.68 1.25 1.46 1.69 1.91 1.26 1.47 2.77 3.33 4.07 5.02 2.44 2.83 3.41 3.95 1.0 1.69 1.28 1.51 1.74 1.98 1.30 1.53 1.78 2.02 1.2 1.08 | 1.29 | 1.51 | 1.74 1.21 1.42 1.65 1.86 1.24 1.47 1.69 1.92 1.26 1.49 1.73 1.96 3.20 3.92 4.96 6.41 2.67 3.20 3.92 4.74 2.36 2.78 3.27 3.94 0.76 0.8 1.01 | 1.20 | 1.39 | 1.59 3.52 4.44 5.85 8.10 2.87 3.49 4.32 5.44 2.52 2.95 3.60 4.20 1.0 1.04 1.23 1.44 1.65 1.06 1.26 1.47 1.69 0.8 0.99 1.17 1.36 1.55 3.68 4.75 6.37 9.25 1.18 1.39 1.60 3.33 4.16 5.35 7.13 1.81 1.20 1.40 1.61 2.99 3.67 4.62 5.93 2.61 3.07 3.80 4.50 1.0 1.02 1.22 1.43 1.65 1.87 2.76 3.36 4.16 5.15 2.43 2.90 3.44 4.20 1.2 1.03 | 1.23 | 1.44 | 1.65 | 1.24 | 1.46 | 1.69 | 1.91 0.96 1.14 1.32 1.51 1.00 1.18 1.37 1.57 1.01 1.20 1.40 1.62 1.15 1.35 1.56 1.77 1.19 1.39 1.60 1.83 1.21 1.42 1.65 1.86 3.47 4.44 5.77 7.96 2.86 3.53 4.44 5.61 2.50 3.02 3.62 4.48 0.80 0.8 3.84 5.10 7.04 10.70 3.10 3.87 4.96 6.50 2.70 3.21 4.00 4.82 1.0

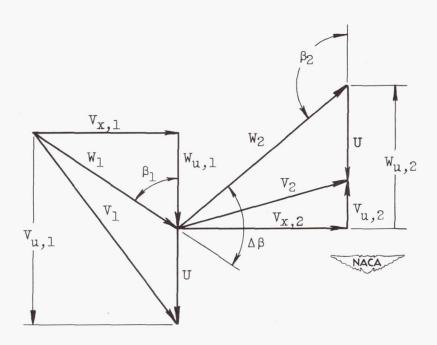


Figure 1. - Typical velocity diagram applicable to any stage.

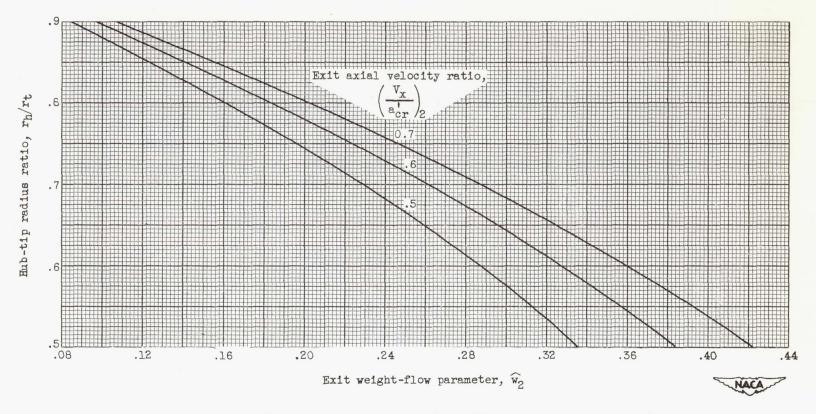


Figure 2. - Variation of hub-tip radius ratio with exit weight-flow parameter for constant values of exit axial velocity ratio and zero exit whirl. For use with chart I and table I.

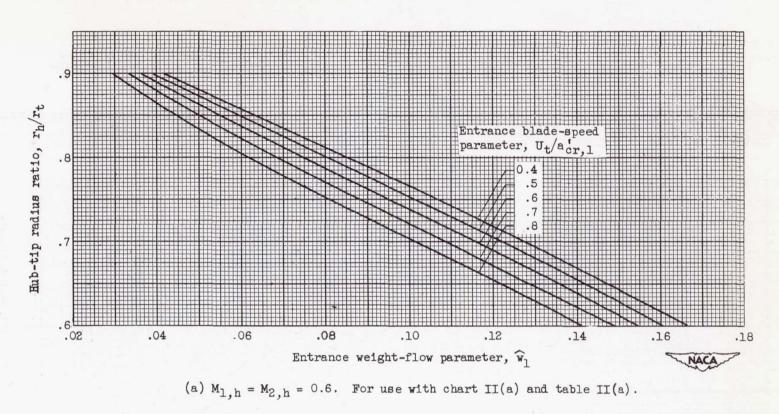
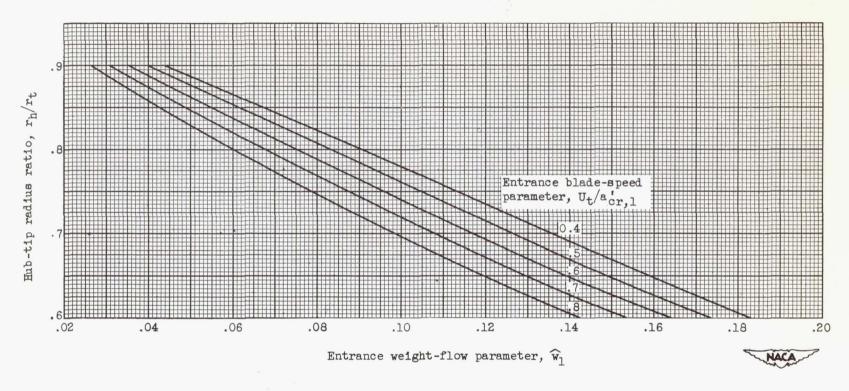
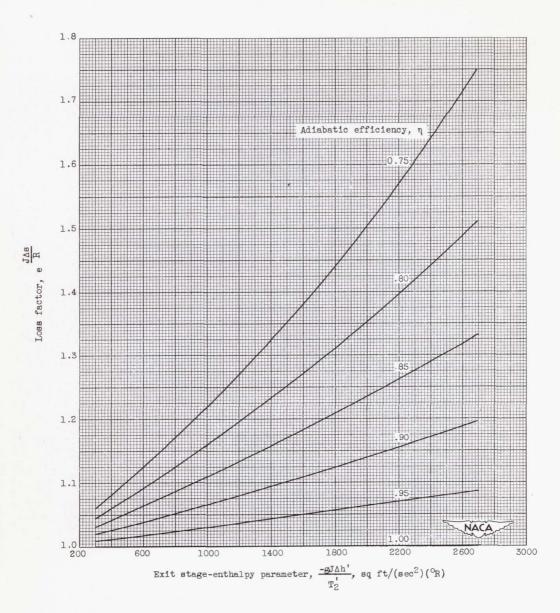


Figure 3. - Variation of hub-tip radius ratio with entrance weight-flow parameter for constant values of entrance blade-speed parameter. Isentropic annular area ratio of 1.0 and 1200 turning angle at hub radius.



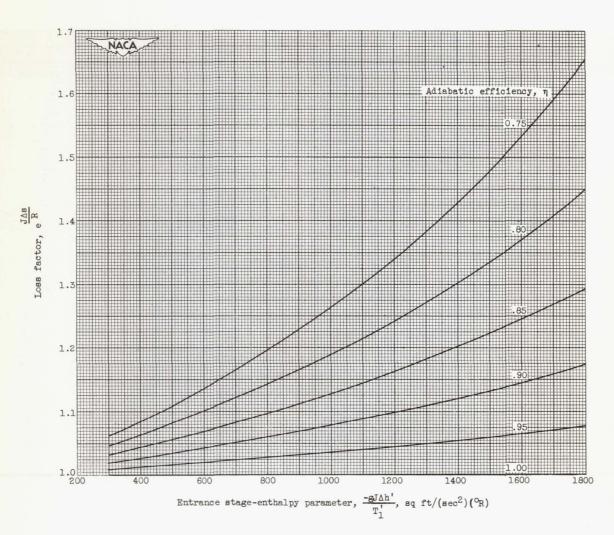
(b) $M_{1,h} = M_{2,h} = 0.8$. For use with chart II(b) and table II(b).

Figure 3. - Concluded. Variation of hub-tip radius ratio with entrance weight-flow parameter for constant values of entrance blade-speed parameter. Isentropic annular area ratio of 1.0 and 120° turning angle at hub radius.



(a) For use with chart I and table I.

Figure 4. - Variation of loss factor with adiabatic efficiency.



(b) For use with chart II and table II.

Figure 4. - Concluded. Variation of loss factor with adiabatic efficiency.

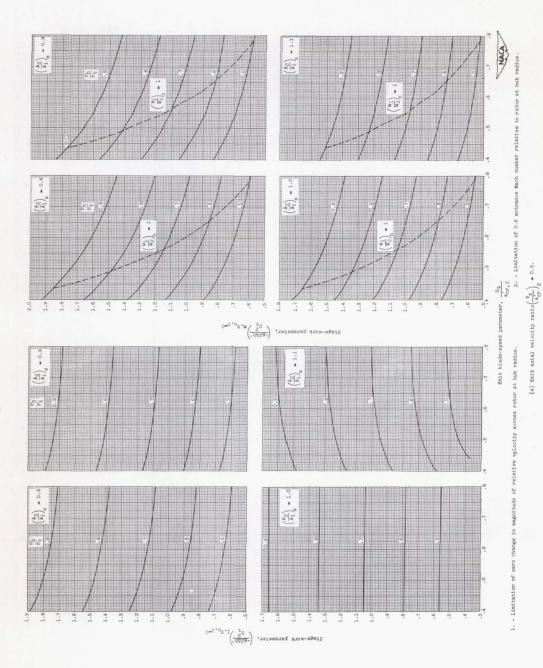
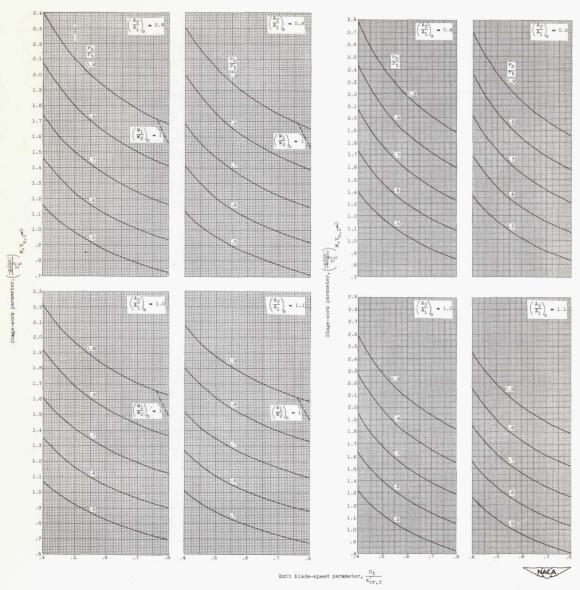


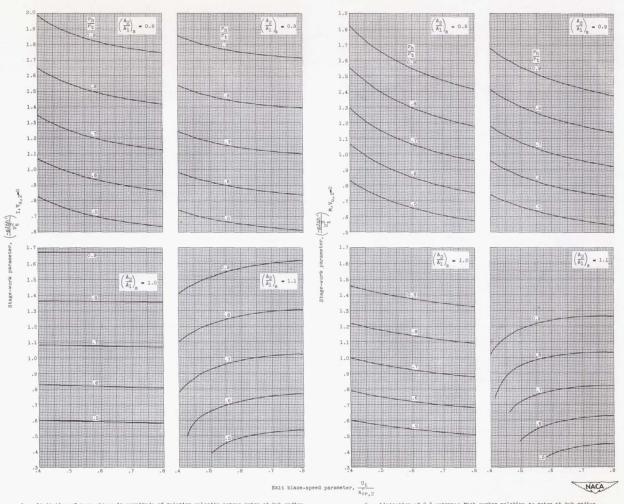
Chart I. - Last stage or single stage with zero exit whirl. (A 17- by 22-in. print of this fig. is attached.)



S. - Limitation of 0.8 entrance Mach number relative to rotor at hub radius.

(a) Concluded. Exit axial velocity ratio $\left(\frac{\mathbf{v}_{\mathbf{x}}}{\mathbf{a}_{ir}}\right)_2$ = 0.5.

Chart I. - Continued. Last stage or single stage with zero exit whirl. (A 17- by 22-in. print of this fig. is attached.)

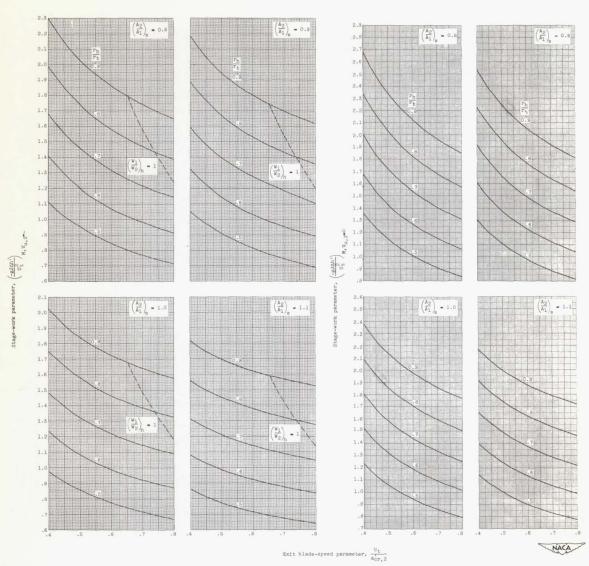


1. - Limitation of zero change in magnitude of relative velocity across rotor at hub radius.

2. - Limitation of 0.6 entrance Mach number relative to rotor at hub radius.

(b) Exit axial velocity ratio $\left(\frac{v_{\chi}}{a_{\rm CP}^{T}}\right)_{2}$ = 0.6.

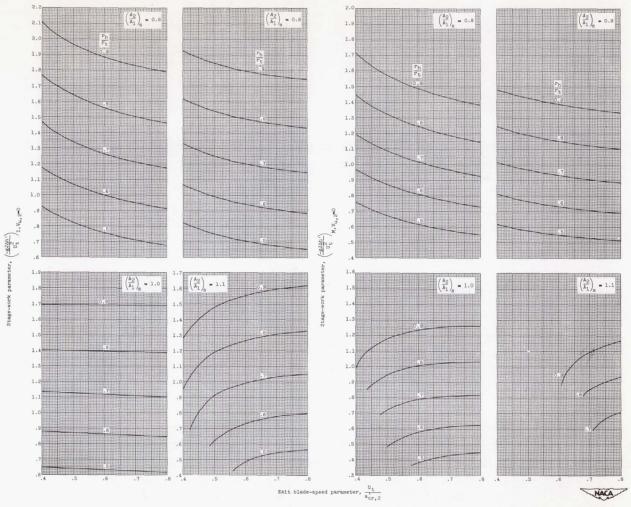
Chart I. - Continued. Last stage or single stage with zero exit whirl. (A 17- by 22-in, print of this fig. is attached.)



3. - Limitation of 0.8 entrance Mach number relative to rotor at hub radius. 4. - Limitation of 1.0 entrance Mach number relative to rotor at hub radius.

(b) Concluded. Exit axial velocity ratio $\left(\frac{V_X}{a_{\rm CP}}\right)_2$ =0.6.

Chart I. - Continued. Last stage or single stage with zero exit whirl. (A 17- by 22-in. print of this fig. is attached.)



1. - Limitation of zero change in magnitude of relative velocity across rotor at hub radius.

2. - Limitation of 0.6 entrance Mach number relative to rotor at hub radius.

(c) Exit axial velocity ratio $\left(\frac{V_X}{a_{cr}}\right)_2 = 0.7$.

Chart I. - Continued. Last stage or single stage with zero exit whirl. (A 17- by 22-in. print of this fig. is attached.)

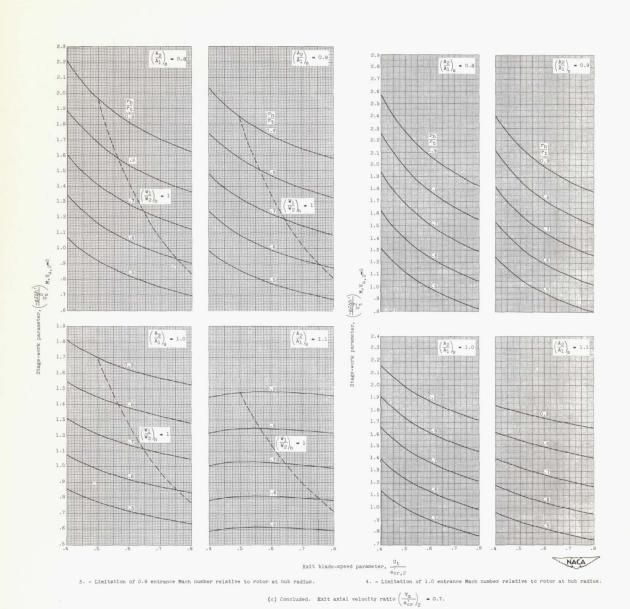


Chart I. - Concluded. Last stage or single stage with zero exit whirl. (A 17- by 22-in. print of this fig. is attached.)

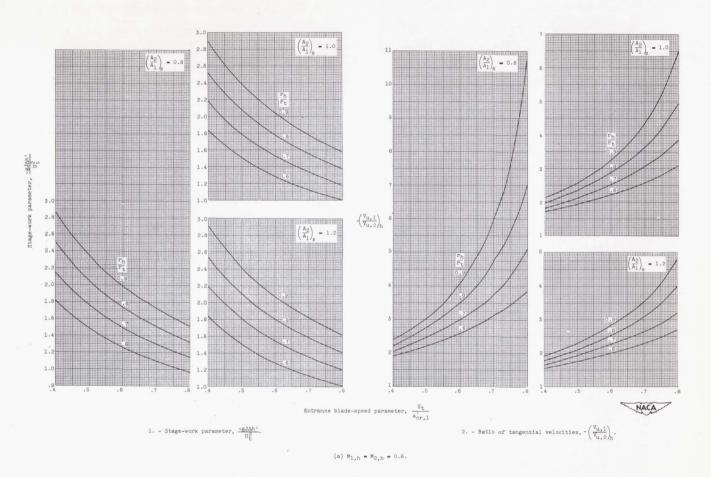


Chart II. - Stage other than last with specified Mach number and 1200 turning angle at hub radius. (A 17- by 22-in. print of this fig. is attached.)

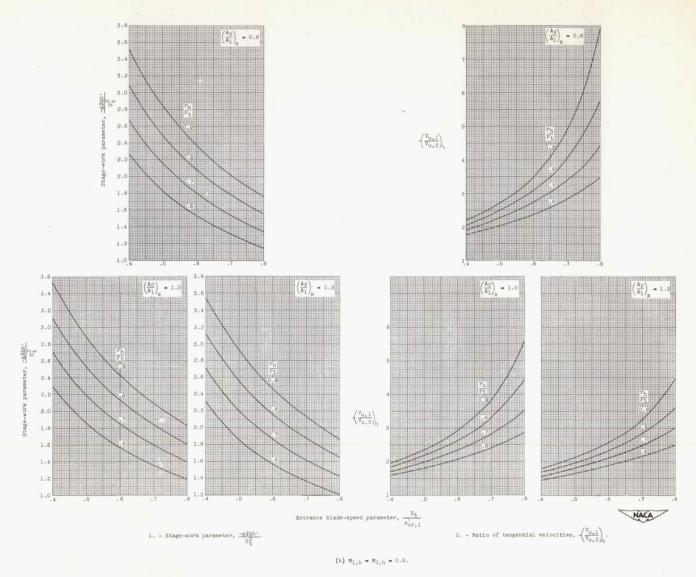
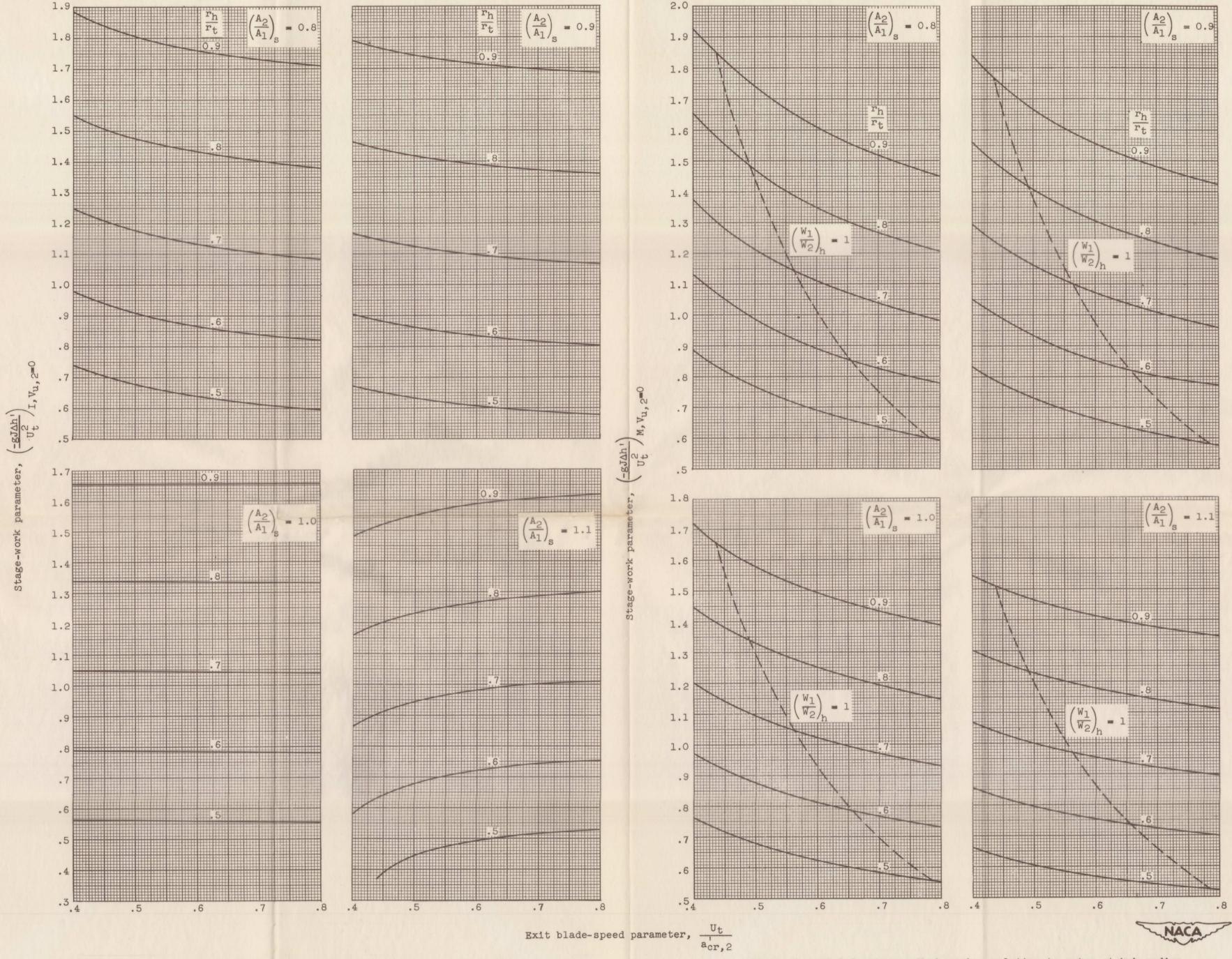


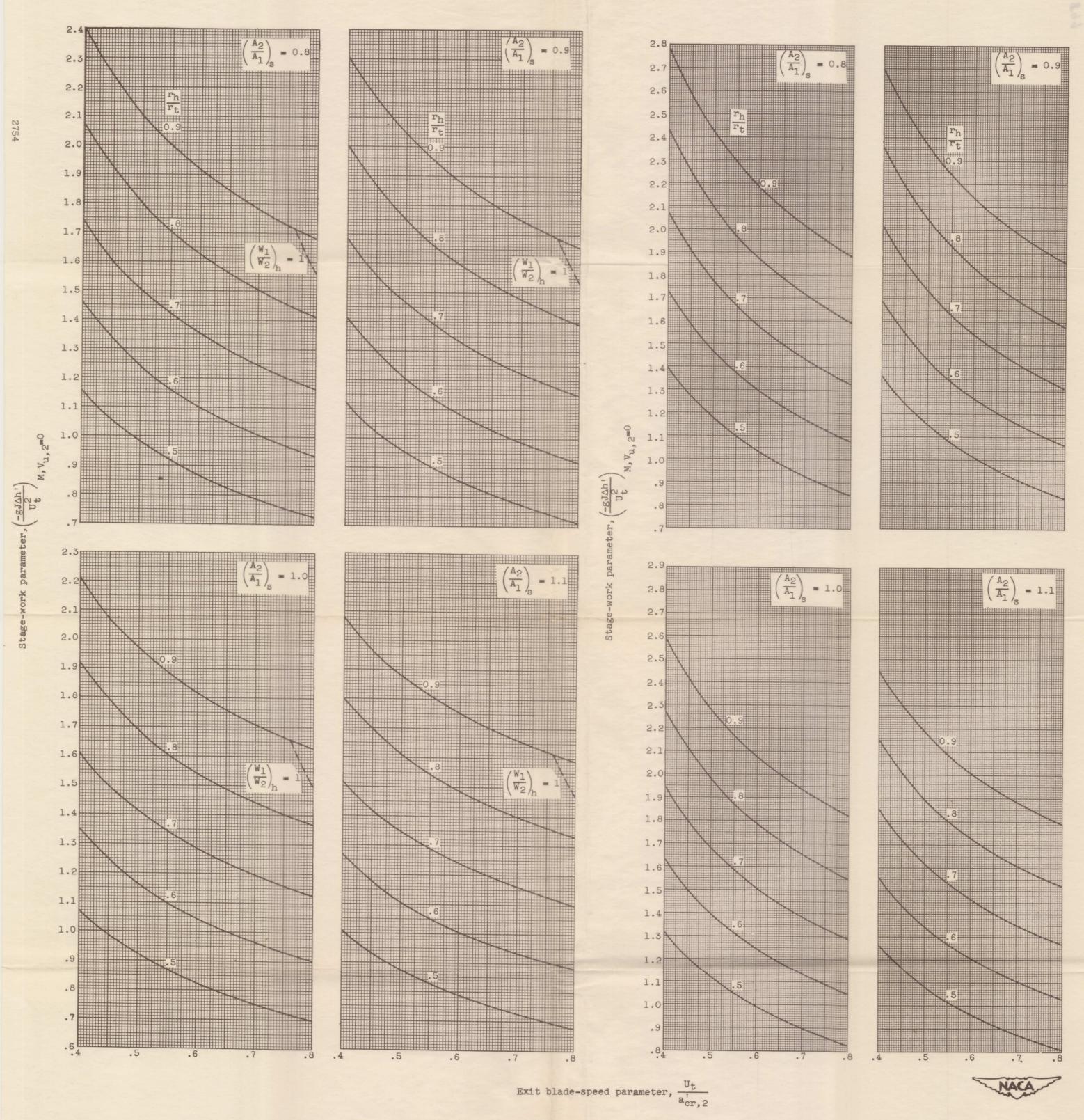
Chart II. - Concluded. Stage other than last with specified Mach number and 120° turning angle at hub radius. (A 17- by 22-in. print of this fig. is attached.)



1. - Limitation of zero change in magnitude of relative velocity across rotor at hub radius.

2. - Limitation of 0.6 entrance Mach number relative to rotor at hub radius.

(a) Exit axial velocity ratio $\left(\frac{V_x}{a_{cr}'}\right)_2 = 0.5$.

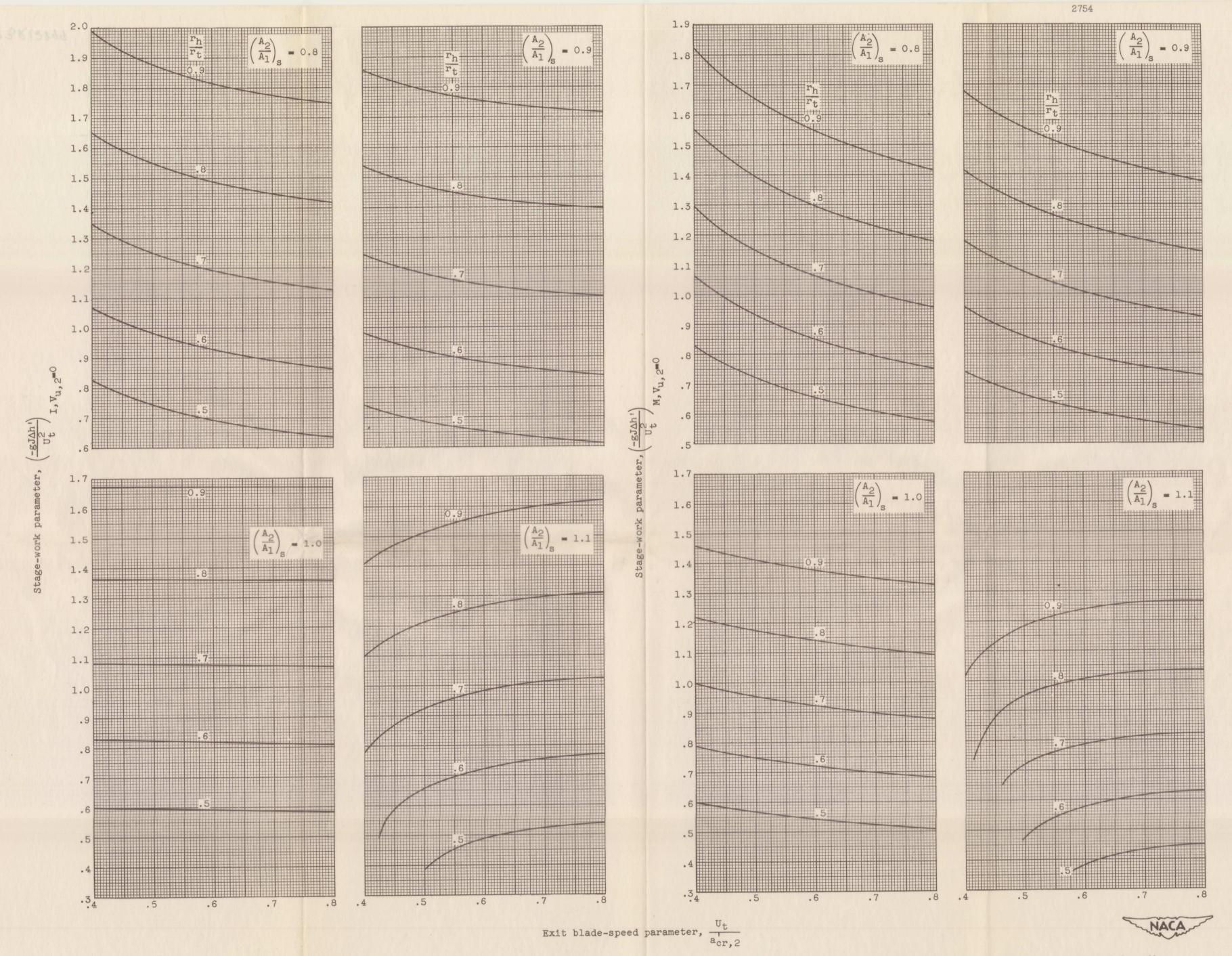


3. - Limitation of 0.8 entrance Mach number relative to rotor at hub radius.

4. - Limitation of 1.0 entrance Mach number relative to rotor at hub radius.

(a) Concluded. Exit axial velocity ratio $\left(\frac{v_x}{a_{cr}'}\right)_2 = 0.5$.

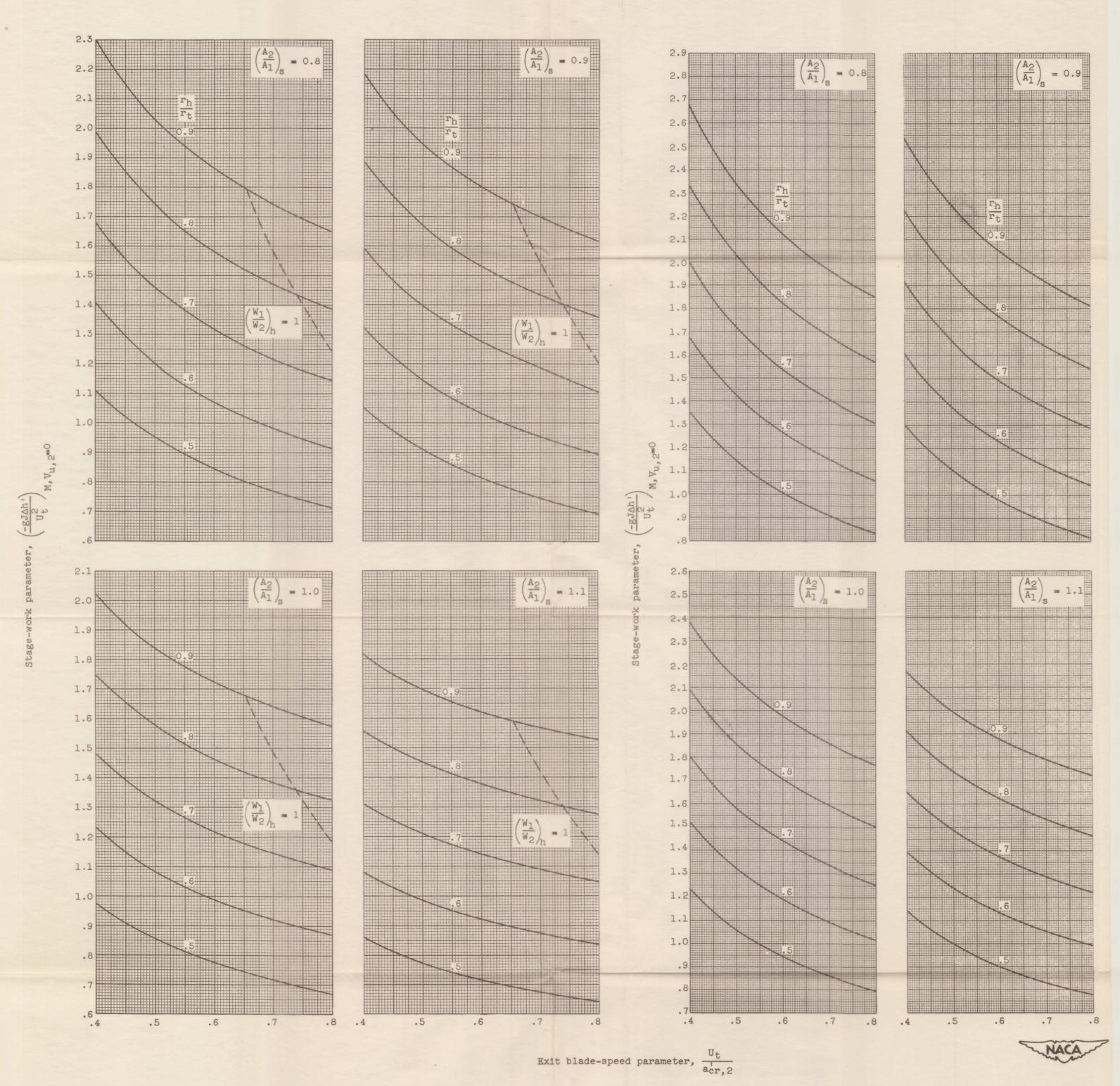
Chart I. - Continued. Last stage or single stage with zero exit whirl.



1. - Limitation of zero change in magnitude of relative velocity across rotor at hub radius.

2. - Limitation of 0.6 entrance Mach number relative to rotor at hub radius.

(b) Exit axial velocity ratio $\left(\frac{V_x}{a_{cr}^{\dagger}}\right)_2 = 0.6$.

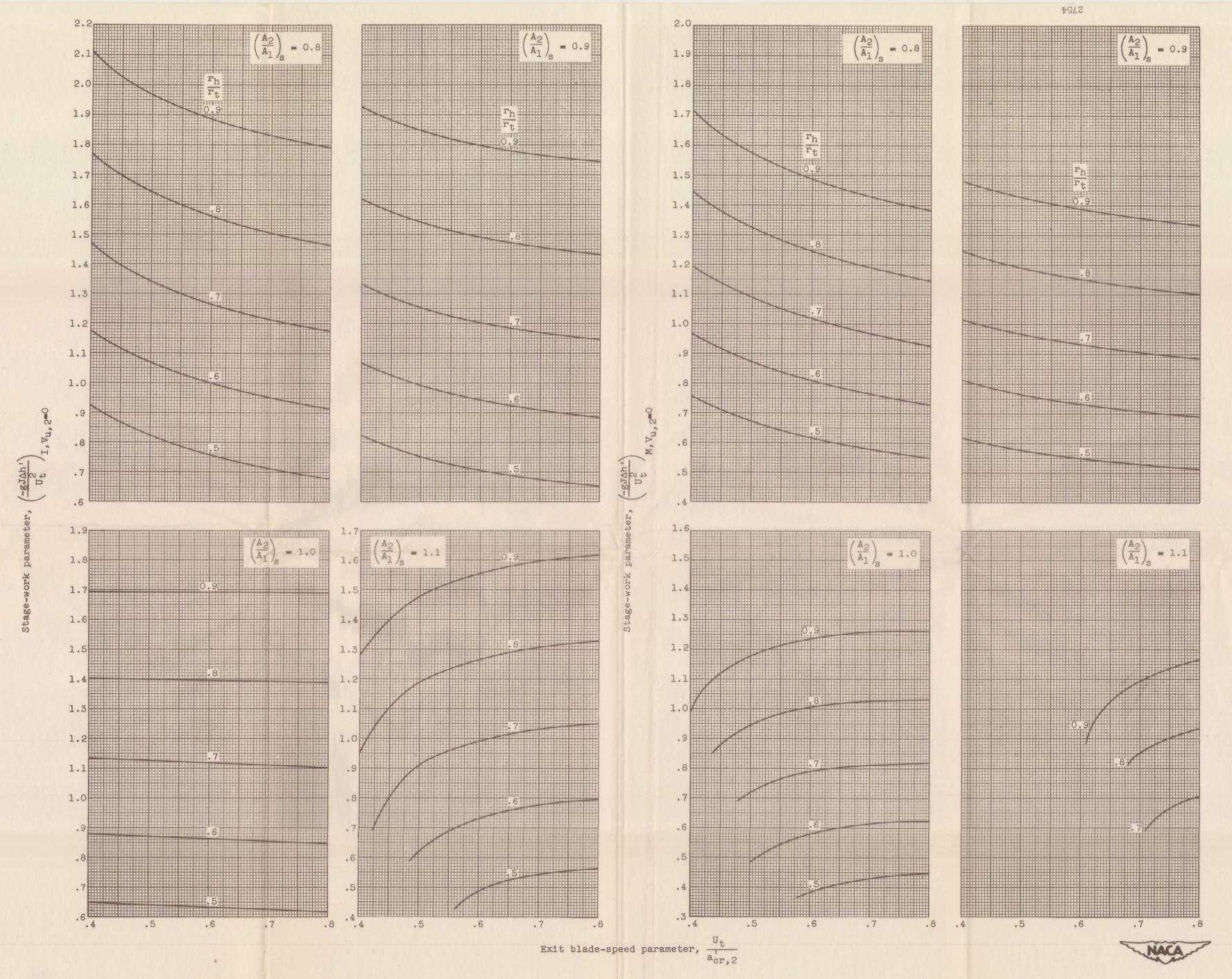


3. - Limitation of 0.8 entrance Mach number relative to rotor at hub radius.

4. - Limitation of 1.0 entrance Mach number relative to rotor at hub radius.

(b) Concluded. Exit axial velocity ratio $\left(\frac{V_X}{a_{cr}^{\dagger}}\right)_2 = 0.6$.

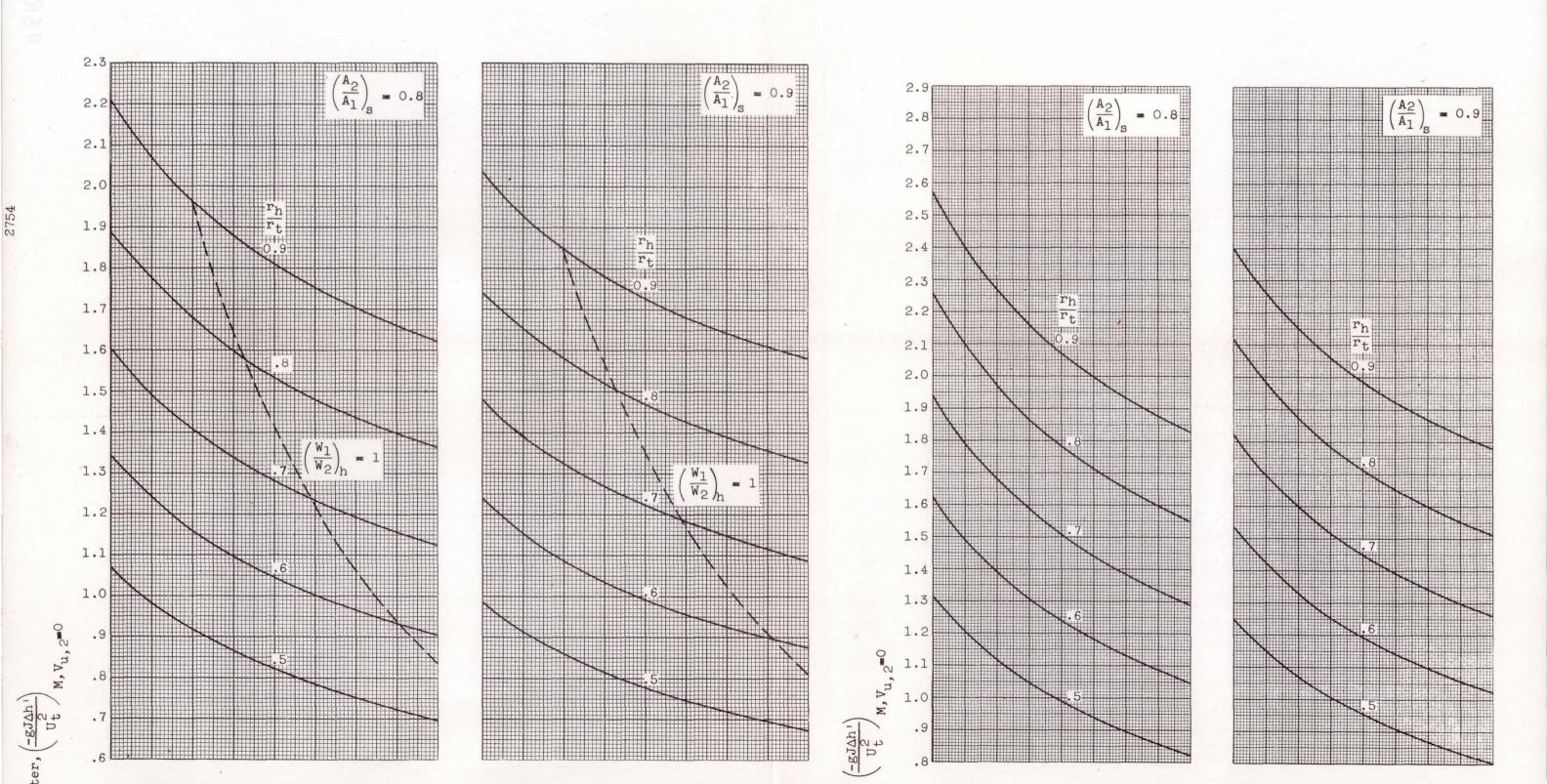
Chart I. - Continued. Last stage or single stage with zero exit whirl.

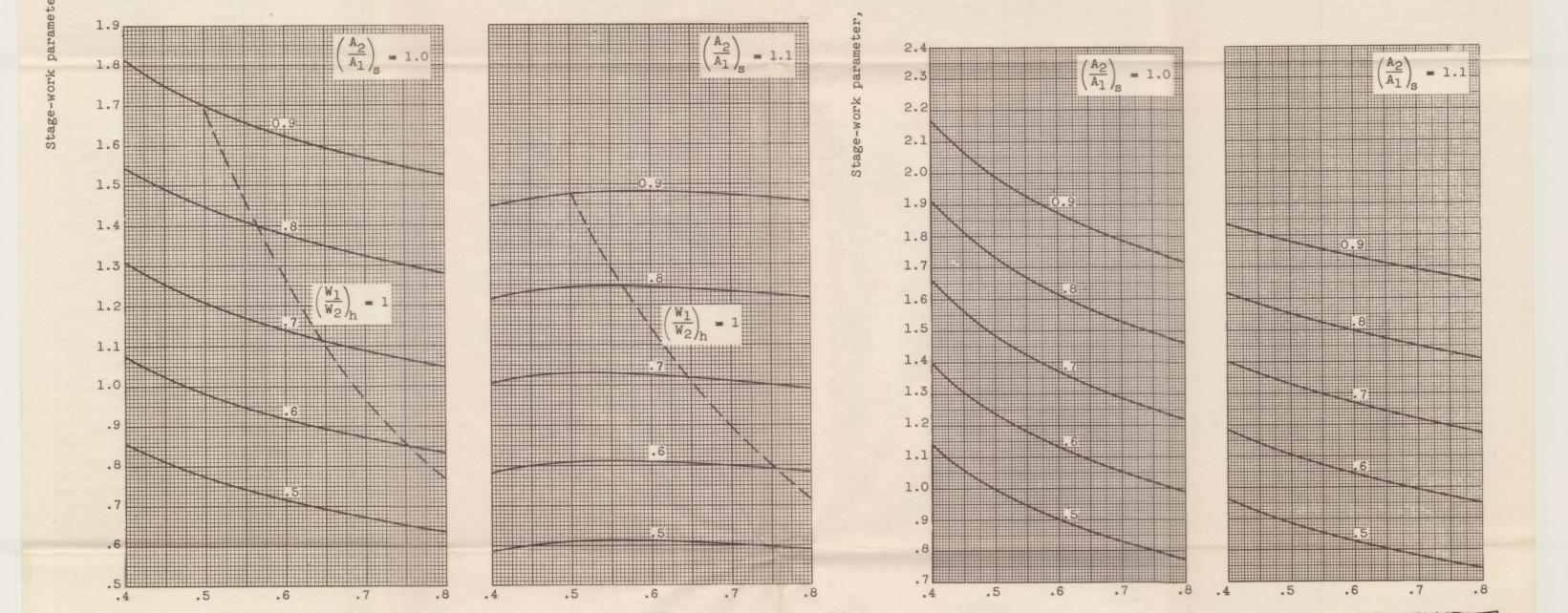


1. - Limitation of zero change in magnitude of relative velocity across rotor at hub radius.

2. - Limitation of 0.6 entrance Mach number relative to rotor at hub radius.

(c) Exit axial velocity ratio $\left(\frac{V_x}{a_{cr}}\right)_2 = 0.7$.





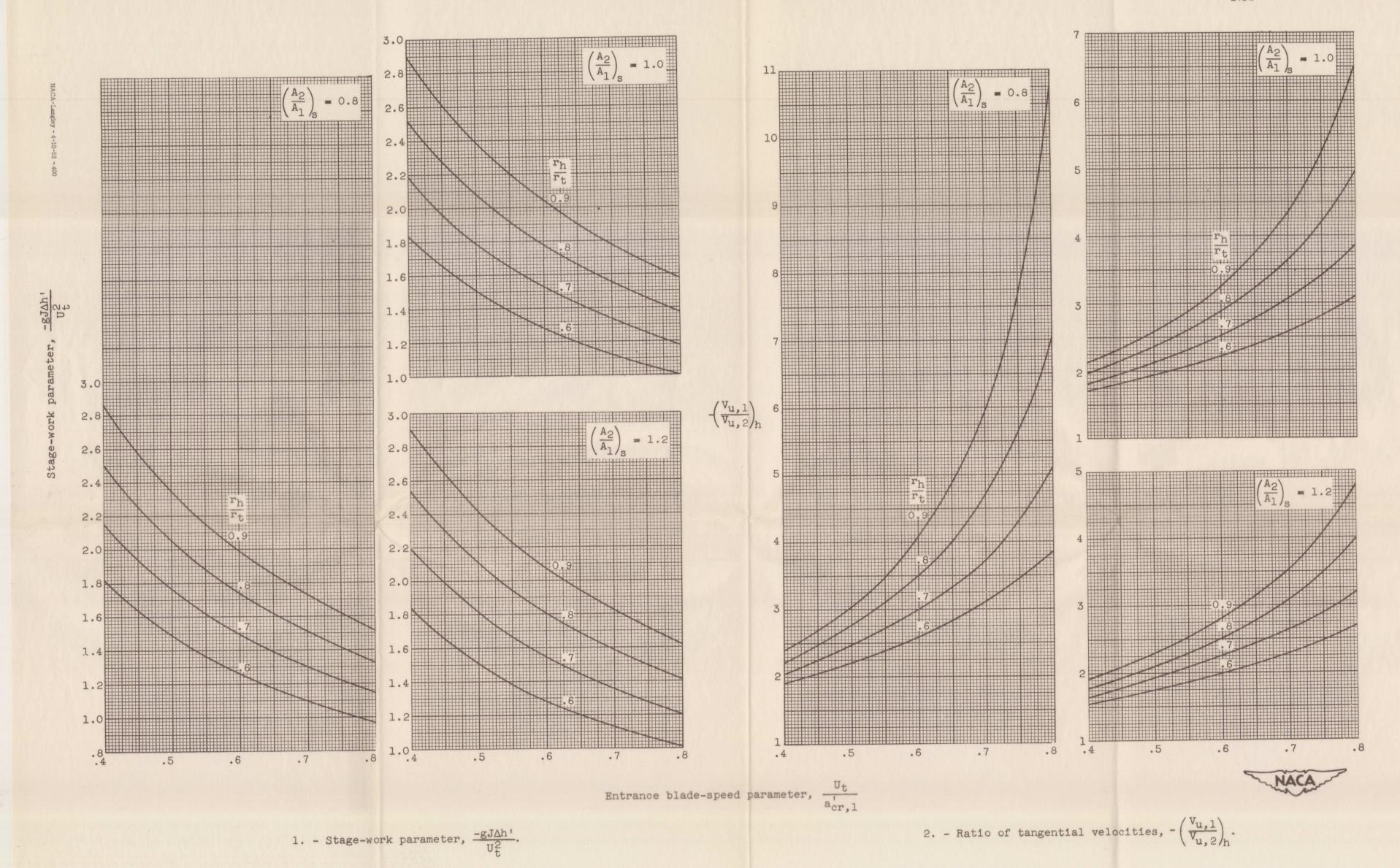
3. - Limitation of 0.8 entrance Mach number relative to rotor at hub radius.

4. - Limitation of 1.0 entrance Mach number relative to rotor at hub radius.

(c) Concluded. Exit axial velocity ratio $\left(\frac{V_X}{a_{cr}'}\right)_2 = 0.7$.

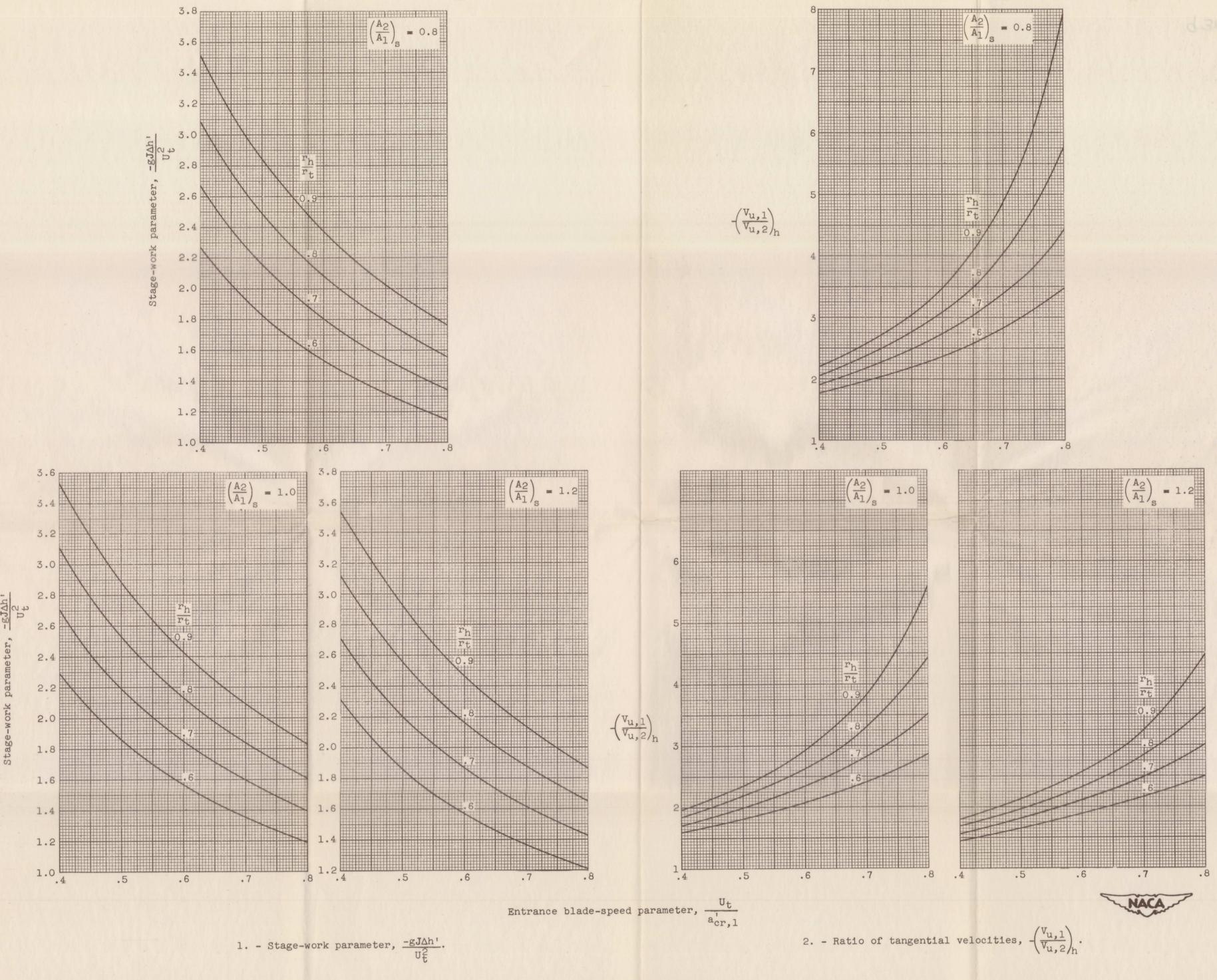
Exit blade-speed parameter, Ut

Chart I. - Concluded. Last stage or single stage with zero exit whirl.



(a) $M_{1,h} = M_{2,h} = 0.6$.

Chart II. - Stage other than last with specified Mach number and 1200 turning angle at hub radius.



(b) $M_{1,h} = M_{2,h} = 0.8$.

NACA-Langley - 4-10-53 - 400